View metadata, citation and similar papers at core.ac.uk

brought to you by CORE

provided by OTHES

universität wien

DISSERTATION

Titel der Dissertation

Analysis of glycopeptides, glycans and polysaccharides by mass spectrometry

angestrebter akademischer Grad

Doktor der Naturwissenschaften (Dr. rer.nat.)

Verfasser:	Roman Ullmer
Matrikel-Nummer:	9600689
Dissertationsgebiet (lt. Studienblatt):	Chemie
Betreuer:	Univ.-Prof. Dr. Andreas Rizzi

Wien, am 22. Oktober 2008

Danksagung

Ich möchte mich sehr herzlich bei folgenden Menschen bedanken, die mich während meines Studiums begleitet haben:

Bei meinem Betreuer Prof. Andreas Rizzi für seine geduldige und freundschaftliche Art und für die wissenschaftliche Begleitung.

Bei den KollegInnen in meiner Arbeitsgruppe Alexander Plematl, Thomas Hrebicek, Sabine Amon, Alexandra Seifner und Michael Lechner in denen ich neue Freunde gefunden habe.

Bei Prof. Irene Schnöll-Bitai und Manuela Belzik für die tolle Zusammenarbeit.

Bei Prof. Ernst Kenndler und seinen MitarbeiterInnen Leopold Kremser, Gerhard Bilek, Madeleine Dell´mour und Victor Weiss für die interessanten wissenschaftlichen und nicht-wissenschaftlichen Diskussionen und den ausgezeichneten Espresso.

Bei Prof. Günter Allmaier und seiner ganzen Arbeitsgruppe, vor allem bei Martina Marchetti-Deschmann, Jasmin Kemptner und Ernst Pittenauer, die mich immer sehr hilfsbereit aufgenommen haben.

Bei Prof. Wolfgang Lindner und seiner Arbeitsgruppe, vor allem bei Alexander Leitner und Peter Frühauf für ihre kompetente Hilfe.

Bei meinen Eltern und meiner Schwester Elisabet, die mich all die Jahre liebevoll unterstützt haben.

Bei meiner Frau Heidi, die immer für mich da ist und mein Leben wunderschön macht.

Content

Introduction.....7

1. Analysis of glycoproteins by MALDI mass spectrometry.....**7**

1.1. Structure of glycoproteins.....7

1.2. MALDI-MS of glycoproteins and glycopeptides.....10

1.3. Separation of glycopeptides and glycans.....11

1.4. Derivatization of glycopeptides prior to mass spectrometry.....12

1.5. Derivatization of glycans prior to mass spectrometry.....13

1.6. Ionic liquid matrices for the MALDI-MS analysis of biopolymers.....14

2. The determination of the molar mass distribution of polymers.....16

2.1. Size-exclusion chromatography of polymers.....16

2.2. MALDI-TOF-MS analysis of polymers.....17

2.3. Pullulans.....18

3. References.....20

Publications.....29

R. Ullmer, A. Plematl and A. Rizzi *„Derivatization by 6-aminoquinolyl-N-hydroxy-succinimidyl carbamate for enhancing the ionization yield of small peptides and glycopeptides in matrix-assisted laser desorption/ionization and electrospray ionization mass spectrometry“*,
Rapid Communications in Mass Spectrometry 2006; 20: 1469-1479.....31

R. Ullmer, A. Rizzi *„Use of a novel ionic liquid matrix for MALDI-MS analysis of glycopeptides and glycans in total tryptic digests”*,
submitted to Journal of Mass Spectrometry 43

I. Schnöll-Bitai, R. Ullmer, T. Hrebicek, A. Rizzi, I. Lacik „*Characterization of the molecular mass distribution of pullulans by matrix-assisted laser desorption/ionization time-of-flight mass spectrometry using 2,5-dihydroxybenzoic acid butylamine (DHBB) as liquid matrix”*,
Rapid Communications in Mass Spectrometry 2008; 22: 2961-2970.....63

Summary.....73

Zusammenfassung.....75

Lebenslauf.....77

Introduction

1. Analysis of glycoproteins by mass spectrometry

1.1. Structure of glycoproteins

Glycoproteins are found in eukaryotes and prokaryotes [1] and have functions that span the entire spectrum of protein activities, including those of enzymes, transport proteins, receptors, hormones and structure proteins. Particularly, secreted and membrane-associated proteins are glycosylated. Their carbohydrate moieties have several important biological roles, for example in cell-cell recognition, protein sorting and metabolism. The structural complexity of glycans allows them to encode information for specific molecular recognition. Changes in carbohydrate structures are also involved in many pathologic states, such as cancer, atherosclerosis and rheumatoid arthritis. Some important monosaccharides are shown in Figure 1, but there is a number of further components present in glycan structures.

The carbohydrate chains are enzymatically generated and covalently linked to the polypeptide without the rigid guidance of nucleic acid templates. The processing enzymes are generally not available in sufficient quantities to ensure the synthesis of uniform products. Glycoproteins therefore have variable carbohydrate compositions, a phenomenon known as microheterogeneity. Three types of direct attachments can be distinguished: *O*-glycosylation, *N*-glycosylation and glycosylphosphatidylinositol (GPI)-membrane anchors.

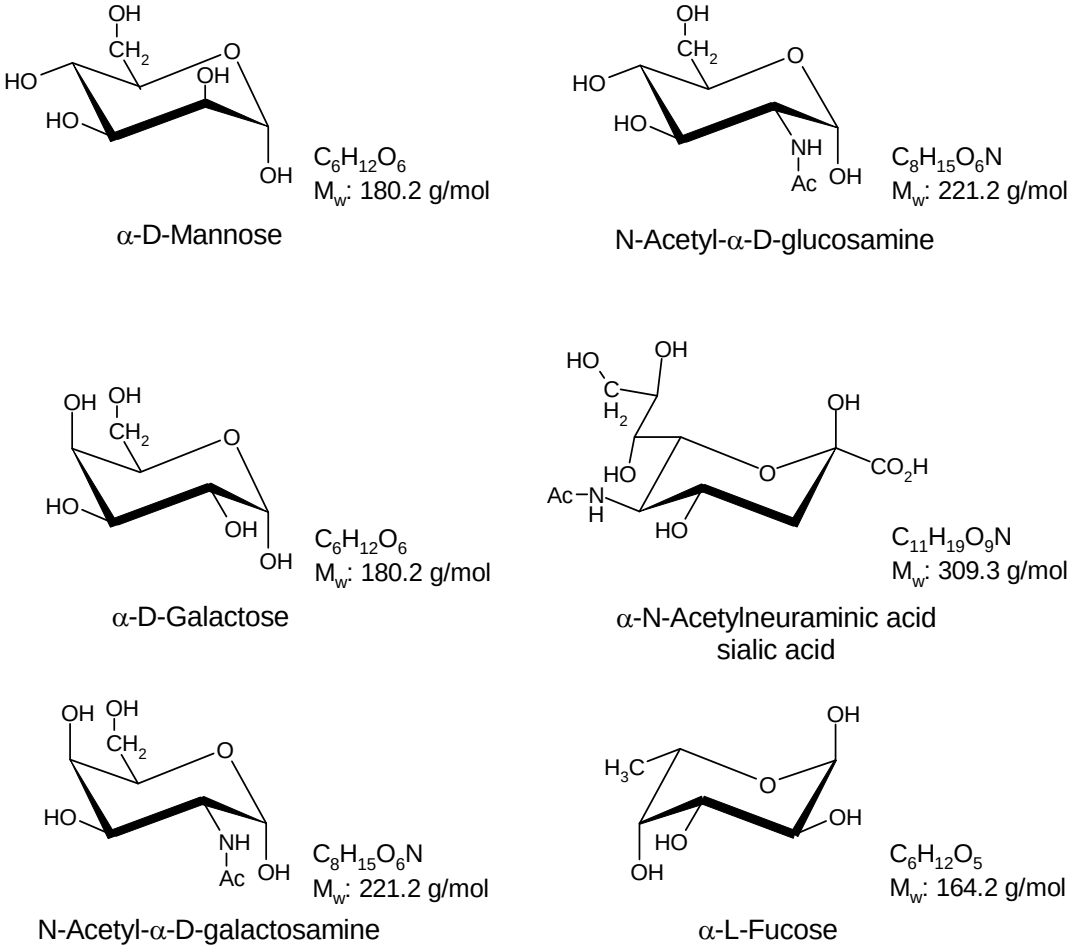

Figure 1: Structures of monosaccharides commonly found in protein attached glycostructures

N-glycosylation

N-glycans are linked to the amide nitrogen of the amino acid asparagine (N) within the consensus sequence N-X-S/T, where X means any amino acid except proline (P) and aspartic acid (D) [2-4]. The carbohydrate chain is characterized by a distinctive pentasaccharide core structure which consists of two *N*-acetyl-glucosamines (GlcNAc) and three mannose (Man) moieties. The biosynthesis of these compounds starts with the attachment of a oligosaccharide containing the core together with additional six mannose

and three glucose residues [5]. Subsequently, the oligosaccharide is processed by various glycosyl transferases and glycosidases to the mature glycan. This processing results in three general types of *N*-linked glycans: The high mannose type, which contains a variable number of mannoses linked to the core structure, the complex type (Figure 2) and the mixture of the these two, the hybrid type. Further structural diversities of *N*-glycans are the so-called bisecting GlcNAc attached to the 4-position of the β-mannose of the core and the α-fucosyl residue attached to the core mannose or to the antennae.

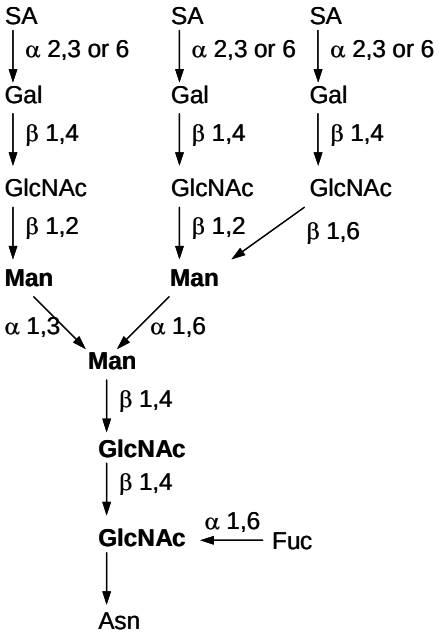

Figure 2: Fucosylated, trisialo, triantennary complex type glycan. The pentasaccharide core common to all *N*-linked oligosaccharides is written in bold type. Asn, asparagine; Fuc, fucose; GlcNAc, N-acetyl-glucoseamine; Man, mannose; Gal, galactose; SA, sialic acid

O-glycosylation

O-linked glycans are much more diverse in structure, ranging from one single galactose residue in collagen to large polysaccharides in proteoglycans and have no common core

structure and no consensus amino acid sequence at the attachment site [6]. They are linked to the hydroxyl group of either serine or threonine. In mammals, normally the *O*-glycosidic attachment do involve a core structure, namely the disaccharide β-Gal-(1-3)-α-GalNAc. The structural diversity introduced through elongation of this basic structure with residues like Gal, Fuc, GlcNAc, xylose and SA can lead to a large number of structural variants.

GPI-linked proteins

GPI-membrane anchors are attached to the polypeptide chain by an amide bond between the C-terminal carboxyl group of the protein and mannose-6-phosphoethanolamine. They function to anchor a wide variety of proteins to the exterior surface of the eukaryotic plasma membrane. GPI anchors thus provide an alternative to protein fixation by transmembrane polypeptide domains.

1.2. MALDI-MS of glycoproteins and glycopeptides

Glycoproteins are among the analytically most challenging classes of biological molecules in mass spectrometry [7]. An important reason is the high number of glycoforms which leads to complex spectra and the certain risk to lose information about low abundant glyco- and isoforms. The glycosylation pattern changes in time and is dependent on the kind and state of the cell. Each glycosylated site may contain many different glycan structures (microheterogeneity). For example, human erythrocyte CD59 has over one hundred different oligosaccharide structures on a single glycosylation site [8,9]. In addition different sites may be only partially glycosylated (macroheterogeneity).

Glycoprotein analysis, particularly the determination of the total number of post-translational modifications (PTMs), can be conducted on the basis of intact glycoprotein isoforms when coupling ESI-MS to high performance separation methods, like high-performance liquid chromatography (HPLC) or high performance capillary zone electrophoresis (CZE) [10-14]. High-resolution mass analyzers combined with electrospray ionization (ESI-MS) were able to differentiate a large number of glyco- and isoforms present in one glycoprotein. Mass accuracy and resolution obtained with matrix-assisted

laser desorption/ ionization mass spectrometry (MALDI-MS) for large glycoproteins, in contrast, are rarely sufficient to distinguish between different iso- and glycoforms present. The detailed analysis of the site-specific positioning and variability in the glycan structures can be rarely done on the basis of the integral glycoprotein.

Site-specific data are mainly gathered by analyzing glycopeptides gained by enzymatic digestion or controlled chemical degradation of the pre-separated or pre-purified glycoprotein. Unfortunately, the ionization yield of different chemical species is very unequal. It has been demonstrated that signals from arginine-containing peptides are generally stronger than that of lysine-containing peptides as a result of its more basic side chain [15]. Oligosaccharides are known to have a relatively low ionization yield compared to, for instance, peptides. Glycopeptides which consist of a large glycan structure in comparison with the peptide backbone deal with the same problem. Small glycosylated peptides are therefore often suppressed and exhibit, if even, low signal intensities in MALDI-MS spectra.

Generally, two different strategies can be applied in order to obtain reproducible spectra of analytes with low ionization yields in MALDI-MS. The first approach deals with the pre-separation of the analytes, the second one with a derivatization step before MS analysis.

1.3. Separation of glycopeptides and glycans

Analytical chemistry offers various methods for the isolation of glycopeptides and glycans. HPLC separation is a well-established method for the analysis of peptides and glycopeptides and is often used in an on-line hyphenation with ESI-MS [16]. Glycopeptides in a protein digest can selectively be detected using multistage LC-ESI-MS/MS by monitoring the oxonium ions from cleaved sugars [17]. The coupling of CE with MS offers a powerful method for the isolation and detection of glycopeptides. To suppress peptide interactions with the fused silica capillary walls and to control the electroosmotic flow (EOF) several approaches have been introduced such as working at extreme pH values, using a high ionic strength buffer and, particularly, modifying the capillary wall applying different coatings [18-20]. The combination of HPLC and CE in a multidimensional approach uses different analytical methods that analyze the sample with independent selectivities [21].

Selective isolation of glycopeptides and glycans can be achieved by affinity chromatography (AFC) with immobilized lectins [22,23], boronic acid groups [24] or by hydrophilic affinity separation with cellulose and sepharose [25]. Commonly used stationary phases for LC analysis of oligosaccharides are anion-exchange materials, reverse-phase (RP), normal-phase (particularly hydrophilic interaction chromatography, HILIC) [26] and porous graphitized carbon (PGC) [27,28] or the combination of two different phases [29,30].

1.4. Derivatization of glycopeptides prior to mass spectrometry

Derivatization of glycopeptides often aims to enhance the ionization yield in the MALDI process and to increased signal intensities in the mass spectrum. These derivatization steps can be carried out either on the peptide backbone or on the glycan structure. Many different methods are available for amino acid derivatization, the reactive groups are in this instance the OH-group in Ser, Thr and Tyr, the COOH-group in Asp and Glu, the NH-group in Lys, Arg and at the N-terminus and the SH-group in Cys. Different types of reactions were carried out including alkylation, acylation, silylation and cyclic reactions [31-34]. Many of these derivatizations were primarily aimed to attach a chromophor or fluorophor label. Some derivatization procedures, however, are exclusively investigated for the enhancement of detection sensitivity of peptides in MALDI-MS. The derivatization with *N*-terminal tags containing a coumarin core was shown to improve the sensitivity for peptides having low ionization yield [35]. The guanidination reaction of lysine residues with *O*-methylisourea results in the more basic side chain homoarginine and in higher peak intensities [36,37]. A highly activated ester containing a permanent charge, S-pentafluorophenyl [tris(2,4,6-triethoxyphenyl) phosphonium] acetate bromide (TMPP-AcSC_6F_5 bromide) was used to derivatize the N-terminus [38,39]. Another strongly basic moiety represents a quaternary ammonium group derived from the reaction of α-amino groups with iodomethane. The resulting signal intensities in MALDI-MS are increased by at least an order of magnitude [40]. Derivatization with 6-aminoquinolyl-*N*-hydroxysuccinimidyl carbamate (AQC), a fluorescent reagent which rapidly reacts with free amino groups resulting in stable urea derivatives, led to an intense increase in ionization yield for small glycopeptides in the presence of non-glycosylated peptides [41].

1.5. Derivatization of glycans prior to mass spectrometry

Derivatization of glycans, although not essential for MALDI analysis, can be advantageous in some cases for improving sensitivity and for influencing fragmentation patterns in MS^n experiments. Reducing sugars are conveniently derivatized with aromatic amines at their reducing terminus by reductive amination with $NaBH_3CN$ or other reactions. The attachment is commonly used for introducing chromophores and fluorophores to aid detection in HPLC and CE experiments and to introduce charges for electrophoretic migration. Enhancement of ionization yield can be achieved by attaching a group with a constitutive charge or high proton affinity. An increase in signal intensity of glycans by up to three orders of magnitude was reported after addition of 4-aminobenzoic acid 2-(diethylamino)ethyl ester (ABDEAE) [42]. Often used reagents in this context are 2-aminopyridine (2-AP) and 2-aminoacridone (AMAC) [43-46]. Whereas the introduced amino groups commonly increase the affinity to protons, the oligosaccharides have higher affinity to sodium adducts. Therefore, a distribution of the derivatized glycans in protonated and sodiated species might lead to a split of the signals and thus to a decrease in sensitivity. 2-aminobenzamide (2-AB) is used to introduce a fluorescent group for detection in HPLC but shows no significant enhancement in sensitivity in MALDI-MS analysis. In this case the MALDI process leads predominantly to $[M+Na^+]^+$ ions. On-target derivatization with aniline in 2,5-dihydroxybezoic acid and *N*,*N*-dimethylaniline via nonreductive amination resulted in increased ionization for glycans and was used for an automated identification of reducing oligosaccharides [47,48]. For the enhancement of ionization yield in the negative ion mode several derivatives capable of forming negative charges were introduced. 2-aminobenzoic acid (2-AA) [49], 8-aminonaphthalene-1,3,6-trisulphonic acid (ANTS) [50] and 1-aminopyrene-3,6,8-trisulfonate (APTS) [51] allow carbohydrates to be examined as negative ions with good sensitivity. Halogeno-substituted 2-aminobenzoic acid derivatives were used for fragmentation studies in negative ion mode [52].

Permetylation with methyl iodide was predominantly carried out to improve the fragmentation pattern in MS^n experiments yielding in cross ring fragmentations even under low energy CID conditions. Such enhanced fragmentation allwos one to extract more information about branching, interglycosidic linkages and the presence of configurational and conformational isomers. For example, the distinction between α2-3 and α2-6 linkages

of the sialic acid residues was elucidated by cross-ring fragments. As important side effects, the permethylation stabilizes the sialic acid residues and enhances the ionization yield [53-56].

The quantitative profiling of oligosaccharides was demonstrated with stable isotope tags based on tetradeuterium-labeled 2-aminopyridine [57]. A multifunctional primary amine tag was introduced employing not only the possibility for relative quantification by stable isotopes but also a UV-active group, a biotin-affinity group and a quaternary amine for ionization enhancement [58]. With these two methods it is possible to compare different glycosylation patterns within different biological samples.

1.6. Ionic liquid matrices

Ionic liquids (ILs) are organic or semiorganic salts melting at temperatures below 100°C and possess a low vapor pressure. Due to their viscous consistence and the ability to dissolve a wide range of analytes they have been used in a number of analytical techniques [59]. In the field of separation science ionic liquids have been used as stationary phases in gas chromatography (GC) [60] and as mobile phase additives in CE [61] and HPLC [62]. The possibility to introduce one or more chiral groups into the IL opens an additional field for analytical as well as synthetic chemistry [63,64]. These chiral ionic liquids (CILs) consist either of a chiral cation or a chiral anion or both. The application of these compounds can be divided into three different groups: Asymmetric synthesis, spectroscopy and separation science. In asymmetric synthesis the CILs act as chiral environment or as catalysts in a large number of chemical reactions. An example of spectroscopic application is the determination of enantiomeric excess of samples by NMR integration [65]. In gas chromatography CILs are used as stationary phases to improve the separation of chiral compounds [66], in electrophoresis as additives in the background electrolyte [67].

In 2001, ionic liquids were introduced as matrices in MALDI-MS for the analysis of biomolecules and synthetic polymers [68]. The first ionic liquid matrices (ILMs) were synthesized of the commonly used matrix substances sinapinic acid (SA) and α-cyano-4-hydroxycinnamic acid (CHCA) combined with a variety of cations based on amine structures [69]. Many different ILMs were investigated for several kinds of analytes,

including polynucleotides [70,71], phospholipids [72], glycolipids [73], heavy oil fractions (asphaltenes) [74] and polyethyleneglycol (PEG) [69,73]. The combination of 2,5-dihydroxybezoic acid with butylamine (DHBB) turned out to be well suited for the analysis of (sulfated) oligosaccharides and glycolipids [73,75]. The same ILM was used for the determination of the molecular mass distribution of polysaccharides (pullulans) which are used as calibration standards in aqueous size-exclusion chromatography [76]. The use of ILM in the analysis of proteins and peptides was also evaluated. It was demonstrated that the use of pyridinium CHCA can lead to a higher sequence coverage in peptide mass fingerprint experiments [77]. In most cases the ionization process in ILMs led to protonated species of the analytes, very similar to solid matrices. However, the analysis of large proteins by ILMs seems to be impeded by the fact that these molecules tend to form adducts with the cations or anions of the matrix, a phenomenon that leads to peak broadening and to a decrease in sensitivity [69,78]. 1,1,3,3-tetramethylguanidinium (TMG) in combination with CHCA in a molar ratio of 2:1 (G_2CHCA) was introduced for the analysis of sulfated oligosaccharides [79]. The resulting mass spectra show very low extent of fragmentation through the loss of SO_3. The TMG salt of *p*-coumaric acid (CA) (in a ratio of 3:1, G_3CA) was used for the analysis of sialylated, sulfated and neutral carbohydrates and glycopeptides and turned out to be well suited for the analysis of sugar containing analytes in the positive and negative ion mode [80].

In comparison to classical crystalline matrices ILMs exhibit one striking advantage: The viscous liquid surface is highly homogeneous and does not tend to build hot spots. The range of the signal intensities between different areas of the spot is very narrow (shot-to-shot reproducibility) and therefore the number of averaged spectra can be reduced [69,73]. This fact could enhance the application of MALDI-MS for quantitative analysis [71,81]. Moreover ILMs are very “cool” matrices, the formation of metastable ions and thus the extent of in-source as well as post-source fragmentation can be reduced.

2. The determination of the molar mass distribution of polymers

2.1. Size-exclusion chromatography of polymers

The most important quantities for the numerical characterization of polymers are the two different average values of the molar mass and the polydispersity. These averages are defined in terms of the molar mass, M_i, of species i, their corresponding number n_i, weight w_i or concentration c_i. The number average molar mass, M_n, is defined as

$$M_n = (\sum n_i M_i) / (\sum n_i)$$

The value of M_n can directly be determined by methods sensitive to the number of molecules like osmometry or cryoscopy.
The weight average molar mass is defined as

$$M_w = (\sum n_i Mi^2) / (\sum n_i M_i) = (\sum w_i M_i) / (\sum w_i) = (\sum c_i M_i) / (\sum c_i)$$

M_w can directly be determined by methods sensitive to the weight of molecules like sedimentation or light scattering.
The polydispersity, D, is a measure of the width of the molar mass distribution and is defined as the ratio of the two average values:

$$D = M_w / M_n$$

Monodisperse samples with all molecules having the same molar mass exhibit a polydispersity of D = 1, technical materials usually have polydispersities up to D = 20.
Size-exclusion chromatography (SEC), also called gel permeation chromatography (GPC), is the most popular method for the determination of the average values of the molar masses of polymers. The separation process is based on the molecular hydrodynamic volume of the polymer species. The polymer solution is passed through a column packed with porous particles with a defined pore volume and narrow pore size distribution. Lower molar mass

species elute later because they can diffuse deeper into the pores. Under ideal conditions there is no separation due to binding to the stationary phase. SEC delivers a linear correlation between log M_i and the elution volume. The system has to be calibrated with a series of narrowly distributed compounds of known molar mass. This calibration is a problem for complex polymers due to the lack of proper standards, the method do not deliver absolute molar mass information. The combination of SEC and MALDI-MS is a commonly used approach to overcome these calibration problems.

2.2. MALDI-TOF-MS analysis of polymers

In recent years mass spectrometry has become a powerful tool for the determination of the characteristic average values of polymers, M_n, M_w and D. MALDI-MS is particularly suitable in this purpose because of its rather simple and straightforward spectrum interpretation. Other techniques like electrospray ionization are known to generate multiple charged ions and provide complex spectra due to a superposition of mass and charge distribution. Due to the huge mass range of polymers with broad distributions it is essential to use a mass analyzer with the lowest mass discrimination possible. The commonly used combination of MALDI ion source and time-of-flight (TOF) analyzer meets this goal and is well suited for the determination of molar mass distributions. Moreover, TOF instruments have a nearly unlimited mass range, masses up to 1.5 MDa have been measured by this method [82]. However, the mass discrimination during the MALDI process itself is still a drawback. This phenomenon leads to an underestimation of higher masses and displaces the peak maximum to somewhat lower masses [83,84]. Especially for polymers with a broad distribution (polydispersity $D > 2$) the discrepancy between the "real" and the measured value is highly pronounced. There have been made some efforts to overcome this problem by means of mathematical models [85]. There are some further effects that influence mass discrimination and lead to a bias towards lower or higher maxima like the voltage parameters of the MALDI-TOF instrument, the laser power, the choice of the matrix and ionizing agent and the nature of the detector [86-92].

In contrast to SEC and most other techniques, MALDI-MS experiments do not only provide molar mass distributions (MMD), but also some other interesting information

concerning the chemical structure of polymers, which might show various types of heterogeneity. The use of different monomers leads to copolymers, this is the chemical heterogeneity (CH). Polymers can show a different molecular architecture (MA), linear, branched or cyclic. And they can contain functional groups at their chain ends leading to a functionality type distribution (FTD). Together with pre-separation techniques MALDI-MS analysis is able to give information about the molecular complexity of polymers.

2.3. Pullulans

Pullulans are polysaccharides produced from different strains of the fungus *Aureobasidium pullulans*. This microorganisms can be found in soil, fruits, effluents and also in building materials, *e.g.* in wood and wallpapers, and are known to elicit hypersensitivity and some kinds of infection. These fungi are converting starch into pullulan and are therefore used in biotechnology. Pullulans are manufactured to edible and tasteless films which are commercially used as food additives in breath freshener or oral hygiene products, as capsules for drugs and as antiseize agent in the production of synthetic fibers [93]. The repeating units of these rather simple carbohydrates are mainly α-(1-6) linked maltotriose units, each of which are composed of three α-(1-4) linked glucoses, and a low extent of α-(1-6) linked maltotetraose units [94] (Figure 3).

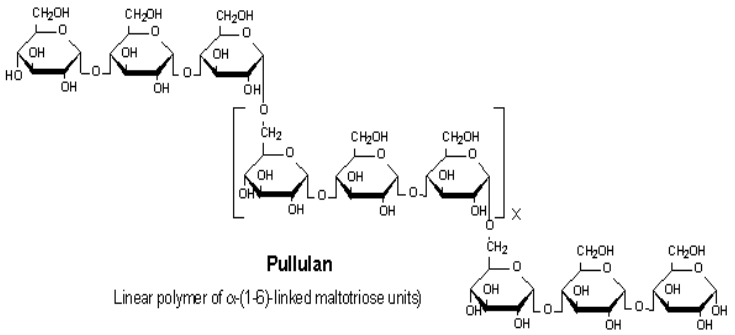

Figure 3: Structure of the polysaccharide pullulan

The polydispersity of pullulans produced by the microorganisms lies between 2.1 and 4.1 [95-97]. Different methods are applied to get more narrow distributions with D values near 1.1. Precipitation followed by gel filtration is carried out yielding fractions of high molar mass pullulans. Intermediate masses are obtained by partial enzymatic degradation by means of pullulanase, masses below 5 kDa are the result of further degradation by HCl [98].

Pullulans play an important role in analytical chemistry since they are commonly used as calibration standards in aqueous SEC [98-101]. Samples with narrow distributions (polydispersity $D < 1.2$) are preferred over those with broad distributions. In this context it is necessary to characterize these samples with respect to the number and weight average molar masses, M_n and M_w, respectively. This characterization is usually carried out by SEC with various types of detectors [94,100,102,103], sedimentation [98,99] or light scattering experiments. Mass spectrometry is an alternative method providing direct data on the molar masses. NanoESI-MS analysis of pullulans was successfully carried out with a sample of a weight average molar mass of approximately 5900 Da [104]. It was possible to obtain a more or less uniform charge state by addition of three sodium ions per molecule. For samples with higher masses it is increasingly difficult to get such simple spectra. The MALDI process is known to produce predominately singly charged ions, MALDI-MS data are therefore more straightforward in this context. The choice of the matrix and the ionizing agent is of huge importance to get reliable data from MALDI-MS experiments, as stated above. Different matrices have been used for the analysis of pullulans, like 2,5-dihydroxybenzoic acid (DHB) [105,106], 2,4,6-trihydroxyacetophenone (THAP) [107] and *nor*-harmane [108]. The use of the ionic liquid matrix like 2,5-dihydroxybenzoic acid butylamine (DHBB) turned out to be well suited for the analysis of pullulan samples in terms of signal intensities of very high mass polymers (up to 100.000 Da) as well as in terms of accuracy of the obtained average molar mass values [76]. Although these carbohydrates are prone to easy fragmentation during the MALDI process, accurate mass distribution and polydispersity data could be assessed when using the ionic liquid matrix.

3. References

1. Moens S, Vanderleyden J. Glycoproteins in prokaryotes. *Archives of Microbiology* 1997; **168**: 169-175.

2. Dwek RA, Edge CJ, Harvey DJ, Wormald MR, Parekh RB. Analysis of glycoprotein-associated oligosaccharides. *Annual Review of Biochemistry* 1993; **62**: 65-100.

3. Gavel Y, Von Heijne G. Sequence differences between glycosylated and non-glycosylated Asn-X-Thr/Ser acceptor sites: implications for protein engineering. *Protein Engineering* 1990; **3**: 433-442.

4. Shakin-Eshleman SH, Spitalnik SL, Kasturi L. The amino acid at the X position of an Asn-X-Ser sequon is an important determinant of N-linked core-glycosylation efficiency. *Journal of Biological Chemistry* 1996; **271**: 6363-6366.

5. Kornfeld R, Kornfeld S. Assembly of asparagine-linked oligosaccharides. *Annual Review of Biochemistry* 1985; **54**: 631-664.

6. Hounsell EF, Davies MJ, Renouf DV. O-linked protein glycosylation structure and function. *Glycoconjugate Journal* 1996; **13**: 19-26.

7. Harvey DJ. Matrix-assisted laser desorption/ionisation mass spectrometry of oligosaccharides and glycoconjugates. *Journal of Chromatography A* 1996; **720**: 429-446.

8. Rudd PM, Elliott T, Cresswell P, Wilson IA, Dwek RA. Glycosylation and the immune system. *Science* 2001; **291**: 2370-2376.

9. Rudd PM, Colominas C, Royle L, Murphy N, Hart E, Merry AH, Hebestreit HF, Dwek RA. A high-performance liquid chromatography based strategy for rapid, sensitive sequencing of N-linked oligosaccharide modifications to proteins in sodium dodecyl sulphate polyacrylamide electrophoresis gel bands. *Proteomics* 2001; **1**: 285-294.

10. Zamfir A, Peter-Katalinic J. Glycoscreening by on-line sheathless capillary electrophoresis/electrospray ionization-quadrupole time of flight-tandem mass spectrometry. *Electrophoresis* 2001; **22**: 2448-2457.

11. Hernandez-Borges J, Neusüß C, Cifuentes A, Pelzing M. On-line capillary electrophoresis-mass spectrometry for the analysis of biomolecules. *Electrophoresis* 2004; **25**: 2257-2281.

12. Bateman KP, White RL, Yaguchi M, Thibault P. Characterization of protein glycoforms by capillary-zone electrophoresis-nanoelectrospray mass spectrometry. *Journal of Chromatography A* 1998; **794**: 327-344.

13. Lai CC, Her GR. Analysis of phospholipase A2 glycosylation patterns from venom of individual bees by capillary electrophoresis/electrospray ionization mass spectrometry using an ion trap mass spectrometer. *Rapid Communications in Mass Spectrometry* 2000; **14**: 2012-2018.

14. Demelbauer UM, Plematl A, Kremser L, Allmaier G, Josic D, Rizzi A. Characterization of glyco isoforms in plasma-derived human antithrombin by on-line capillary zone electrophoresis-electrospray ionization-quadrupole ion trap-mass spectrometry of the intact glycoproteins. *Electrophoresis* 2004; **25**: 2026-2032.

15. Krause E, Wenschuh H, Jungblut PR. The Dominance of Arginine-Containing Peptides in MALDI-Derived Tryptic Mass Fingerprints of Proteins. *Analytical Chemistry* 1999; **71**: 4160-4165.

16. Lo-Guidice JM, Lhermitte M. HPLC of oligosaccharides in glycobiology. *Biomedical Chromatography* 1996; **10**: 290-296.

17. Huddleston MJ, Bean MF, Carr SA. Collisional fragmentation of glycopeptides by electrospray ionization LC/MS and LC/MS/MS: methods for selective detection of glycopeptides in protein digests. *Analytical Chemistry* 1993; **65**: 877-884.

18. Kelly JF, Locke SJ, Ramaley L, Thibault P. Development of electrophoretic conditions for the characterization of protein glycoforms by capillary electrophoresis-electrospray mass spectrometry. *Journal of Chromatography, A* 1996; **720**: 409-427.

19. Rudd PM, Scragg IG, Coghill E, Dwek RA. Separation and analysis of the glycoform populations of ribonuclease B using capillary electrophoresis. *Glycoconjugate Journal* 1992; **9**: 86-91.

20. Amon S, Plematl A, Rizzi A. Capillary zone electrophoresis of glycopeptides under controlled electroosmotic flow conditions coupled to electrospray and matrix-assisted laser desorption/ionization mass spectrometry. *Electrophoresis* 2006; **27**: 1209-1219.

21. Udiavar S, Apffel A, Chakel J, Swedberg S, Hancock WS, Pungor E, Jr. The Use of Multidimensional Liquid-Phase Separations and Mass Spectrometry for the Detailed Characterization of Posttranslational Modifications in Glycoproteins. *Analytical Chemistry* 1998; **70**: 3572-3578.

22. Geng M, Zhang X, Bina M, Regnier F. Proteomics of glycoproteins based on affinity selection of glycopeptides from tryptic digests. *Journal of Chromatography B* 2001; **752**: 293-306.

23. Lis H, Sharon N. Lectins: Carbohydrate-Specific Proteins that Mediate Cellular Recognition. *Chemical Reviews* 1998; **98**: 637-674.

24. Liu X-C, Scouten WH. Miscellaneous methods in affinity chromatography. Part I: boronic acids as selective ligands for affinity chromatography. *Biochromatography* 2002: 307-317.

25. Wada Y, Tajiri M, Yoshida S. Hydrophilic Affinity Isolation and MALDI Multiple-Stage Tandem Mass Spectrometry of Glycopeptides for Glycoproteomics. *Analytical Chemistry* 2004; **76**: 6560-6565.

26. Ruhaak LR, Huhn C, Waterreus W-J, de Boer AR, Neususess C, Hokke CH, Deelder AM, Wuhrer M. Hydrophilic Interaction Chromatography-Based High-Throughput Sample Preparation Method for N-Glycan Analysis from Total Human Plasma Glycoproteins. *Analytical Chemistry* 2008; **80**: 6119-6126.

27. Wuhrer M, Deelder AM, Hokke CH. Protein glycosylation analysis by liquid chromatography-mass spectrometry. *Journal of Chromatography B* 2005; **825**: 124-133.

28. Pabst M, Bondili JS, Stadlmann J, Mach L, Altmann F. Mass + Retention Time = Structure: A Strategy for the Analysis of N-Glycans by Carbon LC-ESI-MS and Its Application to Fibrin N-Glycans. *Analytical Chemistry* 2007; **79**: 5051-5057.

29. Karlsson G, Swerup E, Sandberg H. Combination of two hydrophilic interaction chromatography methods that facilitates identification of 2-aminobenzamide-labeled oligosaccharides. *Journal of Chromatographic Science* 2008; **46**: 68-73.

30. Deguchi K, Keira T, Yamada K, Ito H, Takegawa Y, Nakagawa H, Nishimura S-I. Two-dimensional hydrophilic interaction chromatography coupling anion-exchange and hydrophilic interaction columns for separation of 2-pyridylamino derivatives of neutral and sialylated N-glycans. *Journal of Chromatography, A* 2008; **1189**: 169-174.

31. Halket JM, Zaikin VG. Derivatization in mass spectrometry-1. Silylation. *European Journal of Mass Spectrometry* 2003; **9**: 1-21.

32. Zaikin VG, Halket JM. Derivatization in mass spectrometry-2. Acylation. *European Journal of Mass Spectrometry* 2003; **9**: 421-434.

33. Halket JM, Zaikin VG. Derivatization in mass spectrometry- 3. Alkylation (arylation). *European Journal of Mass Spectrometry* 2004; **10**: 1-19.

34. Zaikin VG, Halket JM. Derivatization in mass spectrometry-4. Formation of cyclic derivatives. *European Journal of Mass Spectrometry* 2004; **10**: 555-568.

35. Pashkova A, Moskovets E, Karger BL. Coumarin Tags for Improved Analysis of Peptides by MALDI-TOF MS and MS/MS. 1. Enhancement in MALDI MS Signal Intensities. *Analytical Chemistry* 2004; **76**: 4550-4557.

36. Bonetto V, Bergman A-C, Joernvall H, Sillard R. C-Terminal Sequence Analysis of Peptides and Proteins Using Carboxypeptidases and Mass Spectrometry after Derivatization of Lys and Cys Residues. *Analytical Chemistry* 1997; **69**: 1315-1319.

37. Beardsley RL, Reilly JP. Optimization of guanidination procedures for MALDI mass mapping. *Analytical Chemistry* 2002; **74**: 1884-1890.

38. Huang Z-H, Wu J, Roth KDW, Yang Y, Gage DA, Watson JT. A Picomole-Scale Method for Charge Derivatization of Peptides for Sequence Analysis by Mass Spectrometry. *Analytical Chemistry* 1997; **69**: 137-144.

39. Strahler JR, Smelyanskiy Y, Lavine G, Allison J. Development of methods for the charge-derivatization of peptides in polyacrylamide gels and membranes for their direct analysis using matrix-assisted laser desorption-ionization mass spectrometry. *International Journal of Mass Spectrometry and Ion Processes* 1997; **169/170**: 111-126.

40. Stewart NA, Pham VT, Choma CT, Kaplan H. Improved peptide detection with matrix-assisted laser desorption/ionization mass spectrometry by trimethylation of amino groups. *Rapid Communications in Mass Spectrometry* 2002; **16**: 1448-1453.

41. Ullmer R, Plematl A, Rizzi A. Derivatization by 6-aminoquinolyl-N-hydroxysuccinimidyl carbamate for enhancing the ionization yield of small peptides and glycopeptides in matrix-assisted laser desorption/ionization and electrospray ionization mass spectrometry. *Rapid Communications in Mass Spectrometry* 2006; **20**: 1469-1479.

42. Takao T, Tambara Y, Nakamura A, Yoshino K-i, Fukuda H, Fukuda M, Shimonishi Y. Sensitive analysis of oligosaccharides derivatized with 4-aminobenzoic acid 2-(diethylamino)ethyl ester by matrix-assisted laser desorption/ionization mass spectrometry. *Rapid Communications in Mass Spectrometry* 1996; **10**: 637-640.

43. Okamoto M, Takahashi K, Doi T, Takimoto Y. High-sensitivity detection and postsource decay of 2-aminopyridine-derivatized oligosaccharides with matrix-assisted laser desorption/ionization mass spectrometry. *Analytical Chemistry* 1997; **69**: 2919-2926.

44. Okafo G, Burrow L, Carr SA, Roberts GD, Johnson W, Camilleri P. A coordinated high-performance liquid chromatographic, capillary electrophoretic, and mass spectrometric approach for the analysis of oligosaccharide mixtures derivatized with 2-aminoacridone. *Analytical Chemistry* 1996; **68**: 4424-4430.

45. Okafo G, Langridge J, North S, Organ A, West A, Morris M, Camilleri P. High-Performance Liquid Chromatographic Analysis of Complex N-Linked Glycans Derivatized with 2-Aminoacridone. *Analytical Chemistry* 1997; **69**: 4985-4993.

46. North S, Birrell H, Camilleri P. Positive and negative ion matrix-assisted laser desorption/ionization time-of-flight mass spectrometric analysis of complex glycans released from hen ovalbumin and derivatized with 2-aminoacridone. *Rapid Communications in Mass Spectrometry* 1998; **12**: 349-356.

47. Snovida Sergei I, Chen Vincent C, Perreault H. Use of a 2,5-dihydroxybenzoic acid/aniline MALDI matrix for improved detection and on-target Derivatization of glycans: A preliminary report. *Analytical Chemistry* 2006; **78**: 8561-8568.

48. Snovida SI, Rak-Banville JM, Perreault H. On the Use of DHB/Aniline and DHB/N,N-Dimethylaniline Matrices for Improved Detection of Carbohydrates:

Automated Identification of Oligosaccharides and Quantitative Analysis of Sialylated Glycans by MALDI-TOF Mass Spectrometry. *Journal of the American Society for Mass Spectrometry* 2008; **19**: 1138-1146.

49. Anumula KR, Dhume ST. High resolution and high sensitivity methods for oligosaccharide mapping and characterization by normal phase high performance liquid chromatography following derivatization with highly fluorescent anthranilic acid. *Glycobiology* 1998; **8**: 685-694.

50. Lemoine J, Cabanes-Macheteau M, Bardor M, Michalski JC, Faye L, Lerouge P. Analysis of 8-aminonaphthalene-1,3,6-trisulfonic acid labelled N-glycans by matrix-assisted laser desorption/ionisation time-of-flight mass spectrometry. *Rapid Communications in Mass Spectrometry* 2000; **14**: 100-104.

51. Suzuki H, Mueller O, Guttman A, Karger BL. Analysis of 1-aminopyrene-3,6,8-trisulfonate-derivatized oligosaccharides by capillary electrophoresis with matrix-assisted laser desorption/ionization time-of-flight mass spectrometry. *Analytical Chemistry* 1997; **69**: 4554-4559.

52. Harvey David J. Halogeno-substituted 2-aminobenzoic acid derivatives for negative ion fragmentation studies of N-linked carbohydrates. *Rapid Communications in Mass Spectrometry* 2005; **19**: 397-400.

53. Mechref Y, Kang P, Novotny MV. Differentiating structural isomers of sialylated glycans by matrix-assisted laser desorption/ionization time-of-flight/time-of-flight tandem mass spectrometry. *Rapid Communications in Mass Spectrometry* 2006; **20**: 1381-1389.

54. Kang P, Mechref Y, Klouckova I, Novotny MV. Solid-phase permethylation of glycans for mass spectrometric analysis. *Rapid Communications in Mass Spectrometry* 2005; **19**: 3421-3428.

55. Viseux N, de Hoffmann E, Domon B. Structural Analysis of Permethylated Oligosaccharides by Electrospray Tandem Mass Spectrometry. *Analytical Chemistry* 1997; **69**: 3193-3198.

56. Delaney J, Vouros P. Liquid chromatography ion trap mass spectrometric analysis of oligosaccharides using permethylated derivatives. *Rapid Communications in Mass Spectrometry* 2001; **15**: 325-334.

57. Yuan J, Hashii N, Kawasaki N, Itoh S, Kawanishi T, Hayakawa T. Isotope tag method for quantitative analysis of carbohydrates by liquid chromatography-mass spectrometry. *Journal of Chromatography A* 2005; **1067**: 145-152.

58. Hsu J, Chang SJ, Franz AH. MALDI-TOF and ESI-MS Analysis of Oligosaccharides Labeled with a New Multifunctional Oligosaccharide Tag. *Journal of the American Society for Mass Spectrometry* 2006; **17**: 194-204.

59. Shamsi SA, Danielson ND. Utility of ionic liquids in analytical separations. *Journal of separation science* 2007; **30**: 1729-1750.

60. Armstrong DW, He L, Liu Y-S. Examination of Ionic Liquids and Their Interaction with Molecules, When Used as Stationary Phases in Gas Chromatography. *Analytical Chemistry* 1999; **71**: 3873-3876.

61. Bao Y, Lantz AW, Crank JA, Huang J, Armstrong DW. The use of cationic surfactants and ionic liquids in the detection of microbial contamination by capillary electrophoresis. *Electrophoresis* 2008; **29**: 2587-2592.

62. Stalcup AM, Cabovska B. Ionic liquids in chromatography and capillary electrophoresis. *Journal of Liquid Chromatography & Related Technologies* 2004; **27**: 1443-1459.

63. Bica K, Gaertner P. Applications of chiral ionic liquids. *European Journal of Organic Chemistry* 2008: 3235-3250.

64. Ding J, Armstrong DW. Chiral ionic liquids. Synthesis and applications. *Chirality* 2005; **17**: 281-292.

65. Wasserscheid P, Boesmann A, Bolm C. Synthesis and properties of ionic liquids derived from the "chiral pool". *Chemical Communications* 2002: 200-201.

66. Ding J, Welton T, Armstrong DW. Chiral ionic liquids as stationary phases in gas chromatography. *Analytical Chemistry* 2004; **76**: 6819-6822.

67. Yanes EG, Gratz SR, Baldwin MJ, Robison SE, Stalcup AM. Capillary electrophoretic application of 1-Alkyl-3-methylimidazolium-based ionic liquids. *Analytical Chemistry* 2001; **73**: 3838-3844.

68. Tholey A, Heinzle E. Ionic (liquid) matrices for matrix-assisted laser desorption/ionization mass spectrometry - applications and perspectives. *Analytical and Bioanalytical Chemistry* 2006; **386**: 24-37.

69. Armstrong DW, Zhang L-K, He L, Gross ML. Ionic liquids as matrixes for matrix-assisted laser desorption/ionization mass spectrometry. *Analytical Chemistry* 2001; **73**: 3679-3686.

70. Carda-Broch S, Berthod A, Armstrong DW. Ionic matrices for matrix-assisted laser desorption/ionization time-of-flight detection of DNA oligomers. *Rapid Communications in Mass Spectrometry* 2003; **17**: 553-560.

71. Li YL, Gross ML. Ionic-liquid matrices for quantitative analysis by MALDI-TOF mass spectrometry. *Journal of the American Society for Mass Spectrometry* 2004; **15**: 1833-1837.

72. Li YL, Gross ML, Hsu F-F. Ionic-liquid matrices for improved analysis of phospholipids by MALDI-TOF aass spectrometry. *Journal of the American Society for Mass Spectrometry* 2005; **16**: 679-682.

73. Mank M, Stahl B, Boehm G. 2,5-Dihydroxybenzoic acid butylamine and other ionic liquid matrixes for enhanced MALDI-MS analysis of biomolecules. *Analytical Chemistry* 2004; **76**: 2938-2950.

74. Hurtado P, Hortal AR, Martinez-Haya B. Matrix-assisted laser desorption/ionization detection of carbonaceous compounds in ionic liquid matrices. *Rapid Communications in Mass Spectrometry* 2007; **21**: 3161-3164.

75. Laremore TN, Murugesan S, Park T-J, Avci FY, Zagorevski DV, Linhardt RJ. Matrix-Assisted Laser Desorption/Ionization Mass Spectrometric Analysis of Uncomplexed Highly Sulfated Oligosaccharides Using Ionic Liquid Matrices. *Analytical Chemistry* 2006; **78**: 1774-1779.

76. Schnoll-Bitai I, Ullmer R, Hrebicek T, Rizzi A, Lacik I. Characterization of the molecular mass distribution of pullulans by matrix-assisted laser desorption/ionization time-of-flight mass spectrometry using 2,5-dihydroxybenzoic acid butylamine (DHBB) as liquid matrix. *Rapid Commun Mass Spectrom* 2008; **22**: 2961-2970.

77. Zabet-Moghaddam M, Heinzle E, Lasaosa M, Tholey A. Pyridinium-based ionic liquid matrices can improve the identification of proteins by peptide mass-fingerprint analysis with matrix-assisted laser desorption/ionization mass spectrometry. *Analytical and Bioanalytical Chemistry* 2006; **384**: 215-224.

78. Zabet-Moghaddam M, Krueger R, Heinzle E, Tholey A. Matrix-assisted laser desorption/ionization mass spectrometry for the characterization of ionic liquids and the analysis of amino acids, peptides and proteins in ionic liquids. *Journal of Mass Spectrometry* 2004; **39**: 1494-1505.

79. Laremore TN, Zhang F, Linhardt RJ. Ionic liquid matrix for direct UV-MALDI-TOF-MS analysis of dermatan sulfate and chondroitin sulfate oligosaccharides. *Analytical Chemistry* 2007; **79**: 1604-1610.

80. Fukuyama Y, Nakaya S, Yamazaki Y, Tanaka K. Ionic Liquid Matrixes Optimized for MALDI-MS of Sulfated/Sialylated/Neutral Oligosaccharides and Glycopeptides. *Analytical Chemistry* 2008; **80**: 2171-2179.

81. Tholey A, Zabet-Moghaddam M, Heinzle E. Quantification of Peptides for the Monitoring of Protease-Catalyzed Reactions by Matrix-Assisted Laser Desorption/Ionization Mass Spectrometry Using Ionic Liquid Matrixes. *Analytical Chemistry* 2006; **78**: 291-297.

82. Schriemer DC, Li L. Detection of High Molecular Weight Narrow Polydisperse Polymers up to 1.5 Million Daltons by MALDI Mass Spectrometry. *Analytical Chemistry* 1996; **68**: 2721-2725.

83. Montaudo G, Montaudo MS, Puglisi C, Samperi F. Characterization of Polymers by Matrix-Assisted Laser Desorption Ionization-Time of Flight Mass Spectrometry. End Group Determination and Molecular Weight Estimates in Poly(ethylene glycols). *Macromolecules* 1995; **28**: 4562-4569.

84. Montaudo G, Scamporrino E, Vitalini D, Mineo P. Novel procedure for molecular weight averages measurement of polydisperse polymers directly from matrix-assisted laser desorption/ionization time-of-flight mass spectra. *Rapid Communications in Mass Spectrometry* 1996; **10**: 1551-1559.

85. Schnoell-Bitai I, Hrebicek T, Rizzi A. Towards a quantitative interpretation of polymer distributions from MALDI-TOF spectra. *Macromolecular Chemistry and Physics* 2007; **208**: 485-495.

86. Schriemer DC, Li L. Mass discrimination in the analysis of polydisperse polymers by MALDI time-of-flight mass spectrometry. 1. Sample preparation and desorption/ionization issues. *Analytical Chemistry* 1997; **69**: 4169-4175.

87. Wetzel SJ, Guttman CM, Flynn KM, Filliben JJ. Significant Parameters in the Optimization of MALDI-TOF-MS for Synthetic Polymers. *Journal of the American Society for Mass Spectrometry* 2006; **17**: 246-252.

88. Wetzel SJ, Guttman CM, Girard JE. The influence of matrix and laser energy on the molecular mass distribution of synthetic polymers obtained by MALDI-TOF-MS. *International Journal of Mass Spectrometry* 2004; **238**: 215-225.

89. Axelsson J, Scrivener E, Haddleton DM, Derrick PJ. Mass discrimination effects in an ion detector and other causes for shifts in polymer mass distributions measured by matrix-assisted laser desorption/ionization time-of-flight mass spectrometry. *Macromolecules* 1996; **29**: 8875-8882.

90. Byrd HCM, McEwen CN. The Limitations of MALDI-TOF Mass Spectrometry in the Analysis of Wide Polydisperse Polymers. *Analytical Chemistry* 2000; **72**: 4568-4576.

91. Shimada K, Lusenkova MA, Sato K, Saito T, Matsuyama S, Nakahara H, Kinugasa S. Evaluation of mass discrimination effects in the quantitative analysis of polydisperse polymers by matrix-assisted laser desorption/ionization time-of-flight mass spectrometry using uniform oligostyrenes. *Rapid Communications in Mass Spectrometry* 2001; **15**: 277-282.

92. Williams JB, Chapman TM, Hercules DM. Matrix-Assisted Laser Desorption/Ionization Mass Spectrometry of Discrete Mass Poly(butylene glutarate) Oligomers. *Analytical Chemistry* 2003; **75**: 3092-3100.

93. Lin Y, Zhang Z, Thibault J. Aureobasidium pullulans batch cultivations based on a factorial design for improving the production and molecular weight of exopolysaccharides. *Process Biochemistry* 2007; **42**: 820-827.

94. Forabosco A, Bruno G, Sparapano L, Liut G, Marino D, Delben F. Pullulans produced by strains of Cryphonectria parasitica-I. Production and characterisation of the exopolysaccharides. *Carbohydrate Polymers* 2006; **63**: 535-544.

95. Petrov PT, Shingel KI, Scripko AD, Tsarenkov VM. Biosynthesis of pullulan by Aureobasidium pullulans strain BMP-97. *Biotekhnologiya* 2002: 36-48.

96. Wiley BJ, Ball DH, Arcidiacono SM, Sousa S, Mayer JM, Kaplan DL. Control of molecular weight distribution of the biopolymer pullulan produced by Aureobasidium pullulans. *Journal of Environmental Polymer Degradation* 1993; **1**: 3-9.

97. Roukas T, Mantzouridou F. Effect of the aeration rate on pullulan production and fermentation broth rheological properties in an airlift reactor. *Journal of Chemical Technology and Biotechnology* 2001; **76**: 371-376.

98. Dubin PL. Nonionic polysaccharides as calibration standards for aqueous size exclusion chromatography. *Carbohydrate Polymers* 1994; **25**: 295-303.

99. Kawahara K, Ohta K, Miyamoto H, Nakamura S. Preparation and solution properties of pullulan fractions as standard samples for water-soluble polymers. *Carbohydrate Polymers* 1984; **4**: 335-356.

100. Roger P, Axelos MAV, Colonna P. SEC-MALLS and SANS Studies Applied to Solution Behavior of Linear a-Glucans. *Macromolecules* 2000; **33**: 2446-2455.

101. Yeung B, Marecak D. Molecular weight determination of hyaluronic acid by gel filtration chromatography coupled to matrix-assisted laser desorption ionization mass spectrometry. *Journal of Chromatography A* 1999; **852**: 573-581.

102. Kasaai MR. Intrinsic viscosity-molecular weight relationship and hydrodynamic volume for pullulan. *Journal of Applied Polymer Science* 2006; **100**: 4325-4332.

103. Zhu H, Yalcin T, Li L. Analysis of the accuracy of determining average molecular weights of narrow polydispersity polymers by matrix-assisted laser desorption ionization time-of-flight mass spectrometry. *Journal of the American Society for Mass Spectrometry* 1998; **9**: 275-281.

104. Bahr U, Pfenninger A, Karas M, Stahl B. High-Sensitivity Analysis of Neutral Underivatized Oligosaccharides by Nanoelectrospray Mass Spectrometry. *Analytical Chemistry* 1997; **69**: 4530-4535.

105. Stahl B, Steup M, Karas M, Hillenkamp F. Analysis of neutral oligosaccharides by matrix-assisted laser desorption ionization mass spectrometry. *Analytical Chemistry* 1991; **63**: 1463-1466.

106. Garozzo D, Spina E, Cozzolino R, Cescutti P, Fett WF. Studies on the primary structure of short polysaccharides using SEC MALDI mass spectroscopy. *Carbohydrate Research* 2000; **323**: 139-146.

107. Hsu N-Y, Yang W-B, Wong C-H, Lee Y-C, Lee RT, Wang Y-S, Chen C-H. Matrix-assisted laser desorption/ionization mass spectrometry of polysaccharides with 2',4',6'-trihydroxy-acetophenone as matrix. *Rapid Communications in Mass Spectrometry* 2007; **21**: 2137-2146.

108. Fukuyama Y, Kolender AA, Nishioka M, Nonami H, Matulewicz MC, Erra-Balsells R, Cerezo AS. Matrix-assisted ultraviolet laser desorption/ionization time-of-flight mass spectrometry of b-(1 -> 3), b-(1 -> 4)-xylans from Nothogenia fastigiata using nor-harmane as matrix. *Rapid Communications in Mass Spectrometry* 2005; **19**: 349-358.

Publications

R. Ullmer, A. Plematl and A. Rizzi *„Derivatization by 6-aminoquinolyl-N-hydroxy-succinimidyl carbamate for enhancing the ionization yield of small peptides and glycopeptides in matrix-assisted laser desorption/ionization and electrospray ionization mass spectrometry“*, Rapid Communications in Mass Spectrometry 2006; 20: 1469-1479

R. Ullmer, A. Rizzi *„Use of a novel ionic liquid matrix for MALDI-MS analysis of glycopeptides and glycans in total tryptic digests”*, submitted to Journal of Mass Spectrometry

I. Schnöll-Bitai, R. Ullmer, T. Hrebicek, A. Rizzi, I. Lacik „*Characterization of the molecular mass distribution of pullulans by matrix-assisted laser desorption/ionization time-of-flight mass spectrometry using 2,5-dihydroxybenzoic acid butylamine (DHBB) as liquid matrix”*, Rapid Communications in Mass Spectrometry 2008; 22: 2961-2970

RAPID COMMUNICATIONS IN MASS SPECTROMETRY
Rapid Commun. Mass Spectrom. 2006; **20**: 1469–1479
Published online in Wiley InterScience (www.interscience.wiley.com) DOI: 10.1002/rcm.2464

Derivatization by 6-aminoquinolyl-*N*-hydroxysuccinimidyl carbamate for enhancing the ionization yield of small peptides and glycopeptides in matrix-assisted laser desorption/ionization and electrospray ionization mass spectrometry

Roman Ullmer, Alexander Plematl and Andreas Rizzi*
Institute of Analytical Chemistry and Food Chemistry, University of Vienna, Währinger Strasse 38, A-1090 Vienna, Austria

Received 2 June 2005; Revised 3 March 2006; Accepted 4 March 2006

The characterization of glycosylation in proteins by mass spectrometry (MS) is often impeded by strong suppression of ionization of glycopeptides in the presence of non-glycosylated peptides. Glycopeptides with a large carbohydrate part and a short peptide backbone are particularly affected by this problem. To meet the goal of generating mass spectra exhibiting glycopeptide coverages as complete as possible, derivatization of glycopeptides offers a practical way to increase their ionization yield. This paper investigated derivatization with 6-aminoquinolyl-*N*-hydroxysuccinimidyl carbamate (AQC) which is a rapid labeling technique commonly used for fluorescence detection in high-performance liquid chromatography (HPLC) and capillary electrophoresis (CE). As test samples we used peptides and glycopeptides obtained by enzymatic digestion of three different glycoproteins, i.e., human antithrombin, chicken ovalbumin, and bovine α1-acid-glycoprotein. It was found that AQC derivatization resulted in strongly increased signal intensities when analyzing small peptides and glycopeptides by matrix-assisted laser desorption/ionization (MALDI)-MS. For these compounds the limit of detection could be reduced to low fmol amounts. Without derivatization only glycopeptides containing large peptide backbones were detected by MALDI-MS. This effect was even significant when glycopeptides were pre-separated and enriched by means of lectin affinity chromatography before MALDI-MS analysis and when using electrospray ionization (ESI). This labeling method, applied in combination with MS detection for the first time, was found to be well suited for the enhancement of detection sensitivity for small glycopeptides in MALDI-MS analysis and thus for reducing the need for pre-separation steps. Copyright © 2006 John Wiley & Sons, Ltd.

The detailed characterization of glycosylation in glycoproteins can still be analytically challenging, especially if a high number of glycoforms are present in one specific sample. The simultaneous presence of many glycan variants leads to complex spectra, and strongly different abundances of these variants increase the risk of missing low-abundance glycoforms. Particularly with therapeutically used, e.g. recombinant, glycoproteins, a detailed characterization of the iso- and glycoforms present in a drug is an essential requirement today and will be even more so in the future. Mass spectrometry (MS) obviously plays the major role in the context of these types of analysis. Glycoprotein analysis, particularly the determination of the number of post-translational modifications (PTMs), can be conducted on the basis of intact glycoprotein isoforms when coupling electrospray ionization (ESI)-MS to high-performance separation methods, e.g., high-performance liquid chromatography (HPLC) or high-performance capillary zone electrophoresis (CZE),[1–3] as recently reviewed by Hernández-Borges *et al*.[4] The mass accuracy and resolution attained with matrix-assisted laser desorption/ionization (MALDI)-MS for large glycoproteins, in contrast, are rarely sufficient to distinguish between different iso- and glycoforms present. High-resolution mass analyzers combined with ESI, e.g., ESI time-of-flight (TOF)-MS, were able to differentiate a large number of glyco- and isoforms present in recombinant human erythropoietin (EPO).[5] However, the detailed analysis of the site-specific positioning and variability in the glycan structures can be rarely done on the basis of the integral glycoprotein. Site-specific data are mainly gathered by analyzing glycopeptides gained by enzymatic digestion

**Correspondence to*: A. Rizzi, Institute of Analytical Chemistry and Food Chemistry, University of Vienna, Währinger Strasse 38, A-1090 Vienna, Austria.
E-mail: andreas.rizzi@univie.ac.at
Contract/grant sponsor: Austrian Science Foundation; contract/grant number: P16414-N03.

Copyright © 2006 John Wiley & Sons, Ltd.

or controlled chemical degradation of the pre-separated or pre-purified glycoprotein.

The MS analysis of glycopeptides, especially when using MALDI-MS, is often impeded by failure to detect the smaller glycosylated peptides, particularly those with a short peptide backbone and large carbohydrate moiety. This failure is due to the strong ionization suppression of molecules in the presence of non-glycosylated peptides for which a high desorption and ionization yield is usually obtained. The detection of glycopeptides within a total enzymatic digest by MALDI-MS often remains incomplete. This effect is not only limited to MALDI-MS; an analogous failure can be observed upon direct infusion of enzymatically digested glycoproteins into ESI-MS instruments. It is frequently observed that the signal intensities are lower when the carbohydrate part of the molecule is larger in relation to the peptide backbone.

Two general strategies can be applied in order to make glycopeptide analysis more complete and thus more reliable. The first one involves a pre-separation of the glycopeptides from the digestion mixture by using either HPLC or CZE, and the second is based on a derivatization or modification step before MS analysis. This second approach is aimed at generation of mass spectra that contain the signals of all glycopeptides present in a protein digest above a certain minimum abundance. The derivatization procedures should be simple, fast and quantitative, as well as compatible with typical MALDI and ESI-MS requirements. Derivatization is, in this context, primarily intended to increase the ionization yield of analytes. For positive ion mode measurements, protonation is stabilized by labels containing basic groups. To a lesser extent the presence of an appropriate label might also influence the homogeneity of the embedding and co-crystallization of the analyte in the matrix. Finally, labels whose absorption maxima are near to the wavelength of the laser might also be directly involved in the energy uptake during the MALDI process.

Several derivatization strategies for proteins, peptides and glycopeptides have been introduced and evaluated in the past. In the case of glycopeptides, the derivatization step can be carried out either on the peptide backbone or on the glycan structure. Many different methods are available for amino acid derivatization. Reactive groups are the OH group in Ser, Thr and Tyr, the COOH group in Asp and Glu, the NH group in Lys, Arg and at the N-terminus, and the SH group in Cys; different reactions can be carried out for each of these reactive groups, as comprehensively reviewed by Halket and Zaikin.[6–9] Many of these derivatizations are primarily intended to attach a chromophore or fluorophore label. Some derivatization procedures, however, have been investigated for the enhancement of detection of peptides in MALDI-MS. Amongst these is the guanidination of lysine residues by *O*-methylisourea to form the more basic side chain of homoarginine.[10] Derivatization with labels containing a dansyl[11] or coumarin core[12,13] attached to the N-terminus was shown to improve the sensitivity for peptides having low ionization yields. Activated esters containing a fixed charge, *S*-pentafluorophenyl[tris(2,4,6-triethoxyphenyl)phosphonium]acetate bromide (TMPP-AcSC_6F_5 bromide), were used for N-terminal derivatization in order to increase signal intensities in MALDI-MS analysis.[14,15] Similarly, signal enhancement was observed by charge-localized derivatization with triphenylphosphonium.[16] A permanently cationic moiety (a quaternary ammonium group) was derived from the reaction of the N-terminus with iodomethane; the resulting signal intensities in MALDI-MS are increased by at least an order of magnitude.[17,18]

Several attempts have been made to derivatize oligosaccharides prior to MS.[19–23] Reductive amination and derivatization with 2-aminopyridine, as well as the formation of hydrazide derivatives, have been investigated. Some of the results represent enhancement of sensitivity between 1000- and 5000-fold over the native oligosaccharides. Permethylation and methyl esterification[24] of the terminal sialic acids, which are easily deprotonated to give rise to negative charges, were used to transform the glycan into a neutral oligosaccharide and to stabilize these groups. Terminal sialic acids can also be removed by enzymatic or soft chemical cleavage.

In this paper we evaluate a further labeling reagent, i.e., 6-aminoquinolyl-*N*-hydroxysuccinimidyl carbamate (AQC), for its potential to enhance the ionization yield of glycopeptides in MALDI-MS analysis. AQC is a fluorescent labeling reagent that preferentially binds to free amino groups forming stable asymmetric urea derivatives. This reagent is widely used for labeling amines, amino acids, peptides and proteins for fluorescence detection in HPLC and CZE,[25–33] since the derivatization step is very fast and simple. To avoid the derivatization of –SH groups in peptides and proteins it might be useful to reduce and alkylate the protein before adding the AQC reagent.

We investigated the benefit of the AQC derivatization for the detection of glycopeptides in an enzymatically digested mixture, giving special emphasis to MALDI-MS. We evaluated the improvement in ionization yields for small peptides carrying large glycans and for low-abundance glycoforms present in this mixture. In this regard we refer to the aspects of completeness and reliability of the analysis. The method was further characterized with respect to low-energy collision-induced dissociation (CID) experiments addressing (i) the stability of labeling and (ii) the prevalence of N-terminally charged fragments (a, b, c) vs. C-terminally charged ones (x, y, z). Finally, analogous ESI experiments were carried out to characterize the performance of the AQC-labeled peptides under the conditions of this alternative soft ionization method.

For this purpose we used mixtures of peptides and glycopeptides obtained by tryptic and chymotryptic digestion of three different glycoproteins: human antithrombin (AT), bovine α1-acid-glycoprotein (AGP) and chicken ovalbumin (OA). The various major- and minor-abundance glycopeptide variants occurring in human AT, and their site-specific occurrences, were known from previous work.[34–36] Bovine AGP contains bi- and triantennary complex type glycans with terminal *N*-acetyl- and *N*-glycolylneuraminic acids.[37–39] Chicken OA contains only one glycosylation site but exhibits a huge heterogeneity. Carbohydrates found in OA comprise a series of high mannose type as well as a number of hybrid and complex type glycans.[37,40]

Copyright © 2006 John Wiley & Sons, Ltd.

DOI: 10.1002/rcm

EXPERIMENTAL

Materials

Antithrombin (AT) derived from lyophilized human plasma, purified from a pool of human blood-donors,[41] was obtained from Octapharma Pharmazeutische Produktionsgesellschaft (Vienna, Austria). Ovalbumin (OA) from chicken egg and bovine α1-acid-glycoprotein (AGP) were purchased from Sigma-Aldrich (St. Louis, MO, USA). Trypsin and chymotrypsin (sequencing grade) were purchased from Roche Diagnostics (Basel, Switzerland). 2,4,6-Trihydroxyacetophenone monohydrate (THAP) (99.5%), α-methyl-D-mannopyranoside (99%) and diammonium hydrogen citrate (99%) were purchased from Fluka (Buchs, Switzerland). Concanavalin A, Sepharose 4B (mean bead size 90 μm, from *Canavalia ensiformis*, Jack Bean), dithiothreitol (DTT), iodoacetamide, tris(hydroxymethyl)aminomethane hydrochloride (TRIS), sodium citrate (99.9 %), trifluoroacetic acid (TFA) and the ProteoMass™ Peptide MALDI-MS calibration kit were obtained from Sigma-Aldrich; all chemicals were of p.a. grade. Guanidinium chloride (99.5%), 2-propanol, acetonitrile, ammonium acetate, NaCl, $CaCl_2$, $MnCl_2$ and $MgCl_2$ were obtained from Merck (Darmstadt, Germany), all of p.a. grade. The AccQ-Fluor™ reagent kit for AQC derivatization and the SEP-PAK® C18 cartridges for purification and solid-phase extraction (SPE) were provided by Waters (Milford, MA, USA). PD-10 desalting columns pre-packed with Sephadex G25 were purchased from Amersham Biosciences (Uppsala, Sweden). HPLC separation was performed using a monolithic Chromolith® CapROD® RP-18e column from VWR-Merck (Darmstadt, Germany) with an i.d. of 0.2 mm and a length of 150 mm. Water was of ultra-high quality prepared using an Elgastat UHQ apparatus (Elga LabWater, Siershahn, Germany).

Sample preparation

Tryptic and chymotryptic digestion

The pure glycoprotein (2.5 mg) was dissolved in 400 μL of denaturing buffer (6 M guanidinium chloride in 1 M TRIS adjusted to pH 8.5 with HCl). To reduce disulfide bonds 6.7 μL of 0.5 M DTT in water were added. The solution was incubated for 1.5 h at a temperature of 37°C and afterwards cooled down to room temperature. Alkylation was carried out by addition of 20 μL of 2 M iodoacetamide solution in denaturing buffer and incubation for 1 h in the dark. PD-10 size-exclusion columns were used to desalt the solution and remove excess reagent. The purified sample was eluted with 600 μL of water, and 67 μL of 0.5 M ammonium acetate buffer at pH 8.2 were added. Then, 25 μg trypsin were dissolved in this solution and digestion was carried out overnight at 37°C. The digested samples were lyophilized by vacuum centrifugation and stored at −20°C.

Digestion with chymotrypsin was carried out like the tryptic digestion but using 0.5 M ammonium acetate buffer at pH 7.8 containing 100 mM $CaCl_2$ and leaving the sample overnight at 25°C.

Pre-separation of the glycopeptides by lectin AFC

If the glycopeptides were pre-separated from the non-glycosylated peptides by means of lectin affinity chromatography (AFC), lyophilized samples were reconstituted with 200 μL of binding buffer.[42] Concanavalin A (Con A) immobilized on Sepharose was chosen as affinity ligand. Binding, washing, elution and column regeneration were performed as described previously.[42] After the separation the samples were purified by SPE in order to remove interfering eluent components.

Derivatization with AQC

The lyophilized sample (0.25 mg) was reconstituted in 60 μL of 20 mM HCl. After adding 180 μL of borate buffer (200 mM, pH 8.9) and 120 μL of AQC reagent (approx. 10 mM in acetonitrile), the mixture was allowed to incubate for 1 min at room temperature. Best results were achieved with a molar ratio of peptides to AQC 1:4. Afterwards the sample was heated for 10 min at 55°C in a water bath. Unwanted salts and buffer components were removed by SPE.

Purification by means of SPE

SPE cartridges (C18 material, 360 mg, pore size 125 Å) were washed with 8 mL of 0.1% TFA in 2-propanol (v/v) followed by 8 mL of 0.1% TFA in water for conditioning. The pressure was applied manually. After the sample had been added, salts and residual reagents were washed off with 4 mL of 0.1% TFA in water. To elute the peptides 4 mL of 75% organic modifier (0.1% TFA in 2-propanol) were added. Afterwards the samples were lyophilized and stored at −20°C.

HPLC/ESI-MS

ESI-MS^n experiments were performed using a Bruker Esquire 3000+ instrument equipped with a quadrupole ion trap (QIT) mass analyzer (Bruker Daltonik, Bremen, Germany). The system uses an orthogonal spray assembly. Nitrogen was used as nebulizing gas (12 psi) and as drying gas (9 L/min at 300°C). Helium served as cooling as well as collision gas for CID experiments at a pressure of about 1.2×10^{-5} mbar. The precursor ion selection width was typically set to 2 *m/z*. The spray voltage was 4000 V (potential between the grounded spray needle and the capillary entrance as cathode). The system was run in positive ion mode with a scan speed of 13 000 $m/z\ s^{-1}$ (MS and MS^n) from 200 to 2000 Da. Data acquisition and processing were managed by Esquire control 5.1 and Bruker Daltonics DataAnalysis 3.1 software. Measurements were accomplished in the MS^1 and MS^2 mode; mass spectra were typically obtained by averaging 10 to 20 unselected scans. Sample introduction was performed by on-line coupling of capillary HPLC to the mass spectrometer via an orthogonal atmospheric pressure ESI interface from Agilent (Waldbronn, Germany). The HPLC instrument consisted of a LC-10AD pump from Shimadzu (Kyoto, Japan) and a Cheminert C2 six-port valve injector from Valco (Houston, TX, USA). The flow was approximately 3 μL/min obtained by a flow splitter. Different mobile phase gradients were applied mixing eluents A (100 mM formic acid in water) and B (100 mM formic acid in acetonitrile).

MALDI-MS

MALDI-MS analysis was carried out using two different mass spectrometers, both obtained from Shimadzu

Copyright © 2006 John Wiley & Sons, Ltd.

DOI: 10.1002/rcm

RCM

Biotech–Kratos Analytical (Manchester, UK). The first instrument, AXIMA-LNR, was equipped with a linear flight tube, a pulsed nitrogen laser working at a wavelength of 337 nm and a pulse width (FWHM) of 4 ns, an integrated 1 GHz recorder and a monochrome CCD camera system for monitoring the sample spots. An accelerating voltage of 20 kV was applied, and molecular ion optimized delayed extraction was used. Data acquisition and processing were managed by Kratos software version 2.3.5. Typically, linear mode mass spectra were acquired by averaging 100–200 unselected single laser shots. Average m/z values were assigned by external mass calibration (using a mixture of bradykinin fragment 1-7, human angiotensin II, synthetic peptide $P_{14}R$, human ACTH fragment 18-39, bovine insulin oxidized chain B and bovine insulin).

MALDI multistage MS experiments with low-energy CID were performed using an AXIMA-QIT instrument consisting of a 3D QIT coupled to a double-stage gridless reflector time-of-flight (RTOF) analyzer. It is equipped with the same laser system as that described above, and uses an accelerating voltage of 4030 V. The ion trap is continuously flooded with helium at a pressure of $5–6 \times 10^{-5}$ mbar to allow cooling of the trapped ions by collision. In addition, a pulse of argon is injected into the QIT shortly before the ion introduction to enhance the cooling of the ions (referred to as 'ultracooling'). An additional argon pulse is applied with the radio frequency (rf)-induced excitation in order to enhance the fragmentation efficiency. Typically, CID spectra were acquired by averaging 2000–5000 unselected single laser shots using a precursor ion selection width of 1/70 or 1/250 of the precursor mass. Monoisotopic masses were assigned by external calibration applying a mixture of fullerenes obtained from Kratos Analytical.

The MALDI sample preparation was performed using standard stainless steel targets, applying the dried droplet technique.[43] A solution of 50 mg/mL diammonium hydrogen citrate in 0.1% TFA was mixed with the same volume of sample solution. A volume of 1.5 μL of this mixture was applied on the target, immediately followed by 1.5 μL of the matrix solution (25 mg/mL THAP in methanol). The droplet was dried at room temperature.

RESULTS AND DISCUSSION

Ionization yields for biomolecules in MALDI- and ESI-MS analysis are often influenced by the presence of concomitant components in the sample solution. The effect of AQC derivatization on ionization yield, charge state distribution, and CID fragmentation pattern was therefore investigated on the basis of two different sample types; the first one consists of a mixture of peptides and glycopeptides obtained directly by tryptic digestion of a selected glycoprotein after reduction and carbamidomethylation of the cysteins; the second type contains only glycopeptides pre-separated by lectin AFC.

Uniformity of AQC derivatization

AQC is reported to bind preferentially to free amino groups, i.e., to the ε-amino group of lysine and to the α-amino group of the N-terminal amino acid. There is a certain risk that the thiol groups of free cysteine residues also become derivatized; this was excluded by carbamidomethylation. On derivatization of a peptide mixture obtained by digestion with trypsin, the lysine-containing peptides will become doubly-labeled; peptides containing a missed lysine-cleavage site will be triply-labeled. Our results showed that, under the conditions chosen in this work, the derivatization with AQC was highly reproducible and complete, i.e., the peptides were not split into two species with different labeling extents. In all instances except some glycopeptides of AGP, only the species with the highest number of possible labels attached were found. Excess reagent interfered with neither the MALDI process nor the crystallization on the target if present in moderate quantity. However, it turned out to be essential to remove the borate reaction buffer after the derivatization step by reversed-phase SPE. It could be shown that the derivatization procedure did not affect the glycan moieties of glycopeptides, and did not cleave off the labile terminal sialic acid residues.

Enhancement of ionization yield of small peptides and glycopeptides in MALDI-MS

Antithrombin

AT contains four peptides carrying one N-linked glycan each, all of which are of complex type with terminal sialic acids.[34,36,42,44] From these glycopeptides only those with a large peptide backbone could be detected when no pre-separation and no derivatization took place; these are the peptides L_{92}-K_{107} (16 amino acids, glycosylated at N_{96}) and S_{151}-K_{169} (19 amino acids, glycosylated at N_{155}). The glycopeptides with a short peptide backbone, K_{133}-K_{136} (4 amino acids, glycosylated at N_{135}) and W_{189}-K_{193} (5 amino acids, glycosylated at N_{192}), could not be detected (Fig. 1(a) and Table 1).

In this paper all peptides will be abbreviated by their first amino acids in a single letter code plus their position number in the protein sequence, i.e., L_{92}, K_{133}, S_{151} and W_{189}. After derivatization the small glycopeptides K_{133} and W_{189} were found in the spectra as well, and showed signal intensities comparable to those of the larger ones (Fig. 1(b)). By chance, the signals of glycopeptide K_{133} (plus three attached AQC labels) and glycopeptide W_{189} (plus two attached labels) were coincident with an observed average molecular mass of 3179 Da. The corresponding theoretical average masses were 3177.06 and 3180.13 Da. The linear-TOF analyzer employed could not resolve this mass difference, but the identities of these glycopeptides were verified by the QIT-RTOF instrument providing much higher resolution (about 8000 FWHM) and by MS/MS analysis. The limit of detection for the small glycopeptides out of the total tryptic digest could be evaluated as approximately 500 fmol.

Signal enhancement upon derivatization was investigated in the positive ion mode as well as in the negative mode; however, this enhancement was seen exclusively in the positive ion mode. This was expected, as the heterocyclic quinoline ring introduced by the AQC label is assumed to stabilize the proton transfer because of its basicity. An analogous effect cannot be utilized in the negative ion mode.

When dealing with the entire peptide mixture, the ionization yield of the small, non-glycosylated peptides

Copyright © 2006 John Wiley & Sons, Ltd.

DOI: 10.1002/rcm

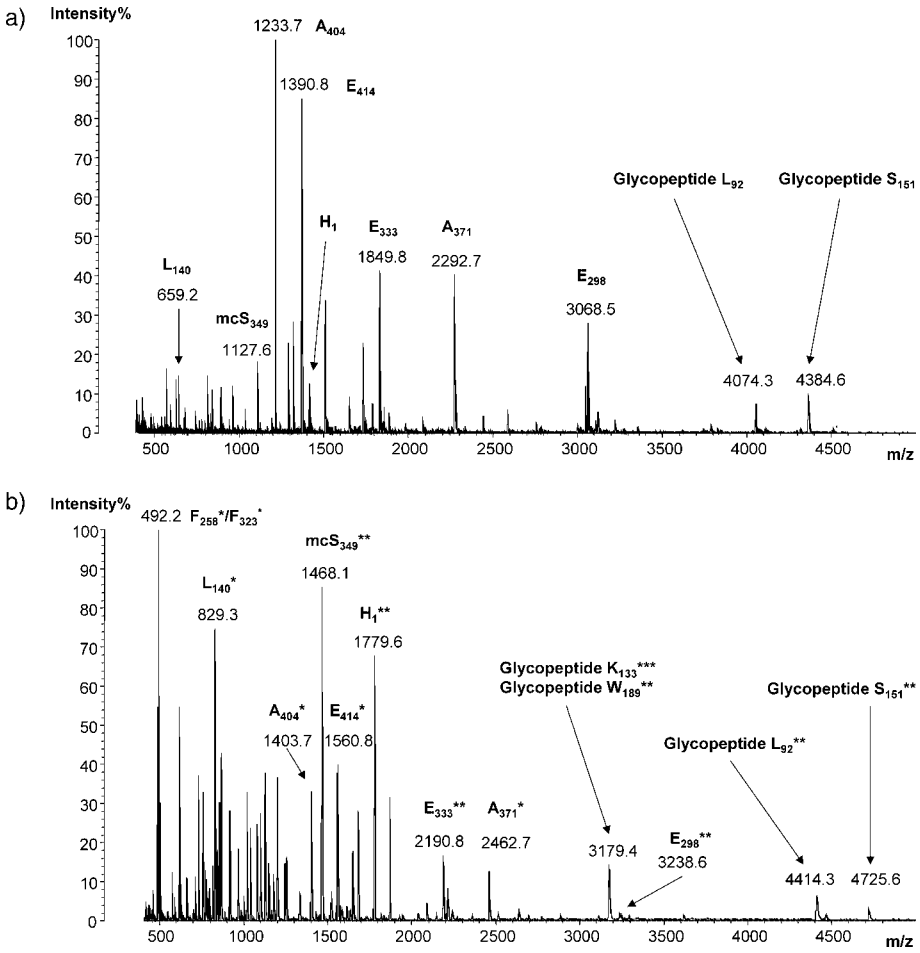

Figure 1. MALDI mass spectra of the total tryptic digest of human AT obtained using a linear TOF analyzer; without derivatization (a), and after AQC derivatization (b). Numerical values specify the average masses of the $[M+H]^+$ ions. The asterisk (*) symbolizes the number of attached AQC labels. Prominent peptide peaks are identified.

Table 1. Compilation of known glycopeptides of antithrombin and their appearance in MALDI-TOFMS spectra with and without derivatization. Triantennary structures present with very low abundances are not mentioned

		Total tryptic digest		AFC pre-separated tryptic digest	
Glycopeptide/amino acid sequence	Attached glycan structure	Not derivatized	Derivatized with AQC	Not derivatized	Derivatized with AQC
KANK		—	✓	—	✓
133-136		—	✓	—	✓
WVSNK		—	✓	—	✓
189-193		—	✓	—	✓
LGACNDTLQQLMEVFK		✓	✓	✓	✓
92-107		—	—	✓	✓
SLTFNETYQDISELVYGAK		✓	✓	✓	✓
		—	—	✓	✓
151-169		✓	—	✓	✓

Symbols: ○ hexose, □ HexNAc, ◇ sialic acid, ▼ desoxyhexose (fucose)

Copyright © 2006 John Wiley & Sons, Ltd.

DOI: 10.1002/rcm

was very low, and many of them could not be detected. A further problem in finding these low M_r peptides was the presence of peaks originating from matrix components. The most prominent peaks in the spectra originated from peptides with long backbones (Fig. 1(a)). After AQC derivatization the small peptides were measured with enhanced relative and absolute signal intensities, while those of the large peptides were reduced in relative but not absolute intensities (Fig. 1(b)). This complementary preference might be helpful, as the combination of the spectra with and without derivatization led to a peptide coverage of together 98%; only one expected peptide was not detected either with or without derivatization. A list of detected peptides, without and with AQC derivatization, is given in Table 2.

Table 2. Compilation of the tryptic peptides from antithrombin and their appearance in MALDI-TOFMS spectra with and without AQC derivatization (complete cleavage). Calculated *m/z* values are printed in normal type, experimental *m/z* values in bold type

		Theoretical average peptide masses				
			Sample derivatized with AQC			
			Number of attached labels			
Peptide/amino acid sequence	Modification	Sample without derivatization	Non-derivatized	1 AQC	2 AQC	3 AQC
K		147.2	147.2	317.4	**487.6**	
R		175.2	175.2	**345.4**		
SK		234.3	234.3	404.5	**574.7**	
SSK		321.4	321.4	491.6	**661.8**	
FR		322.4	322.4	**492.6**		
YR		338.4	338.4	**508.6**		
VEK		375.4	375.4	545.6	**715.8**	
SLAK		418.5	418.5	588.7	**758.9**	
ANSR		447.5	447.5	**617.7**		
LYR		**451.5**	451.5	**621.7**		
SPEK		460.5	460.5	630.7	**800.9**	
TEGR		462.5	462.5	**632.7**		
VTFK		**494.6**	494.6	664.8	**835.0**	
GLWK		**503.6**	503.6	673.8	**844.0**	
AAINK		**516.6**	516.6	686.8	**857.0**	
LN**C**R		**562.7**	562.7	**732.9**		
LFGDK		**579.7**	579.7	749.9	**920.1**	
LVSANR		**659.8**	659.8	**830.0**		
ELFYK		**699.8**	699.8	870.0	**1040.2**	
SLNPNR		**700.8**	700.8	**871.0**		
VWELSK		**761.9**	761.9	932.1	**1102.3**	
VANP**C**VK		**788.0**	788.0	**958.2**	**1128.4**	
IPEATNR		**800.9**	800.9	**971.1**		
ENAEQSR		**833.8**	833.8	**1004.0**		
FDTISEK		**839.9**	839.9	1010.1	**1180.3**	
FSPENTR		**850.9**	850.9	**1021.1**		
LQPLDFK		**861.0**	861.0	1031.2	**1201.4**	
IEDGFSLK		**909.0**	909.0	1079.2	**1249.4**	
LPGIVAEGR		**912.1**	912.1	**1082.3**		
ATEDEGSEQK		**1094.1**	1094.1	1264.3	**1434.5**	
ANRPFLVFIR		**1233.5**	1233.5	**1403.7**		
DDLYVSDAFHK		**1310.4**	1310.4	1480.6	**1650.8**	
TSDQIHFFFAK		**1341.5**	1341.5	1511.7	**1681.9**	
EVPLNTIIFMGR		**1390.7**	1390.7	**1560.9**		
DIPMNPM**C**IYR		1410.7	1410.7	1580.9		
VAEGTQVLELPFK		**1431.7**	1431.7	1601.9	**1772.1**	
HGSPVDI**C**TAKPR		**1438.6**	1438.6	1608.8	**1779.0**	
FATTFYQHLADSK		**1529.7**	1529.7	1699.9	**1870.1**	
GDDITMVLILPKPEK		**1670.0**	1670.0	1840.2	2010.4	2180.5
ADGES**C**SASMMYQEGK		**1751.9**	1751.9	1922.1	**2092.3**	
EQLQDMGLVDLFSPEK		**1850.1**	1850.1	2020.3	**2190.5**	
AFLEVNEEGSEAAASTAVVI AGR		**2292.5**	2292.5	**2462.7**		
NDNDNIFLSPLSISTAFAMT K		**2300.6**	2300.6	2470.8	**2641.0**	
KA**N**K	N-glycan 135	2665.3	2666.6	2836.8	3007.0	**3177.1**
ITDVIPSEAINELTVLVLVNTIYFK		**2806.3**	2806.3	2976.5	3146.7	
WVS**N**K	N-glycan 192	2838.5	2839.7	3009.9	**3180.1**	
ELTPEVLQEWLDELEEMMLVVHMPR		**3068.6**	3068.6	**3238.8**		
LGA**CN**DTLQQLMEVFK	N-glycan 96	**4072.9**	4074.2	4244.4	**4414.6**	
SLTF**N**ETYQDISELVYGAK	N-glycan 155	**4384.2**	4385.4	4555.6	**4725.8**	

Copyright © 2006 John Wiley & Sons, Ltd.

DOI: 10.1002/rcm

Glycopeptide mixture obtained from AT after pre-enrichment by AFC

Pre-separation and enrichment of glycopeptides by lectin AFC generally led to higher absolute signal intensities of the glycopeptides, allowing detection of even minor populated isoforms of the large glycopeptides, i.e., the fucosylated and the mono-sialo forms. The AQC derivatization resulted in a further significant increase in signal intensities, allowing observation of also the mono-sialo forms of the small glycopeptides; Table 1 summarizes these results. After derivatization the limit of detection for the two small peptides could be evaluated as approximately 50 fmol. It is important with respect to the reliability of glycosylation analysis that, even in AFC pre-separated and enriched samples, the non-derivatized glycopeptides with small peptide backbones could not be detected in MALDI-MS analysis. Derivatization turned out to be necessary in order not to miss these small glycopeptides. Alternatively, these small non-derivatized glycopeptides could be detected by MALDI-MS only after complete pre-separation from the larger glycopeptides, e.g., by reversed-phase HPLC (data not shown).

Ovalbumin

The glycans in OA attached to N_{292} show a high heterogeneity and belong to the hybrid and high mannose types.[37] The corresponding glycopeptides obtained by chymotryptic digestion could not be seen in the MALDI spectra (Fig. 2(a)).

After derivatization with AQC the glycopeptides could be detected out of the total chymotryptic digest (Fig. 2(b)). Both spectra shown in Fig. 2 were achieved with the same amount of analytes, i.e., approximately 6 pmol. The signals originating from the glycopeptides (shown in the inset in Fig. 2(b)) exhibit the typical mass differences of 162.1 and 203.2 Da corresponding to the molecular masses of single hexoses and *N*-acetylhexosamines, respectively.

α1-Acid-glycoprotein

Bovine AGP consists of three N-glycosylation sites with bi- and triantennary complex type structures containing *N*-acetylneuraminic acids (sialic acids) and/or *N*-glycolyl-neuraminic acids showing a typical mass difference of 16 Da.[37,39] Without derivatization two glycopeptides could be detected out of the total tryptic digest by MALDI-MS

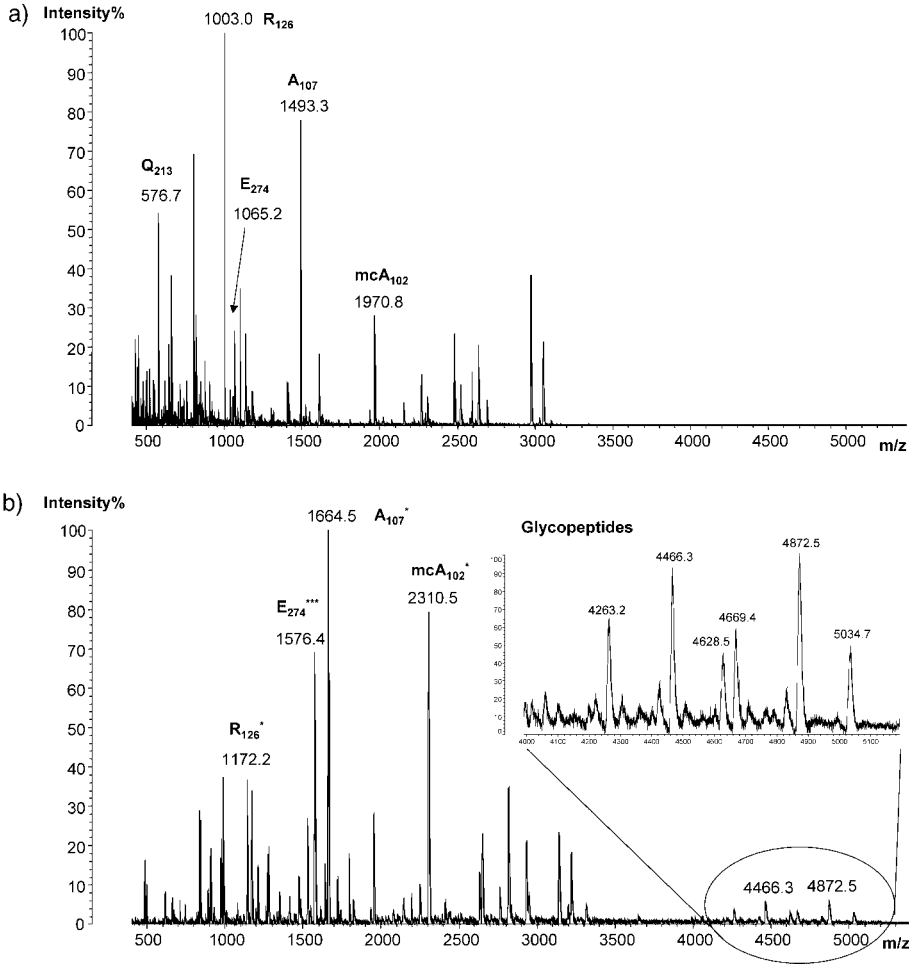

Figure 2. MALDI mass spectra of the total chymotryptic digest of chicken OA obtained using a linear TOF analyzer; without derivatization (a), and after AQC derivatization (b). The insert shows an expanded region for AQC-labeled glycopeptides of OA showing the typical mass differences of hexoses (162.1 Da) and *N*-acetylhexosamines (203.2 Da). Numerical values specify the average masses of the $[M+H]^+$ ions. The asterisk (*) symbolizes the number of attached AQC labels.

Copyright © 2006 John Wiley & Sons, Ltd.

DOI: 10.1002/rcm

RCM

measurements, i.e., glycopeptide C_{77} with 9 amino acids and T_{114} with 12 amino acids (Fig. 3(a)). Derivatization with AQC allowed detection of one additional glycopeptide, i.e., N_{39} with 6 amino acids (Fig. 3(b)). In this case the derivatization was not quantitative and the glycopeptides were split in two different signals, carrying one or two AQC labels. All non-glycosylated tryptic peptides could be detected both without and with label.

Stability of labeling in multistage MALDI-MS involving CID

Glycopeptides

Glycopeptide analysis was carried out also under conditions of multistage MS, using a hybrid instrument combining MALDI with a quadrupole ion trap (QIT) for the precursor ion selection and CID. When using this MALDI-QIT-RTOF instrument in the MS^1 mode (i.e., without precursor ion selection and CID) considerable metastable (post-source decay) fragmentation was observed. For glycopeptides with terminal sialic acids (SA) the complete depletion of these SA units as well as further partial fragmentation of the glycan were found already in these MS^1 spectra, as reported previously.[42] When choosing a metastable fragment ion (produced in the MS^1 mode) containing still the nearly complete glycan structure (but no SAs) as precursor ion, the MS^2 spectra exhibited almost all those fragments which sequentially differ just by one or two sugar units, as illustrated by Fig. 4. It was found that many fragments still carried the AQC label on the peptide when some or all of the saccharide units were cleaved off. Other fragments, however, had lost the label but not all of the saccharide units. These data indicate that, under the chosen experimental conditions, the binding of the label was approximately as stable as the glycosidic bonds between the sugar units and as the binding between asparagine and the first GlcNAc.

Figure 4 shows the MS^2 spectrum of the labeled glycopeptide W_{189} from AT, using an ion with nearly the

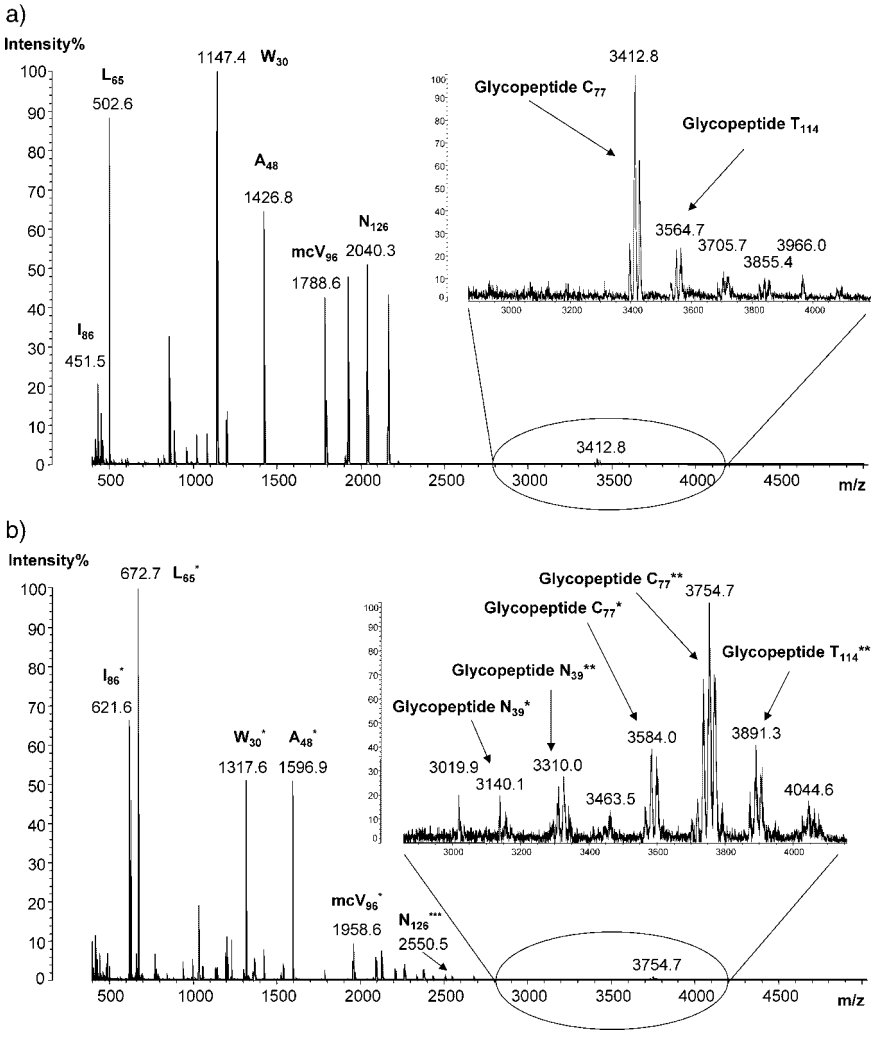

Figure 3. MALDI mass spectra of the total tryptic digest of bovine AGP obtained using a linear TOF analyzer; without derivatization (a), and after AQC derivatization (b). The inserts show the glycopeptides of AGP with the typical mass differences of 16 Da, the difference between *N*-acetylneuraminic acid (sialic acid) and *N*-glycolylneuraminic acid. Numerical values specify the average masses of the $[M+H]^+$ ions. The asterisk (*) symbolizes the number of attached AQC labels.

Copyright © 2006 John Wiley & Sons, Ltd.

DOI: 10.1002/rcm

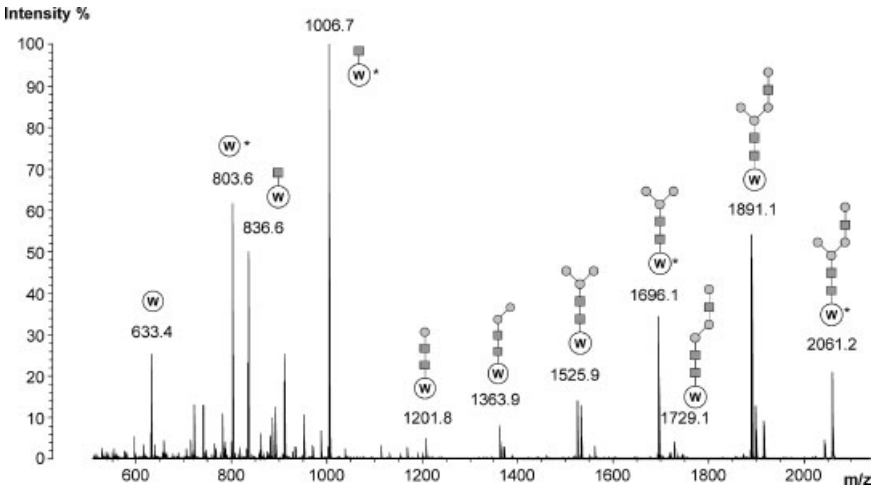

Figure 4. MS^2 spectrum of the AFC-enriched and AQC-derivatized glycopeptides of human AT obtained using a MALDI-QIT-MS instrument. The precursor ion was the singly protonated glycopeptide WVSNK+($GlcNAc_3Man_3Gal$)+1AQC with *m/z* 2061.2. Numerical values specify the monoisotopic masses for the $[M+H]^+$ ions. Symbols as in Table 1.

complete glycan structure attached as precursor. Typically, the signal corresponding to the peptide with the innermost GlcNAc with attached label was found as the most intense peak (in this case *m/z* 1006.7). Between this signal and that of the intact labeled peptide there was typically a series of intense peaks present which were derived from stepwise neutral losses of water and from ring fragmentations taking place in the N-linked GlcNAc moiety.[45] Although the AQC label is partially lost during this CID step it is worth mentioning that without previous derivatization the small glycopeptides were not detectable in the MS^1 mode even after AFC enrichment; the AQC label seemed to be necessary for the ionization of these glycopeptides.

Non-glycosylated peptides

On submitting non-glycosylated labeled peptides to MS experiments in the MALDI-QIT-RTOF instrument, an extensive but not complete depletion of the AQC label was observed already in the MS^1 mode as a consequence of metastable fragmentation. It seemed that the binding of the label was weaker than the peptide bonds. Choosing a non-glycosylated peptide with one label attached as precursor ion for CID in the MS^2 mode, the spectra exhibited one predominant signal representing the precursor ion minus the label. The other fragment ions (originating from peptide backbone fragmentation) were present with low intensities only. This peptide backbone fragment spectrum achieved from the labeled peptide was more or less identical to that gained from the non-labeled peptide (data not shown). It was not observed that the N-terminally attached label favors the presence of b-ions over that of y-ions.

All MALDI-MS investigations in this work were done with one type of matrix, i.e., a mixture of THAP and ammonium citrate applied in the dried-droplet technique as described in the Experimental section. This mixture was found to be useful for the analysis of glycopeptides with anionic glycans.[46] Whether similar results will be obtained when using other commonly employed matrices like 2,5-dihydroxybenzoic acid (DHB), 3,5-dimethoxy-4-hydroxycinnamic acid (sinapinic acid),[47,48] α-cyano-4-hydroxycinnamic acid (HCCA),[49,50] and particularly 3-hydroxy-2-pyridinecarboxylic acid (HPA)[51] and D-arabinosazone,[52,53] remains to be shown in a forthcoming work.

HPLC/ESI-QIT-MS experiments

Using HPLC/ESI-MS analysis, the suppression effects for small glycopeptides are generally not as problematic as in MALDI-MS analysis because of the pre-separation step.[36] The small glycopeptides of the test sample were easily detectable even without the AQC label, but with significantly lower signal intensities in comparison to the larger ones. However, after derivatization, these signals were increased by a factor of approximately 10, whereas the intensities of the large glycopeptides were not affected. Hence, the labeled glycopeptides occurred in the spectra with comparable signal intensities (data not shown). A further effect observed with AQC-derivatized peptides/glycopeptides in ESI-MS experiments was a slight shift within the charge state distribution to higher protonated species.

Looking at the results obtained by measurements of non-glycosylated peptides in the MS^2 mode, one could distinguish between peptides containing lysine and those with arginine at the C-terminus. Lysine-containing peptides were doubly-labeled and the MS^2 spectra were dominated by a peak corresponding to the unlabeled peptide (loss of two labels) and a signal representing the peptide with one attached AQC label (loss of one label). The spectra exhibited complete b- and y-series; some of the fragments still contained the attached AQC group, and some of them did not (see Fig. 5). Again, the labeling seemed to be as stable as the peptide bond in these low-energy CID experiments. The arginine-containing peptides were derivatized at the N-terminus only, and therefore the y-fragments lack the AQC group. The comparison between the MS^2 spectra of derivatized and non-derivatized peptides showed that the labeling did not significantly influence the relative intensities

Copyright © 2006 John Wiley & Sons, Ltd.

DOI: 10.1002/rcm

RCM

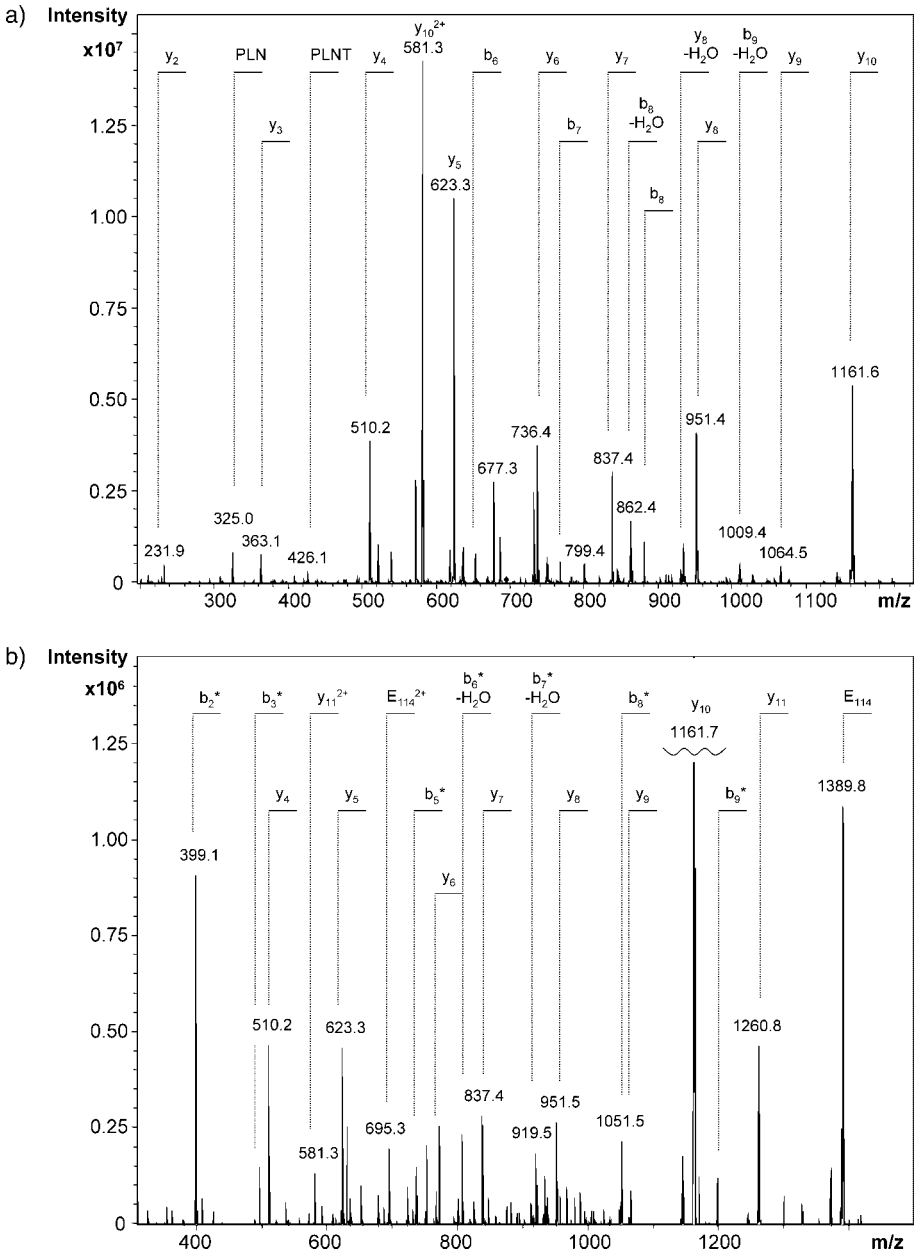

Figure 5. MS^2 spectra of the doubly protonated peptide E_{414} (EVPLNTIIFMGR) out of the total tryptic digest of human AT obtained by using an ESI-QIT-MS instrument; without derivatization, precursor ion *m/z* 695.3 (a), and plus one attached label, precursor ion *m/z* 780.4 (b). Numerical values specify the monoisotopic masses for the $[M+H]^+$ and $[M+2H]^{2+}$ ions, respectively. The intensity of the y_{10} ion is truncated in (b). The asterisk (*) symbolizes the number of attached AQC labels.

of the b- vs. the y-series ions. However, the labeling resulted in a shift within the b- and y-series; after derivatization the b-series ions occurred as shorter fragments (often the b_2+AQC ion as first fragment of the series), while the ions belonging to the y-series became larger on average.

CONCLUSIONS

The intention of this work was to evaluate the potential of a well-established fluorescent label (AQC) for the enhancement of the ionization yield in MALDI- and ESI-MS analysis. This derivatization strategy was particularly aimed at overcoming ionization suppression effects regarding small glycopeptides present in mixtures of glycosylated and non-glycosylated peptides as obtained by enzymatic digestion of glycoproteins.

This labeling method, here applied in combination with MS detection for the first time, led to a significant increase in signal intensities of the small glycopeptides in MALDI-MS analysis. The limit of detection for the small glycopeptides investigated could be reduced to low fmol quantities. The benefit of this procedure was thus an increase in detection sensitivity, the finding of more and even low-abundant glycoforms and higher sequence coverages, as could be demonstrated by the examples of three glycoproteins, i.e., AT, OA and AGP.

Copyright © 2006 John Wiley & Sons, Ltd.

DOI: 10.1002/rcm

The influence of the AQC label on the fragmentation pattern in low-energy CID of peptides was found to be not very significant. For peptides singly-labeled at the N-terminus it was not possible to observe any decisive shift in the intensities of b-ions vs. y-ions; the presence of such a shift would have opened a potential to identify ions belonging to a particular series. With glycopeptides the AQC label was found to be still present in most of the fragments having lost already parts of their glycans. Fragment ions obtained by peptide backbone fragmentation have commonly lost all their labels. The binding strength of the labels is thus assumed to range near to that of the glycosidic linkages.

In the context of MALDI-MS, the main benefit of this AQC-labeling procedure can thus be seen in the enhanced ionization yield that is particularly valuable in the context of glycopeptide analysis. The increased ionization yield might be in many cases the prerequisite for enabling MALDI-MS^n analyses of otherwise ionization-suppressed analytes.

In the corresponding ESI-MS experiments the signal intensities of small glycopeptides were also found to be increased when using this labeling procedure, and a shift to higher protonated species was observed. Again, the relative signal intensities of the b- vs. y-series in multistage MS experiments were hardly influenced by AQC derivatization. In most of the mentioned aspects MALDI and ESI data turned out to be widely corresponding.

Acknowledgements

The authors thank Octapharma Pharmazeutische Produktionsgesellschaft (Vienna, Austria) for generously providing the highly purified human antithrombin. Financial support was given by the Austrian Science Foundation (grant P16414-N03).

REFERENCES

1. Bateman KP, White RL, Yaguchi M, Thibault P. *J. Chromatogr. A* 1998; **794**: 327.
2. Lai CC, Her GR. *Rapid Commun. Mass Spectrom*. 2000; **14**: 2012.
3. Zamfir A, Peter-Katalinic J. *Electrophoresis* 2001; **22**: 2448.
4. Hernández-Borges J, Neusüß C, Cifuentes A, Pelzing M. *Electrophoresis* 2004; **25**: 2257.
5. Neusüß C, Demelbauer U, Pelzing M. *Electrophoresis* 2005; **26**: 1442.
6. Halket JM, Zaikin VG. *Eur. J. Mass Spectrom*. 2003; **9**: 1.
7. Zaikin VG, Halket JM. *Eur. J. Mass Spectrom*. 2003; **9**: 421.
8. Halket JM, Zaikin VG. *Eur. J. Mass Spectrom*. 2004; **10**: 1.
9. Zaikin VG, Halket JM. *Eur. J. Mass Spectrom*. 2004; **10**: 555.
10. Krause E, Wenschuh H, Jungblut PR. *Anal. Chem*. 1999; **71**: 4160.
11. Park S-J, Song J-S, Kim H-J. *Rapid Commun. Mass Spectrom*. 2005; **19**: 3089.
12. Pashkova A, Moskovets E, Karger BL. *Anal. Chem*. 2004; **76**: 4550.
13. Deng H-M, Zhang Z-Y, Deng Q-Y, Zhao S-K. *Zhipu Xuebao* 2004; **25**: 145.
14. Huang Z-H, Wu J, Roth KDW, Yang Y, Gage DA, Watson JT. *Anal. Chem*. 1997; **69**: 137.
15. Strahler JR, Smelyanskiy Y, Lavine G, Allison J. *Int. J. Mass Spectrom. Ion Processes* 1997; **169/170**: 111.
16. Liao P-C, Allison J. *J. Mass Spectrom*. 1995; **30**: 511.
17. Stewart NA, Pham VT, Choma CT, Kaplan H. *Rapid Commun. Mass Spectrom*. 2002; **16**: 1448.
18. Spengler B, Luetzenkirchen F, Metzger S, Chaurand P, Kaufmann R, Jeffery W, Bartlet-Jones M, Pappin DJC. *Int. J. Mass Spectrom. Ion Processes* 1997; **169/170**: 127.
19. Poulter L, Burlingame AL. *Methods Enzymol*. 1990; **193**: 661.
20. Yoshino K, Takao T, Murata H, Shimonishi Y. *Anal. Chem*. 1995; **67**: 4028.
21. Okamoto M, Takahashi K, Doi T, Takimoto Y. *Anal. Chem*. 1997; **69**: 2919.
22. Shinohara Y, Furukawa J, Niikura K, Miura N, Nishimura S. *Anal. Chem*. 2004; **76**: 6989.
23. Mechref Y, Novotny MV. *Chem. Rev*. 2002; **102**: 321.
24. Powell AK, Harvey DJ. *Rapid Commun. Mass Spectrom*. 1996; **10**: 1027.
25. Cohen SA, Michaud DP. *Anal. Biochem*. 1993; **211**: 279.
26. De Antonis KM, Brown PR, Cohen SA. *Anal. Biochem*. 1994; **223**: 191.
27. Cladrowa-Runge S, Rizzi A. *J. Chromatogr. A* 1997; **759**: 167.
28. Shindo N, Nojima S, Fujimura T, Taka H, Mineki R, Murayama K. *Anal. Biochem*. 1997; **249**: 79.
29. Liu H, Sanuda-Pena MC, Harvey-White JD, Kalra S, Cohen SA. *J. Chromatogr. A* 1998; **828**: 383.
30. Liu H, Cho B-Y, Strong R, Krull IS, Cohen S, Chan KC, Issaq HJ. *Anal. Chim. Acta* 1999; **400**: 181.
31. Strong RA, Liu H, Krull IS, Cho B-Y, Cohen SA. *J. Liquid Chromatogr. Relat. Technol*. 2000; **23**: 1775.
32. Uchikoba T, Fukumoto S, Itakura T, Okubo M, Tomokiyo K, Arima K, Yonezawa H. *Biosci. Biotechnol. Biochem*. 2004; **68**: 222.
33. Liu H, Cho BY, Krull IS, Cohen SA. *J. Chromatogr. A* 2001; **927**: 77.
34. Franzen LE, Svensson S, Larm O. *J. Biol. Chem*. 1980; **255**: 5090.
35. Demelbauer UM, Plematl A, Kremser L, Allmaier G, Josic D, Rizzi A. *Electrophoresis* 2004; **25**: 2026.
36. Demelbauer UM, Plematl A, Josic D, Allmaier G, Rizzi A. *J. Chromatogr. A* 2005; **1080**: 15.
37. Kuster B, Wheeler SF, Hunter AP, Dwek RA, Harvey DJ. *Anal. Biochem*. 1997; **250**: 82.
38. Nashabeh W, El Rassi Z. *J. Chromatogr*. 1991; **536**: 31.
39. Hunter AP, Games DE. *Rapid Commun. Mass Spectrom*. 1995; **9**: 42.
40. Yet MG, Chin CCQ, Wold F. *J. Biol. Chem*. 1988; **263**: 111.
41. Buchacher A, Schulz P, Choromanski J, Schwinn H, Josic D. *J. Chromatogr. A* 1998; **802**: 355.
42. Demelbauer UM, Zehl M, Plematl A, Allmaier G, Rizzi A. *Rapid Commun. Mass Spectrom*. 2004; **18**: 1575.
43. Karas M, Hillenkamp F. *Anal. Chem*. 1988; **60**: 2299.
44. Plematl A, Demelbauer UM, Josic D, Rizzi A. *Proteomics* 2005; **5**: 4025.
45. Wuhrer M, Hokke CH, Deelder AM. *Rapid Commun. Mass Spectrom*. 2004; **18**: 1741.
46. Papac DI, Wong A, Jones AJS. *Anal. Chem*. 1996; **68**: 3215.
47. Strupat K, Karas M, Hillenkamp F. *Int. J. Mass Spectrom. Ion Processes* 1991; **111**: 89.
48. Beavis RC, Chait BT. *Rapid Commun. Mass Spectrom*. 1989; **3**: 432.
49. Beavis RC, Chaudhary T, Chait BT. *Org. Mass Spectrom*. 1992; **27**: 156.
50. Kussmann M, Nordhoff E, Rahbek-Nielsen H, Haebel S, Rossel-Larsen M, Jakobsen L, Gobom J, Mirgorodskaya E, Kroll-Kristensen A, Palm L, Roepstorff P. *J. Mass Spectrom*. 1997; **32**: 593.
51. Stahl B, Steup M, Karas M, Hillenkamp F. *Anal. Chem*. 1991; **63**: 1463.
52. Chen P, Baker AG, Novotny MV. *Anal. Biochem*. 1997; **244**: 144.
53. Wheeler SF, Harvey DJ. *Anal. Chem*. 2000; **72**: 5027.

Copyright © 2006 John Wiley & Sons, Ltd.

DOI: 10.1002/rcm

Use of a novel ionic liquid matrix for MALDI-MS analysis of glycopeptides and glycans in total tryptic digests

Roman Ullmer and Andreas Rizzi*

Institute of Analytical Chemistry and Food Chemistry, University of Vienna, Austria
Währinger Straße 38, A-1090 Vienna, Austria

key-words:
MALDI-MS, ionic liquid matrix, glycopeptides, glycans

**Correspondence to*:
A. Rizzi, Institute of Analytical Chemistry and Food Chemistry, University of Vienna, Währinger Straße 38, A-1090 Vienna, Austria
E-mail: andreas.rizzi@univie.ac.at

ABSTRACT

In this work we investigated a novel ionic liquid matrix (ILM), namely the 1,1,3,3-tetramethylguanidinium (TMG) salt of 2,4,6-trihydroxyacetophenone (THAP). This matrix (GTHAP) turned out to be well suited for the matrix-assisted laser desorption/ionization mass spectrometry (MALDI-MS) analysis of glycopeptides and glycans and overcomes the well-known suppression of ionization of carbohydrate structures in the presence of peptides. The matrix was evaluated by two different series of experiments and compared to crystalline matrix THAP. First we measured mass spectra of the unseparated tryptic digest of three glycoproteins. Particularly those glycopeptides containing short backbones but large carbohydrate moieties did not appear in the THAP spectra but gave high signal intensities with the ILM. Secondly the total tryptic digests were treated with endoglycosidase PNGase F. When measured with solid matrix THAP the cleaved glycans were suppressed in the MALDI process, exclusively signals of peptides could be achieved. In case of the GTHAP matrix it was possible to detect the glycans with high intensities in presence of the tryptic peptides.

INTRODUCTION

Ionic liquids (ILs) are salts melting at temperatures below 100°C, they exhibit low vapor pressure and the ability to dissolve a wide range of analytes. Therefore, they have been utilized in a number of analytical techniques, for instance gas chromatography (GC)[1] and capillary electrophoresis (CE)[2]. Armstrong and co-workers applied ionic liquids as matrices in matrix-assisted laser desorption/ionization mass spectrometry (MALDI-MS) by combining a variety of cations based on amine structures and the commonly used matrix substances sinapinic acid (SA) and α-cyano-4-hydroxycinnamic acid (CHCA)[3]. Since then these ionic liquid matrices (ILMs) are used in MALDI-MS of biomolecules and synthetic polymers[4]. In comparison to classical crystalline matrices they exhibit one striking advantage: The viscous liquid surface is highly homogeneous and does not tend to build hot spots. The range of the signal intensities between different areas of the spot is very narrow (shot-to-shot reproducibility) and, therefore, the number of spectra to be averaged can be reduced[3,5]. This fact could also enhance the application of MALDI-MS for quantitative analysis[6,7]. Many research groups have investigated ILMs for different kinds of analytes, including proteins, peptides, carbohydrates, polynucleotides[7,8], phospholipids[9], glycolipids[5], polyethyleneglycol (PEG)[3,5] and heavy oil fractions (asphaltenes)[10]. It was shown that the use of pyridinium CHCA can lead to a higher sequence coverage in peptide mass fingerprint experiments[11]. The analysis of proteins by using ILMs, however, seems to be impeded by the fact that proteins tend to form undefined multiple adducts with the cations or anions of the matrix. This phenomenon leads to peak broadening and to a decrease in the accuracy of mass determination, as well as to a decrease in sensitivity[3,12]. The combination of 2,5-dihydroxybezoic acid with butylamine (DHBB) turned out to be well suited for the analysis of (sulfated) oligosaccharides and glycolipids[5,13]. The same ILM was used for the determination of the molecular mass distribution of polysaccharides (pullulans), which are used as calibration standards in aqueous size-exclusion chromatography[14]. Although these carbohydrates are prone to easy fragmentation during the MALDI process, accurate mass distribution and polydispersity data could be assessed.
Recently, Laremore et al. introduced a new cation, 1,1,3,3-tetramethylguanidinium (TMG), in combination with the commonly used matrix α-cyano-4-hydroxycinnamic acid (CHCA) in a molar ration of 2:1 (G_2CHCA) for the analysis of sulfated oligosaccharides[15]. The resulting mass spectra show very low extent of in-source fragmentation by loss of SO_3.

Fukuyama et al. combined TMG with *p*-coumaric acid (G_3CA) and used this matrix for the analysis of sialylated, sulfated and neutral carbohydrates and glycopeptides[16].

In this work we investigated the 1,1,3,3-tetramethylguanidinium (TMG) salt of 2,4,6-trihydroxyacetophenone (THAP) as a new ionic liquid matrix and evaluated the advantages of this matrix (GTHAP) by two different experiments: In the first one we generated spectra of total tryptic digests of standard glycoproteins and compared the solid matrix THAP and the ionic liquid matrix GTHAP with respect to the ionization yield of the glycopeptides. In the second one we cleaved the *N*-glycans on the glycopeptide level by means of PNGase F and measured the unseparated mixture of peptides and oligosaccharides. In both cases significantly improved signal intensities of the carbohydrate containing analytes could be achieved when using the GTHAP matrix.

EXPERIMENTAL

Materials

Bovine fetuin (FET) and bovine α1-acid-glycoprotein (AGP) were obtained from Sigma-Aldrich (St. Louis, MO, USA), human antithrombin (AT) from Octapharma Pharmazeutische Produktionsgesellschaft (Vienna, Austria). PNGase F (recombinant from *Flavobacterium meningosepticum*) was purchased from Roche Diagnostics (Basel, Switzerland). Guanidinium chloride and ammonium acetate were obtained from Merck (Darmstadt, Germany), trypsin (modified, sequencing grade), 2,4,6-trihydroxyacetophenone (THAP), 1,1,3,3-tetramethylguanidine (TMG), di-ammonium hydrogen citrate, trifluoroacetic acid (TFA), dithiothreitol (DTT), iodoacetamide, tris-(hydroxymethyl)-aminomethan hydrochloride (TRIS), methanol and LC-MS grade water from Sigma-Aldrich (St. Louis, MO, USA). PD-10 desalting columns pre-packed with Sephadex G25 were purchased from GE Healthcare (Uppsala, Sweden).

Preparation of the ionic liquid matrix

To a 150 mM solution of THAP in methanol an equimolar amount of TMG was added and shaken at room temperature for 1 min. Methanol was removed in a vacuum evaporator. Subsequently, the viscous 1,1,3,3-tetramethylguanidinium 2,4,6-trihydroxyacetophenone (GTHAP) was redissolved in methanol to a concentration of 100 mg/mL. The ionic liquid matrix was prepared freshly and used within several hours.

Sample preparation

2.5 mg of glycoprotein were dissolved in 400 µL of denaturing buffer (6 M guanidinium chloride in 500 mM TRIS-HCl, pH 8.5). 6.7 µL of 500 mM DTT in water were added and the solution was incubated for 1 hour at 37°C. Alkylation was carried out by addition of 20 µL of 2 M iodoacetamide in denaturing buffer and incubation for 1 hour in the dark. Excess reagent was removed by PD-10 size-exclusion columns. The sample was eluted with pure water. After addition of 67 µL 500 mM ammonium acetate buffer at pH 8.2 and 20 µg trypsin the digestion was carried out overnight at 37°C. Afterwards the sample was evaporated in a speed-vac and stored at –25°C.

The release of the N-glycans was done with PNGase F. The enzyme was purified by PD-10 size-exclusion to remove the interfering salts and buffers, evaporated in a speed-vac and dissolved in 100 mM ammonium acetate pH 7.4 (1U/µL). 2 µL of the enzyme solution were added to 10 µL of the tryptic digest (100pmol/µL pure water) and left at 37°C for 4 hours.

MALDI-QIT-RTOFMS

The matrices were applied using the dried droplet technique: The ionic liquid matrix GTHAP (100 mg/mL in methanol) was deposited on a standard stainless steel MALDI target and mixed with the same volume of aqueous sample solution (10 pmol/µL). The solid matrix 2,4,6-trihydroxyacetophenone (THAP) was applied as follows: 0.5 µL of di-ammonium hydrogen citrate (50 mg/mL in 0.1% TFA in water), 0.5 µL of the sample solution and 1 µL of the matrix solution (25 mg/mL THAP in methanol) were deposited on the target and dried at room temperature.

MALDI-MS and MALDI-MS/MS experiments with low-energy CID were performed on an AXIMA-QIT instrument (Shimadzu Biotech - Kratos Analytical, Manchester, UK) consisting of a 3D quadrupole ion trap followed by a reflector TOF mass analyzer. It was equipped with a pulsed nitrogen laser working at a wavelength of 337 nm and a pulse width of 4 ns. The ion trap was continuously flooded with helium at a pressure of 5 – 6 x 10^{-5} mbar to allow cooling of the trapped ions by collision. Typically, spectra were acquired by averaging 200-500 unselected single laser shots in the positive ion mode. External calibration was done with a mixture of fullerenes obtained from Kratos Analytical. Data acquisition and processing were managed by Kratos software version 2.7.2.

RESULTS AND DISCUSSION

Ionic liquid matrix GTHAP

GTHAP is a yellow viscous liquid made of equimolar amounts of 1,1,3,3-tetramethylguanidine (TMG) and 2,4,6-trihydroxyacetophenone (THAP). It is soluble in water, methanol, ethanol and acetonitrile (and some further solvents) and remains fluid in high vacuum. In a concentration of 100 mg/mL it forms a thin film on the MALDI stainless steel target after evaporation of the solvent.

The specific advantages of GTHAP for carbohydrate containing analytes was evaluated by means of three well-known glycoproteins, *i.e.,* bovine α1-acid-glycoprotein (AGP), bovine fetuin (FET) and human antithrombin (AT). Particularly, the enhancement of the ionization yield for these types of analytes was investigated in presence of non-glycosylated peptides. The performance in these respects was compared with that of the commonly used solid matrix THAP, which is known to be well suited for the analysis of glycopeptides[17]. In the first experiment we investigated signal intensities of glycopeptides in mixtures with non-glycosylated peptides, in a second experiment those of enzymatically cleaved glycans in the entire reaction mixture.

Glycopeptide analysis

Bovine α1-acid-glycoprotein (AGP) has five glycosylation sites with bi- and triantennary complex type glycans containing a varying number of terminal *N*-acetyl- and *N*-glycolyl-neuraminic acids, the majority of the oligosaccharides belonging to the biantennary type[18-20]. Two of the corresponding tryptic glycopeptides have rather short peptide backbones, namely six and seven amino acids, respectively. These small glycopeptides were not efficiently ionized and, thus, could not be seen in the positive ion spectra of the total tryptic digest when using the solid matrix THAP (Figure 1a). Three larger glycopeptides appear in the positive ion spectrum with high signal intensities, as expected. When analyzing the identical sample by using GTHAP, all five glycopeptides could be detected in their high abundant glycoforms out of the non-separated tryptic digest mixture (Figure 1b).

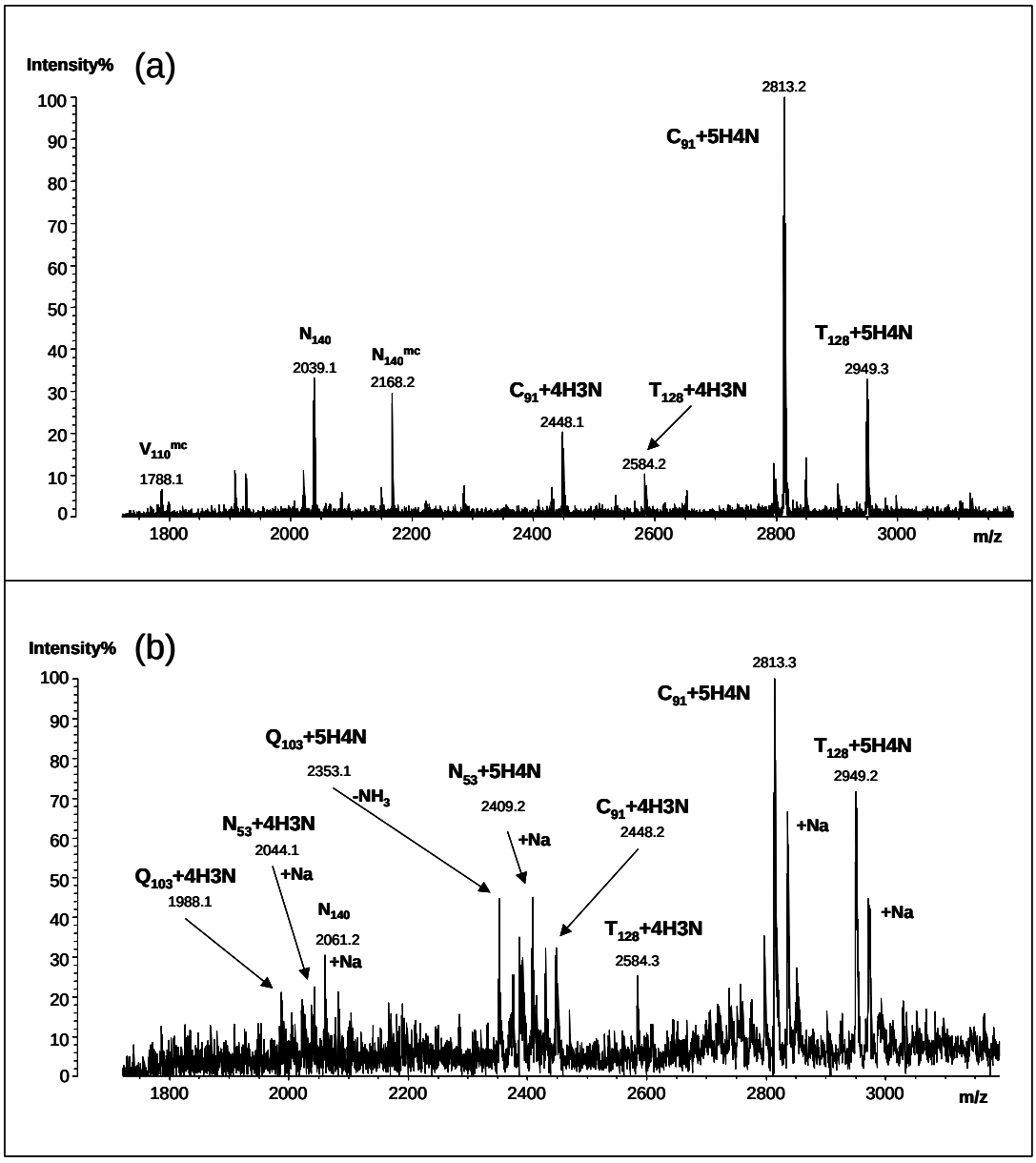

Figure 1: MALDI-QIT-RTOF mass spectra in the positive ion mode of a total tryptic digest of bovine AGP using (a) THAP as solid matrix, and (b) GTHAP as ionic liquid matrix. Numerical values specify the monoisotopic masses of the $[M+H]^+$ ions. Peptides are indicated by the one letter symbol and the sequence number of the first amino acid. mc, missed cleavage; H, hexose (Hex); N, N-acetyl-hexoseamine (HexNAc)

Astonishingly, in this spectrum almost exclusively glycopeptides were observed, non-glycosylated peptides were suppressed in contrast to all commonly used solid MALDI matrices. Low abundant triantennary glycoforms were not detected. However, two general drawbacks were observed: First, the signal-to-noise (S/N) ratio was decreased when using the ILM leading to a loss in sensitivity. The limit of detection (LOD) for glycopeptides was found to be in the high femtomole range. Secondly, oligosaccharide containing molecules tended to build sodium adducts in addition and competitive to protonation. Guanidinium adducts were not observed with peptides and glycopeptides, unlike to the situation with proteins. It turned out that the relative intensities of sodiated versus protonated species were dependent on the laser fluence. Measuring at the laser intensity threshold value led to a shift towards the protonated species. When using the MALDI-QIT-RTOF instrument, all glycopeptides were detected without the terminal *N*-acetyl- and *N*-glycolyl-neuraminic acids, even in the MS^1 mode and using positive ions. The loss of these moieties was found with all types of matrices, solid as well as ionic liquid. Moreover, with both matrices the loss of one hexose plus one *N*-acetyl-hexose could be observed for all glycopeptides to a small extent. These fragmentations are inherent to the MALDI-QIT instrument[21], in which metastable ions are trapped in a time range of milliseconds and in which labile linkages can be broken during the deceleration of fast ions in the ion trap (ion cooling). The extent of metastable ion formation in the ILM is obviously still high, although this phenomenon can be reduced to some extent by the choice of the matrix[16] and the cooling gas.

Human antithrombin (AT) possesses four glycosylation sites each of them exhibiting biantennary disialylated complex type glycans with only minor variability. Triantennary, monosialo and fucosylated glycoforms can be found to very small extents only[22-24]. The tryptic digest of antithrombin contains four peptides with *N*-linked glycans, two of them with short amino acid chains, *i.e.*, the peptide $K_{165\text{-}168}$ with four amino acids (containing one missed cleavage site near to the attached glycan) and the peptide $W_{221\text{-}225}$ with five amino acids. Both of them do not appear in the spectrum taken with the solid THAP matrix (Figure 2a), but are represented with high signals when using GTHAP as ILM (Figure 2b). Interestingly, the non-glycosylated peptides are not suppressed in this case, about the same number of signals assigned to peptides could be seen compared to the solid matrix. The lower extent of metastable ion fragmentation in the case of ILMs is demonstrated by the signals originating from peptide A_{403}.

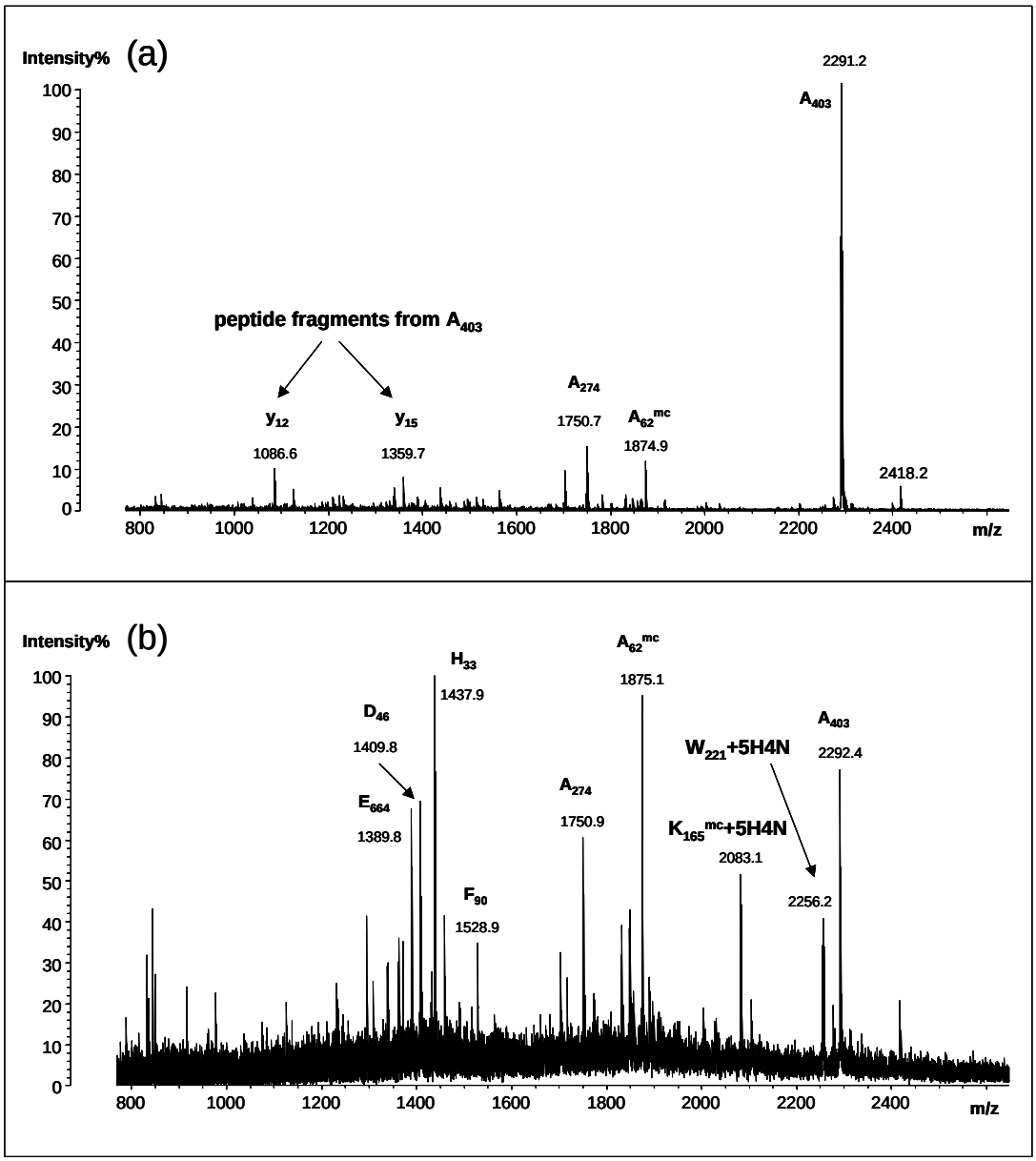

Figure 2: MALDI-QIT-rTOF mass spectra in the positive ion mode of a total tryptic digest of human AT using (a) solid matrix THAP, and (b) ionic liquid matrix GTHAP. Numerical values specify the monoisotopic masses of the $[M+H]^+$ ions. Peptides are indicated by the one letter symbol and the sequence number of the first amino acid. mc, missed cleavage; H, hexose (Hex); N, N-acetyl-hexoseamine (HexNAc)

When measured with the crystalline matrix, A_{403} showed a high ionization yield and two fragments of the y-series gave significant signals already in the MS^1 mode (Figure 2a). This metastable fragmentation leads to a more complex spectrum interpretation and might lead, in other cases, to the complete missing of the parent ion peak. This phenomenon could be widely eliminated by use of GTHAP, in this instance only intact peptides were detected. However, the cleavage of the terminal acidic sugar moieties (sialic acids) still took place in all cases.

The three tryptic *N*-linked glycopeptides of bovine fetuin (FET) consist of rather large amino acid backbones and are therefore usually not suppressed in the MALDI process, the corresponding signals can be seen with both the solid THAP and the liquid GTHAP matrices. FET contains also three *O*-linked glycans with a GalGalNAc core and some heterogeneity in the terminal moieties, all of them linked to the same tryptic peptide[25]. Each of the resulting glycopeptides sums up to more than 6000 Da, they could be detected from solid as well as liquid matrices with the MALDI-QIT instrument (data not shown).

Glycan analysis

The second series of experiments addressed the detection of glycan structures after release from the glycopeptides by endoglycosidase PNGase F. The enzymatic reaction and the MALDI measurements were done in the unseparated total tryptic digest. Figure 3 shows spectra from tryptic digest of AGP after PNGase F treatment from solid (a) and liquid (b) matrix. In the spectrum generated from THAP (Figure 3a) no signal which derives from oligosaccharides can be seen besides the peptide signals. In contrast, when using GTHAP the signal corresponding to the sodium adduct of the biantennary glycan (without the terminal *N*-acetyl- and *N*-glycolyl-neuraminic acids) was the most intense peak in the spectrum. The signals of the peptides were decreased or completely missing. The identity of the glycan species was proved in the MS/MS mode by means of collision induced dissociation (CID) (Figure 4). Again, this MS/MS spectrum was generated out of the total mixture of peptides and glycans. It was not possible to detect minor abundant triantennary glycan structures in the APG sample.

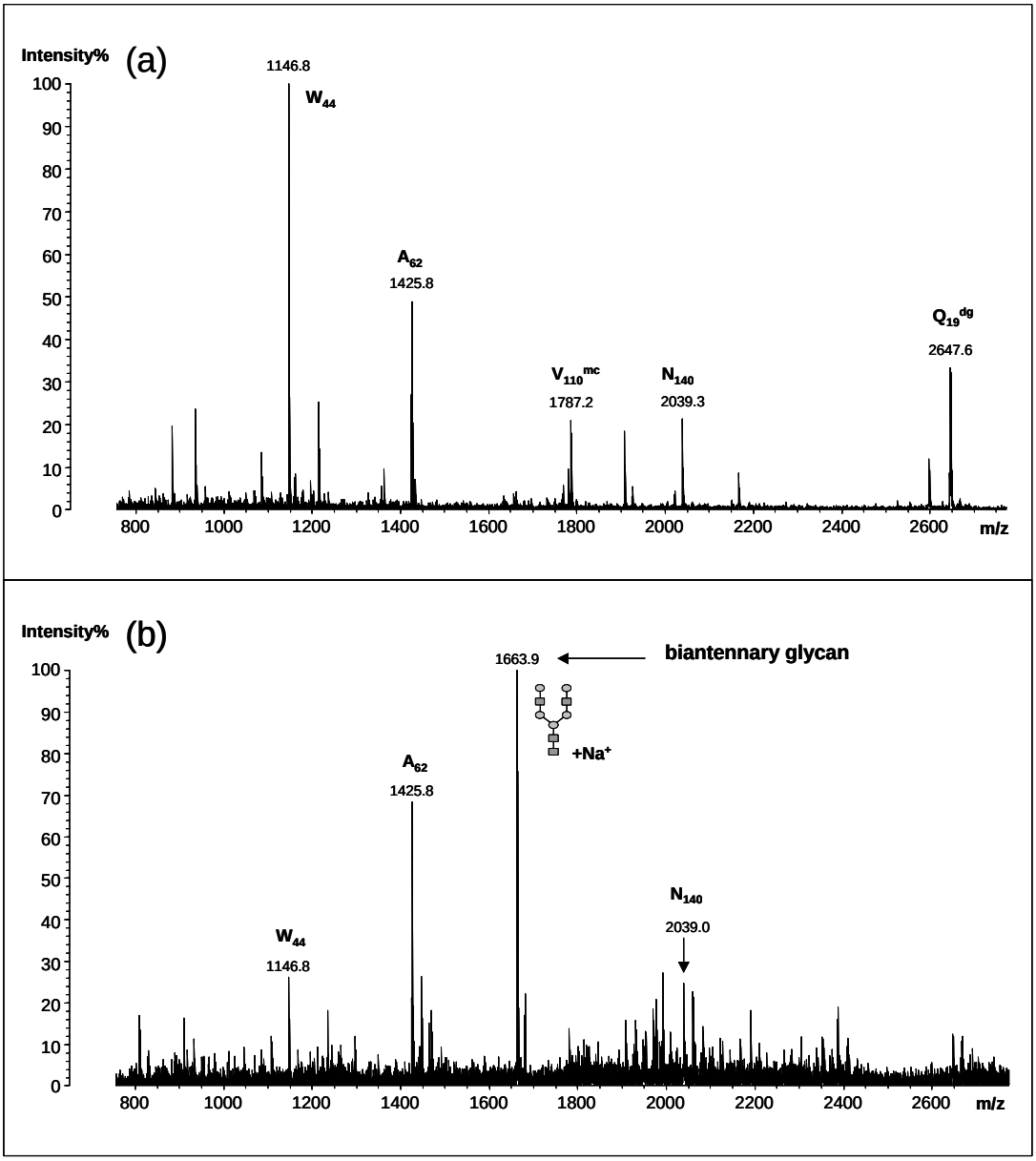

Figure 3: MALDI-QIT-rTOF mass spectra in the positive ion mode of the tryptic peptides and glycans of bovine AGP after PNGase F treatment using (a) solid matrix THAP, and (b) ionic liquid matrix GTHAP. Numerical values specify the monoisotopic masses of the $[M+H]^+$ ions. Symbols : ○ Hexose, ■ HexNAc; dg, deglycosylated peptide

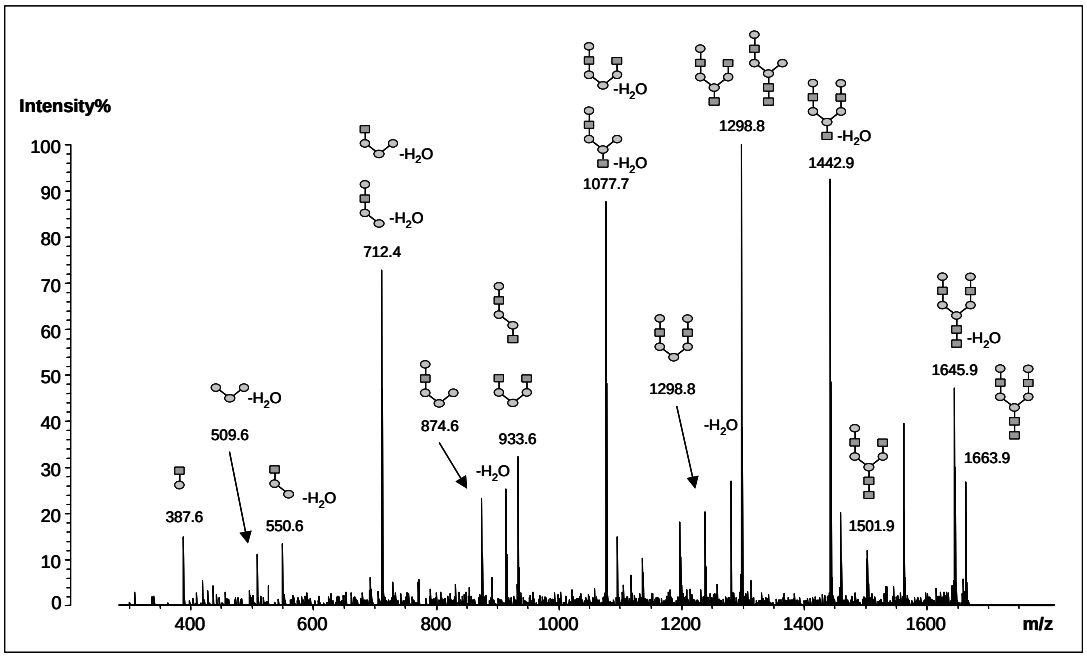

Figure 4: MALDI-QIT-rTOF MS/MS spectrum in the positive ion mode of biantennary complex type glycan of bovine AGP without terminal N-acetyl- and N-glycolyl-neuraminic acids. The spectrum was taken out of the unseparated tryptic and PNGase F digest with the ionic liquid matrix GTHAP. Numerical values specify the monoisotopic masses of the $[M+Na]^+$ ions. Symbols: ○ Hexose, ■ HexNAc

Very similar results were achieved with the AT sample. No glycan structures could be assigned to the peaks in the spectrum gained with THAP, it exhibited only signals originating from peptides (Figure 5a). With GTHAP a very intense signal was observed for the glycan (biantennary, without NeuAc), whereas peptide signals were completely suppressed and did not appear in the spectrum (Figure 5b).

Also with bovine fetuin the detection of the released glycans in presence of the peptides was only possible when using the ionic liquid matrix GTHAP (Figures 6a and b). The glycans of this protein exhibit highly sialylated bi- and triantennary complex type structures. The two major forms could be seen in the spectrum taken from the total enzymatic digest mixture and could be verified by MS/MS measurements (data not shown). Other low abundant glycoforms like fucosylated and tetra-antennary structures[18,26,27] were not found in the spectrum.

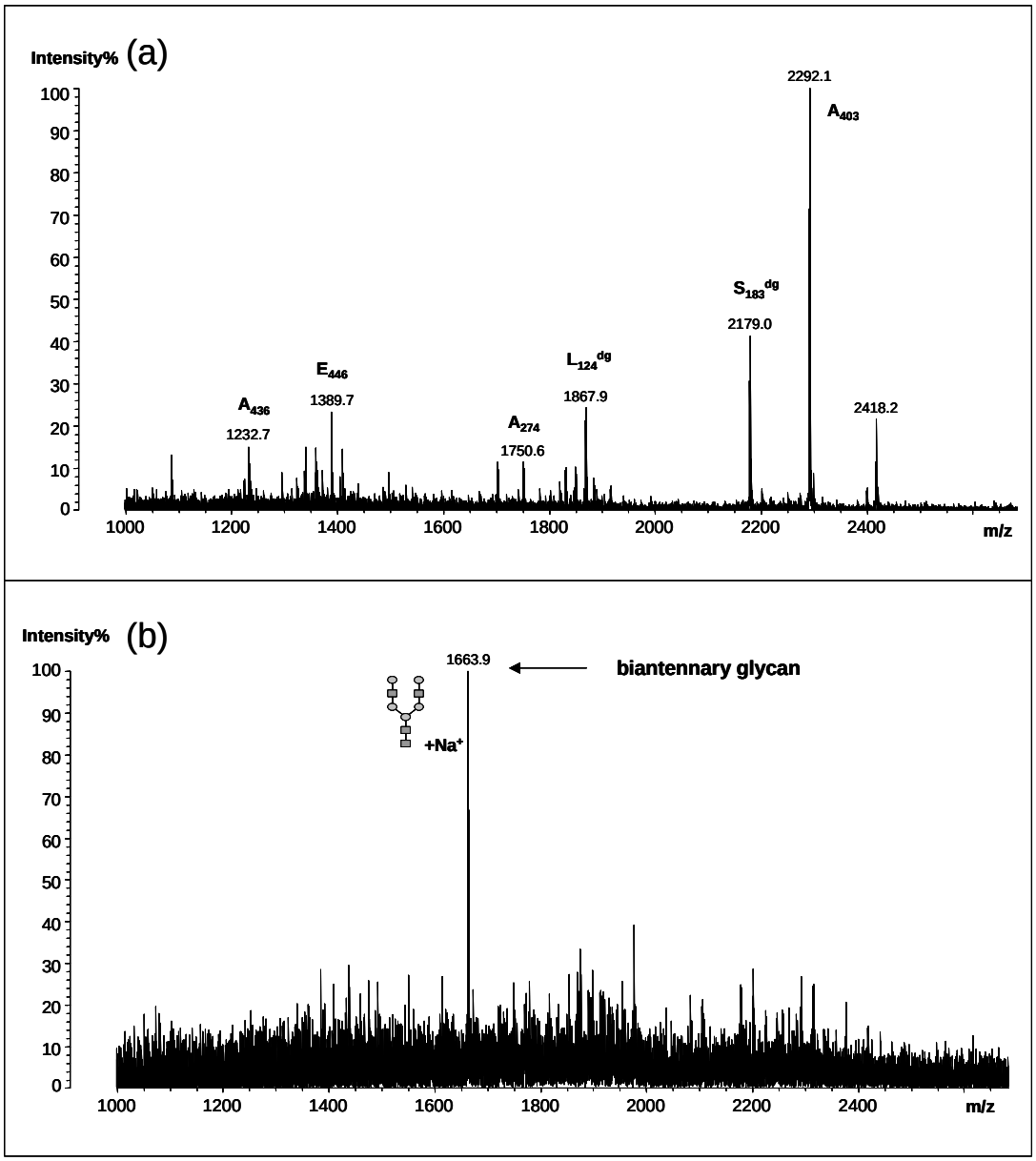

Figure 5: MALDI-QIT-rTOF mass spectra in the positive ion mode of the tryptic peptides and glycans of human AT after PNGase F treatment using (a) solid matrix THAP, and (b) ionic liquid matrix GTHAP. Numerical values specify the monoisotopic masses of the $[M+H]^+$ ions. dg, deglycosylated peptide

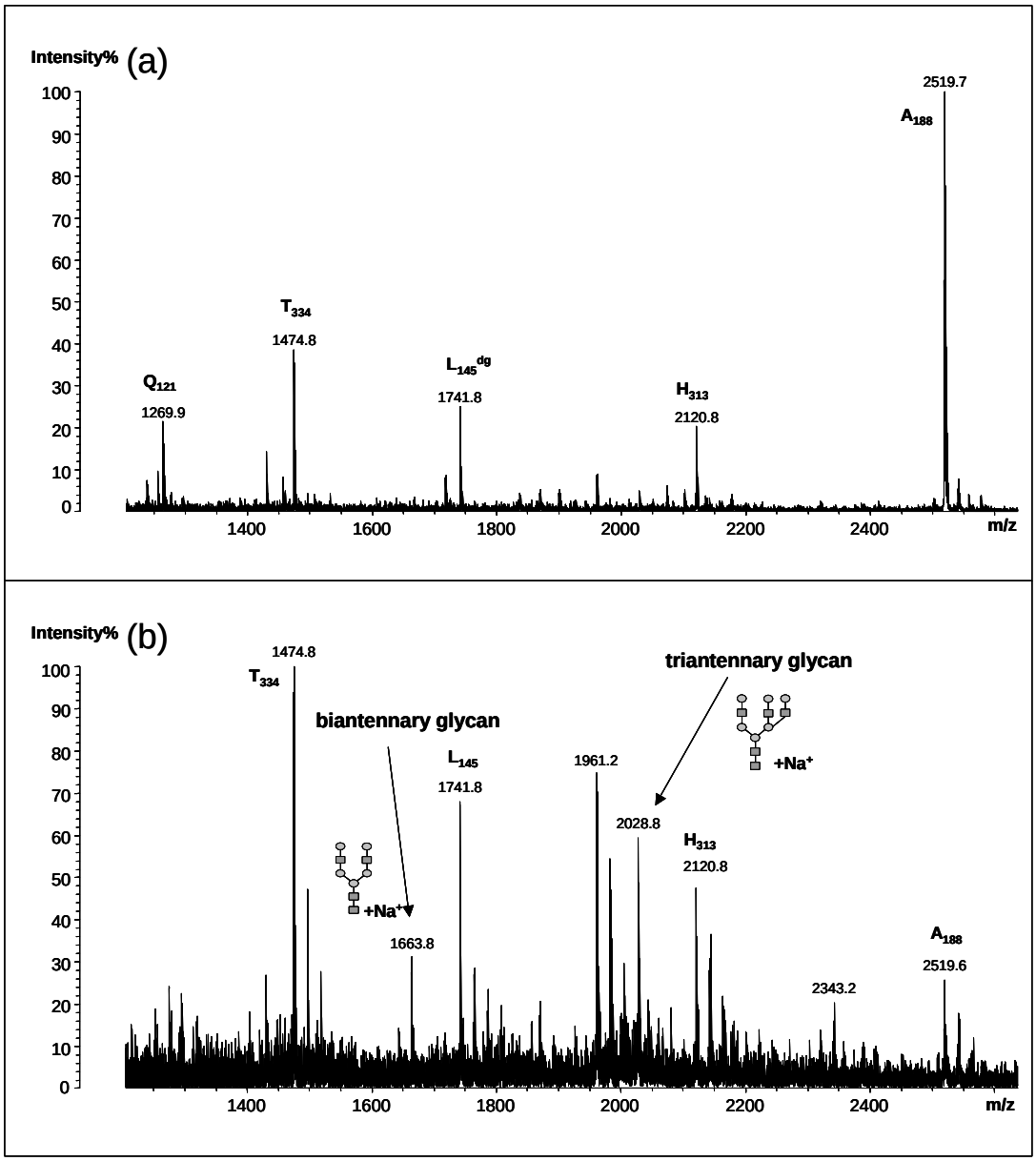

Figure 6: MALDI-QIT-rTOF mass spectra in the positive ion mode of the tryptic peptides and glycans of bovine Fetuin after PNGase F treatment using (a) solid matrix THAP, and (b) ionic liquid matrix GTHAP. Numerical values specify the monoisotopic masses of the $[M+H]^+$ ions. Glycans without terminal N-acetylneuraminic acids. mc, missed cleavage; dg, deglycosylated peptide

CONCLUSIONS

The ionic liquid matrix GTHAP introduced in this paper was evaluated regarding ionization efficiency and fragmentation extent in MALDI-MS analysis of glycopeptides and glycans. Appling the commonly used solid matrices like THAP or DHB the ionization yield of oligosaccharides is low compared to peptides, and glycan containing analytes are suppressed in MALDI-MS spectra. When using GTHAP the results are completely different. It seems that carbohydrate structures are favored in the MALDI process. The ionic liquid matrix GTHAP was well suited for the analysis of glycopeptides and glycans out of complex mixtures. Post source fragmentation of metastable ions, a key issue when using analyzer systems with long residence times like ion traps, could be reduced when looking at peptide structures. However, cleavage of the sialic acid residues were observed to occur to completeness. The switch to ionic liquid matrices led to a decrease in absolute sensitivity by a factor of 10 to 100, dependent on the matrix preparation and the type of analytes and to a decrease in the signal-to-noise ratio. As sodium adducts of carbohydrates are present with increased intensities when using GTHAP, S/N ratio is further compromised and due to this reasons it was not possible to detect low abundant glycoforms. In future investigations it will be necessary to address the improvement of sensitivity and signal-to-noise ratio.

REFERENCES

1. Armstrong DW, He L, Liu Y-S. Examination of Ionic Liquids and Their Interaction with Molecules, When Used as Stationary Phases in Gas Chromatography. *Analytical Chemistry* 1999; **71**: 3873-3876.
2. Bao Y, Lantz AW, Crank JA, Huang J, Armstrong DW. The use of cationic surfactants and ionic liquids in the detection of microbial contamination by capillary electrophoresis. *Electrophoresis* 2008; **29**: 2587-2592.
3. Armstrong DW, Zhang L-K, He L, Gross ML. Ionic liquids as matrixes for matrix-assisted laser desorption/ionization mass spectrometry. *Analytical Chemistry* 2001; **73**: 3679-3686.
4. Tholey A, Heinzle E. Ionic (liquid) matrices for matrix-assisted laser desorption/ionization mass spectrometry - applications and perspectives. *Analytical and Bioanalytical Chemistry* 2006; **386**: 24-37.
5. Mank M, Stahl B, Boehm G. 2,5-Dihydroxybenzoic acid butylamine and other ionic liquid matrixes for enhanced MALDI-MS analysis of biomolecules. *Analytical Chemistry* 2004; **76**: 2938-2950.
6. Tholey A, Zabet-Moghaddam M, Heinzle E. Quantification of Peptides for the Monitoring of Protease-Catalyzed Reactions by Matrix-Assisted Laser Desorption/Ionization Mass Spectrometry Using Ionic Liquid Matrixes. *Analytical Chemistry* 2006; **78**: 291-297.
7. Li YL, Gross ML. Ionic-liquid matrices for quantitative analysis by MALDI-TOF mass spectrometry. *Journal of the American Society for Mass Spectrometry* 2004; **15**: 1833-1837.
8. Carda-Broch S, Berthod A, Armstrong DW. Ionic matrices for matrix-assisted laser desorption/ionization time-of-flight detection of DNA oligomers. *Rapid Communications in Mass Spectrometry* 2003; **17**: 553-560.
9. Li YL, Gross ML, Hsu F-F. Ionic-liquid matrices for improved analysis of phospholipids by MALDI-TOF aass spectrometry. *Journal of the American Society for Mass Spectrometry* 2005; **16**: 679-682.
10. Hurtado P, Hortal AR, Martinez-Haya B. Matrix-assisted laser desorption/ionization detection of carbonaceous compounds in ionic liquid matrices. *Rapid Communications in Mass Spectrometry* 2007; **21**: 3161-3164.

11. Zabet-Moghaddam M, Heinzle E, Lasaosa M, Tholey A. Pyridinium-based ionic liquid matrices can improve the identification of proteins by peptide mass-fingerprint analysis with matrix-assisted laser desorption/ionization mass spectrometry. *Analytical and Bioanalytical Chemistry* 2006; **384**: 215-224.
12. Zabet-Moghaddam M, Krueger R, Heinzle E, Tholey A. Matrix-assisted laser desorption/ionization mass spectrometry for the characterization of ionic liquids and the analysis of amino acids, peptides and proteins in ionic liquids. *Journal of Mass Spectrometry* 2004; **39**: 1494-1505.
13. Laremore TN, Murugesan S, Park T-J, Avci FY, Zagorevski DV, Linhardt RJ. Matrix-Assisted Laser Desorption/Ionization Mass Spectrometric Analysis of Uncomplexed Highly Sulfated Oligosaccharides Using Ionic Liquid Matrices. *Analytical Chemistry* 2006; **78**: 1774-1779.
14. Schnoll-Bitai I, Ullmer R, Hrebicek T, Rizzi A, Lacik I. Characterization of the molecular mass distribution of pullulans by matrix-assisted laser desorption/ionization time-of-flight mass spectrometry using 2,5-dihydroxybenzoic acid butylamine (DHBB) as liquid matrix. *Rapid Communications in Mass Spectrometry* 2008; **22**: 2961-2970.
15. Laremore TN, Zhang F, Linhardt RJ. Ionic liquid matrix for direct UV-MALDI-TOF-MS analysis of dermatan sulfate and chondroitin sulfate oligosaccharides. *Analytical Chemistry* 2007; **79**: 1604-1610.
16. Fukuyama Y, Nakaya S, Yamazaki Y, Tanaka K. Ionic Liquid Matrixes Optimized for MALDI-MS of Sulfated/Sialylated/Neutral Oligosaccharides and Glycopeptides. *Analytical Chemistry* 2008; **80**: 2171-2179.
17. Papac DI, Wong A, Jones AJS. Analysis of Acidic Oligosaccharides and Glycopeptides by Matrix-Assisted Laser Desorption/Ionization Time-of-Flight Mass Spectrometry. *Analytical Chemistry* 1996; **68**: 3215-3223.
18. Kuster B, Wheeler SF, Hunter AP, Dwek RA, Harvey DJ. Sequencing of N-linked oligosaccharides directly from protein gels: in-gel deglycosylation followed by matrix-assisted laser desorption/ionization mass spectrometry and normal-phase high-performance liquid chromatography. *Analytical Biochemistry* 1997; **250**: 82-101.
19. Nakano M, Kakehi K, Tsai M-H, Lee YC. Detailed structural features of glycan chains derived from a1-acid glycoproteins of several different animals: the presence

of hypersialylated, O-acetylated sialic acids but not disialyl residues. *Glycobiology* 2004; **14**: 431-441.

20. Snovida SI, Chen VC, Krokhin O, Perreault H. Isolation and Identification of Sialylated Glycopeptides from Bovine a1-Acid Glycoprotein by Off-Line Capillary Electrophoresis MALDI-TOF Mass Spectrometry. *Analytical Chemistry* 2006; **78**: 6556-6563.
21. Demelbauer UM, Zehl M, Plematl A, Allmaier G, Rizzi A. Determination of glycopeptide structures by multistage mass spectrometry with low-energy collision-induced dissociation: Comparison of electrospray ionization quadrupole ion trap and matrix-assisted laser desorption/ionization quadrupole ion trap reflectron time-of-flight approaches. *Rapid Communications in Mass Spectrometry* 2004; **18**: 1575-1582.
22. Demelbauer UM, Plematl A, Josic D, Allmaier G, Rizzi A. On the variation of glycosylation in human plasma derived antithrombin. *Journal of Chromatography A* 2005; **1080**: 15-21.
23. Franzen LE, Svensson S, Larm O. Structural studies on the carbohydrate portion of human antithrombin III. *Journal of Biological Chemistry* 1980; **255**: 5090-5093.
24. Plematl A, Demelbauer UM, Josic D, Rizzi A. Determination of the site-specific and isoform-specific glycosylation in human plasma-derived antithrombin by IEF and capillary HPLC-ESI-MS/MS. *Proteomics* 2005; **5**: 4025-4033.
25. Medzihradszky KF, Gillece-Castro BL, Townsend RR, Burlingame AL, Hardy MR. Structural elucidation of O-linked glycopeptides by high energy collision-induced dissociation. *Journal of the American Society for Mass Spectrometry* 1996; **7**: 319-328.
26. Balaguer E, Neususs C. Glycoprotein Characterization Combining Intact Protein and Glycan Analysis by Capillary Electrophoresis-Electrospray Ionization-Mass Spectrometry. *Analytical Chemistry* 2006; **78**: 5384-5393.
27. Green ED, Adelt G, Baenziger JU, Wilson S, Van Halbeek H. The asparagine-linked oligosaccharides on bovine fetuin. Structural analysis of N-glycanase-released oligosaccharides by 500-megahertz proton NMR spectroscopy. *Journal of Biological Chemistry* 1988; **263**: 18253-18268.

RAPID COMMUNICATIONS IN MASS SPECTROMETRY
Rapid Commun. Mass Spectrom. 2008; **22**: 2961–2970
Published online in Wiley InterScience (www.interscience.wiley.com) DOI: 10.1002/rcm.3655

Characterization of the molecular mass distribution of pullulans by matrix-assisted laser desorption/ionization time-of-flight mass spectrometry using 2,5-dihydroxybenzoic acid butylamine (DHBB) as liquid matrix

Irene Schnöll-Bitai[1]*, Roman Ullmer[2], Thomas Hrebicek[2], Andreas Rizzi[2] and Igor Lacik[3]

[1]University of Vienna, Department of Physical Chemistry, Währinger Str. 42, A-1090 Vienna, Austria
[2]University of Vienna, Department of Analytical Chemistry and Food Chemistry, Währinger Str. 38, A-1090 Vienna, Austria
[3]Polymer Institute of the Slovak Academy of Sciences, Dúbravská cesta 9, 842 36 Bratislava, Slovak Republic

Received 26 May 2008; Revised 20 June 2008; Accepted 23 June 2008

The performances of several matrices were investigated for the accurate determination of the molecular mass distributions of pullulans by matrix-assisted laser desorption/ionization time-of-flight mass spectrometry (MALDI-TOFMS). The ionic liquid matrix (ILM) 2,5-dihydroxybenzoic acid butylamine (DHBB) gave better and more reliable results than the crystalline matrices 2,5-dihydroxybenzoic acid (DHB) and 2,4,6-trihydroxyacetophenone (THAP). With the ILM it was possible to obtain spectra of pullulans up to more than 100 kDa, the highest molar mass reported thus far. Owing to the known advantages of liquid matrices providing better spot-to-spot reproducibility, an almost noise-free spectrum and constant baselines were obtained when working under optimized conditions. In particular, the extent of in-source fragmentation occurring with this group of fragile polymers was considerably and decisively reduced. Thus, a more reliable representation of the true oligomer and polymer distributions is experimentally attainable, especially for distributions with small polydispersity values. The maximum error in the measured distribution associated with fragmentation was estimated by model calculations describing the changes in the polymer distribution upon different probabilities of fragmentation events. These simulation results indicated that the data obtained by MALDI-TOFMS using the liquid DHBB matrix were of high reliability. In particular, the average value of the distributions, M_w, and the polydispersity were obtained with predicted uncertainties of between 3 and 15% depending on the width of the distribution and the mass of the polymers. **Copyright © 2008 John Wiley & Sons, Ltd.**

Pullulans are an interesting group of polysaccharides which are frequently used as food additives.[1] They are naturally occurring water-soluble, biodegradable polyhydroxyl compounds which are also capable of forming hydrogels or liquid crystalline phases.[2] Due to these features they are also used for biomedical and cosmetic applications. The repeating unit of pullulans is a trisaccharide composed of mainly α-(1 → 6) linked maltotriose subunits (i.e. three α-(1-4) linked glucoses) and a low extent of α-(1 → 6) maltotetraose units.[3]

Pullulans are, in addition, of considerable interest as standards for the calibration of aqueous size-exclusion chromatography (SEC).[4–8] In this context it is essential to have standard samples well characterized with respect to the number, M_n, and weight, M_w, average molar masses, and especially samples with narrow distributions (polydispersities $D = M_w/M_n$ smaller than 1.2) are preferred over those with broad distributions. As the polydispersity of pullulans produced by different types and strains of microorganisms (*Aureobasidium* pullulans[5,9] and CP159, CP263 and CP102[3] strains of *Cryphonectria parasitica*) lies usually between 2.1 and 4.1,[10–12] the pullulans must be fractionated and characterized before they can be used as calibration standards. Large-scale coarse fractionation is carried out by precipitation followed by gel filtration yielding fractions of high molar mass pullulans. Pullulans with intermediate molar masses (<50 kDa) are obtained via partial enzymatic degradation by pullulanase whereas masses below 5 kDa are obtained by further proteolytic degradation with HCl.[4] Polymer distributions with D values near 1.1 can be obtained in this way. A newly developed fractionation technique, the so-called continuous spin fractionation,[13] yields pullulans with somewhat broader distributions ($D \approx 2$).

Characterization of fractionated pullulans is usually carried out by viscosity, sedimentation,[4,5] osmotic pressure and light scattering measurements (providing average values M_n and M_w) as well as by SEC measurements

*Correspondence to: I. Schnöll-Bitai, University of Vienna, Institute of Physical Chemistry, Vienna, Austria.
E-mail: irene.schnoell-bitai@univie.ac.at

Copyright © 2008 John Wiley & Sons, Ltd.

involving various types of detectors (providing also the molecular mass distributions).[3,7,14–16] As an alternative method, mass spectrometry (MS) can be employed for the direct determination of the molecular mass distribution of synthetic[17] and biologically produced polymers,[18–20] and this method offers the advantage of providing direct data on the molar masses of the individual polymers.

In general, matrix-assisted laser desorption/ionization time-of-flight mass spectrometry (MALDI-TOFMS) has been used for this purpose and several matrices have been tested. Analyses of polysaccharides, especially pullulans, carried out with the matrices 2,5-dihydroxybenzoic acid (DHB),[18,19] 2′,4′,6′-trihydroxyacetophenone (THAP),[21] and *nor*-hamane[22] have been described. With the widely used and thoroughly studied matrix DHB[23] reasonable results were obtained up to a molar mass of 22.8 kDa. Hsu and coworkers[21] were able to extend the experimentally accessible molecular mass range up to 47.3 kDa with THAP; the mass resolution for the sample with 23 kDa was good enough to reveal the molar mass of the repeating anhydromaltotriose moiety and a minor additional series shifted to higher masses by 162 Da relative to the main distribution. Despite these improvements, these measurements displayed a non-constant baseline, high noise, and strong fragmentation.

Armstrong *et al.*[24] investigated the potential benefits of a variety of ionic liquids (covering primarily alkylammonium, pyridinium and substituted anilinium salts of sinapinic acid and α-cyano-4-hydroxycinnamic acid) when used as matrices for the analysis of peptides,[25] proteins and synthetic polymers (polyethylene glycols, PEGs). These ionic liquid matrices (ILMs) exhibited the particular advantage of allowing enhanced sensitivity and good spot-to-spot reproducibility due to the more homogeneous mixing of analyte and matrix. Using 2,5-dihydroxybenzoic acid butylamine (DHBB) and other ILMs as matrix, Stahl and coworkers[26] investigated oligosaccharides in the positive ion mode up to a molar mass of 2.2 kDa and found for PEGs a lower extent of MALDI-induced fragmentation. Various ILMs were also successfully tested[27,28] for the analysis of sulphated oligosaccharides in the positive ion mode.

In the context of analyzing molecular mass distributions of polymers it is essential that the ionization process does not alter the distribution either by forming unspecified adducts, by mass discrimination during the ionization or by fragmentation of the analytes. Poly- and oligosaccharides are known to be easily cleaved at the glycosidic bonds. DHBB has been investigated here as an ILM for the accurate determination of polymer distributions of oligosaccharides, particularly pullulans, and its performance is compared with that of crystalline matrices (particularly DHB). Pullulan standards characterized by means of various methods by the suppliers were used as test analytes. The impact of fragmentation on the measured molecular mass distribution of the polymers is analyzed by means of model calculations carried out under the assumption of realistic model parameters.

EXPERIMENTAL

Materials

The ProteoMassTM Peptide and Protein MALDI-MS calibration kit, *nor*-harmane, LC/MS grade water and trifluoroacetic acid (TFA) were obtained from Sigma-Aldrich (St. Louis, MO, USA). Ethanol was purchased from Merck (Darmstadt, Germany), acetonitrile and methanol from Baker (Deventer, The Netherlands), and 2,5-dihydroxybenzoic acid (DHB), 2,4,6-trihydroxyacetophenone (THAP), sinapinic acid (SA), α-cyano-4-hydroxycinnamic acid (CHCA) and butylamine were from Fluka (Buchs, Switzerland). Pullulans were purchased from Polymer Laboratories (Church Stretton, UK); their descriptors were chosen according to the M_w value given by the supplier (cf. Table 1).

Sample preparation

The pullulan samples were dissolved in LC/MS grade water at a concentration of 5 mg/mL. The concentrations of the solid matrices were: (a) DHB: 50 mg/mL dissolved in a mixture of acetonitrile 75% (v/v) and water; (b) *nor*-harmane: 10 mg/mL in 3:1 (v/v) methanol/water; (c) THAP: 25 mg/mL methanol; (d) SA: 10 mg/mL 1:1 (v/v) methanol/water. The samples were applied using the dried-droplet technique by depositing 0.5 μL matrix solution mixed with 0.5 μL sample solution onto the MALDI target.

The ionic liquid matrix was prepared freshly as described by Stahl and coworkers.[26] To a 200 mM solution of DHB in

Table 1. Compilation of the weight average molar mass, M_w [kDa], and the polydispersity values, D, as specified by the supplier and as measured by means of MALDI-TOFMS. The molar mass of the repeating unit, M_0 [Da], was determined using the Kratos software-routine 'polymer' and the given integration limits (in kDa). Values in italics were calculated from exported data by numerical integration using a home-made plot software.[29] Smoothing (sm.) of raw mass spectra was performed by means of the Savitzky-Golay routine where indicated (SG) using a width parameter of 30

Supplier's data			MALDI-TOFMS-based data							
			DHB			DHBB				
Sample	M_w	D	M_0	M_w	D	M_0	M_w	D	sm.	integration limits
Pul-5,900	5.9	1.09	486.4	5.4	1.023	486.4	5.4 *5.5*	1.019 *1.020*	none	2–10
Pul-11,800	11.8	1.10	486.5	9.3	1.031	485.1	9.2 *9.4*	1.009 *1.011*	none	4–14
Pul-22,800	22.8	1.07	—	—	—	478	17.2 *17.9*	1.003 *1.023*	SG	11–27
Pul-47,300	47.3	1.06	—	—	—	—	*44.6*	*1.017*	SG	20–70
Pul-112,000	112.0	1.12	—	—	—	—	*87.6*	*1.026*	SG	50–130

Copyright © 2008 John Wiley & Sons, Ltd.

DOI: 10.1002/rcm

methanol an equimolar amount of butylamine was added and shaken at room temperature for 1 min. Methanol and free butylamine were then removed in a vacuum evaporator. Subsequently, the viscous 2,5-dihydroxybenzoic acid butylamine (DHBB) was mixed with the same volume of ethanol. Then 1 μL of the ethanolic ILM was deposited on a standard stainless steel MALDI target followed by deposition of 1 μL of the aqueous sample solution. The mixture was homogenized on the target by repeated pipetting and dispensing.

MALDI-MS

MALDI-TOFMS analysis was carried out using a linear TOF instrument (AXIMA-LNR, Shimadzu Biotech – Kratos Analytical, Manchester, UK). It was equipped with a pulsed nitrogen laser working at a wavelength of 337 nm and a pulse width (FWHM) of 4 ns, an integrated 1 GHz recorder and a monochrome CCD camera system for monitoring the sample spots. An accelerating voltage of 20 kV was applied and delayed extraction was used. Data acquisition and processing were performed using Kratos software version 2.4.1. Mass spectra were acquired in the positive ion mode by averaging 200 unselected single laser shots. External mass calibration was done by use of two different mixtures of peptides and proteins. For the lower mass range the $[M+H]^+$ ions of a mixture of the following peptides and proteins was measured with THAP as matrix: bradykinin fragment 1-7, human angiotensin II and III, bovine insulin and ubiquitin. For the higher mass range $[M+H]^+$ ions of a mixture of the following proteins were measured with SA (10 mg/mL in acetonitrile, 0.1% TFA) as matrix: equine cytochrome c, equine apomyoglobin, rabbit muscle aldolase and bovine serum albumin. The laser power was set to the threshold of the specific analyte. The MALDI-MS-based M_w data were obtained by using the Kratos software option 'polymer' or by numerical integration of exported data.[29]

RESULTS AND DISCUSSION

In the MALDI-TOFMS spectra of pullulans published to date,[3,18,19,21,30] and those presented in this work, the major ions were separated by a mass difference of 486.43 *m/z* units which corresponds to the mass of a trisaccharide, the repeating unit in pullulans. In addition, less abundant ions peaks were separated by a mass difference of 162 *m/z* units corresponding to the mass of a monosaccharide increment. So far, these less abundant ions have been interpreted as originating primarily from the incorporation of one tetraose or pentaose unit[3] during the synthesis of pullulans by microorganisms.

With the acidic crystalline matrices used the principal ions in the spectra corresponded to sodiated and potassiated molecules, $[M+Na^+]^+$ and $[M+K^+]^+$. With the liquid ion-pair matrix DHBB, the principal ions were butylammonium (BA) adducts $[M+C_4H_9NH_3^+]^+$.

Choice of matrices

Several MALDI matrices were used and evaluated with regard to various criteria including accessible mass range, extent of fragmentation and base-line noise. The classical protein matrix SA[31] was inadequate for the analysis of pullulans as no useful signal could be obtained, CHCA led to very broad and noisy signals, and *nor*-hamane[22] yielded only very weak signals for the smallest pullulan sample (Pul-5,900) and none for samples with higher molecular masses. With DHB[18] reasonable results were obtained up to a molecular mass of 22.8 kDa, and with THAP it was possible to measure even Pul-47,000 but fragmentation and baseline problems were already becoming obvious for Pul-11,800. The liquid ion-pair matrix DHBB definitely outperformed all the other tested matrices with respect to resolution, signal-to-noise (S/N) ratio, absence of baseline noise and drift, absence (or less severe presence) of fragmentation, and the accessible mass range. It was possible to measure pullulans with molecular masses up to 112 kDa (shown below).

Influence of oligomer chain length on the quality of spectra

Pullulans with short chain length

The spectrum of Pul-738 (not shown) obtained with the solid matrix DHB exhibited two ions at *m/z* 689.4 and 705.3 identified as the sodium and potassium adducts of an oligosaccharide with a monoisotopic relative mass of 666.4 consisting of four glucose units. In the spectrum measured with DHBB there is only a single ion present at *m/z* 740.7 corresponding to the butylammonium adduct of this oligosaccharide. A very weak additional ion at *m/z* 903.2 corresponds to maltopentaose ($M_r = 828.6$ Da). Obviously, there is a mismatch between the supplier's molar mass data and the values determined here.

The spectra of Pul-5,900 measured in DHB matrix (Figs. 1(a) and 1(b)) displayed an oligomer distribution where the major ions were the sodium adducts of the polysaccharides separated by the expected mass increment of approximately 486.4 *m/z* units. The ion at *m/z* 4905.7 thus conforms to the mass calculated for ten trisaccharide units (i.e. $10 \times 486.43 + 18.0 + 23.0 = 4905.3$), and the corresponding potassium adduct is seen at *m/z* 4921.0. The low abundance ions between the major ions are separated by approximately 162 *m/z* units, corresponding to one monosaccharide unit. One might interpret the spectrum as composed of three distributions where each of them has the expected mass difference between neighbouring ions of 486.4 *m/z* units (repeating trisaccharide unit), but are shifted relative to each other by 162.1 *m/z* units, corresponding to one glucose unit. The abundances of these ions with a mass difference of 162.1 *m/z* units increase drastically in the *m/z* range below 2000 indicating a considerable extent of in-source or most probably on-target fragmentation of the labile glycosidic linkage.

Figures 1(c) and 1(d) show the spectra of the same pullulan sample measured with the liquid matrix DHBB. The major ions correspond to 7 to 16 maltotriose units present in the oligosaccharides. The ion at *m/z* 4957.8 corresponds to the BA adduct of ten trisaccharide units (i.e., $10 \times 486.43 + 18.0 + 74.1 = 4956.4$). Near these major ions, low abundance sodium adducts can be seen, whereas the potassium adducts solely contribute to the tailing of the low abundance ions.

Copyright © 2008 John Wiley & Sons, Ltd.

DOI: 10.1002/rcm

RCM

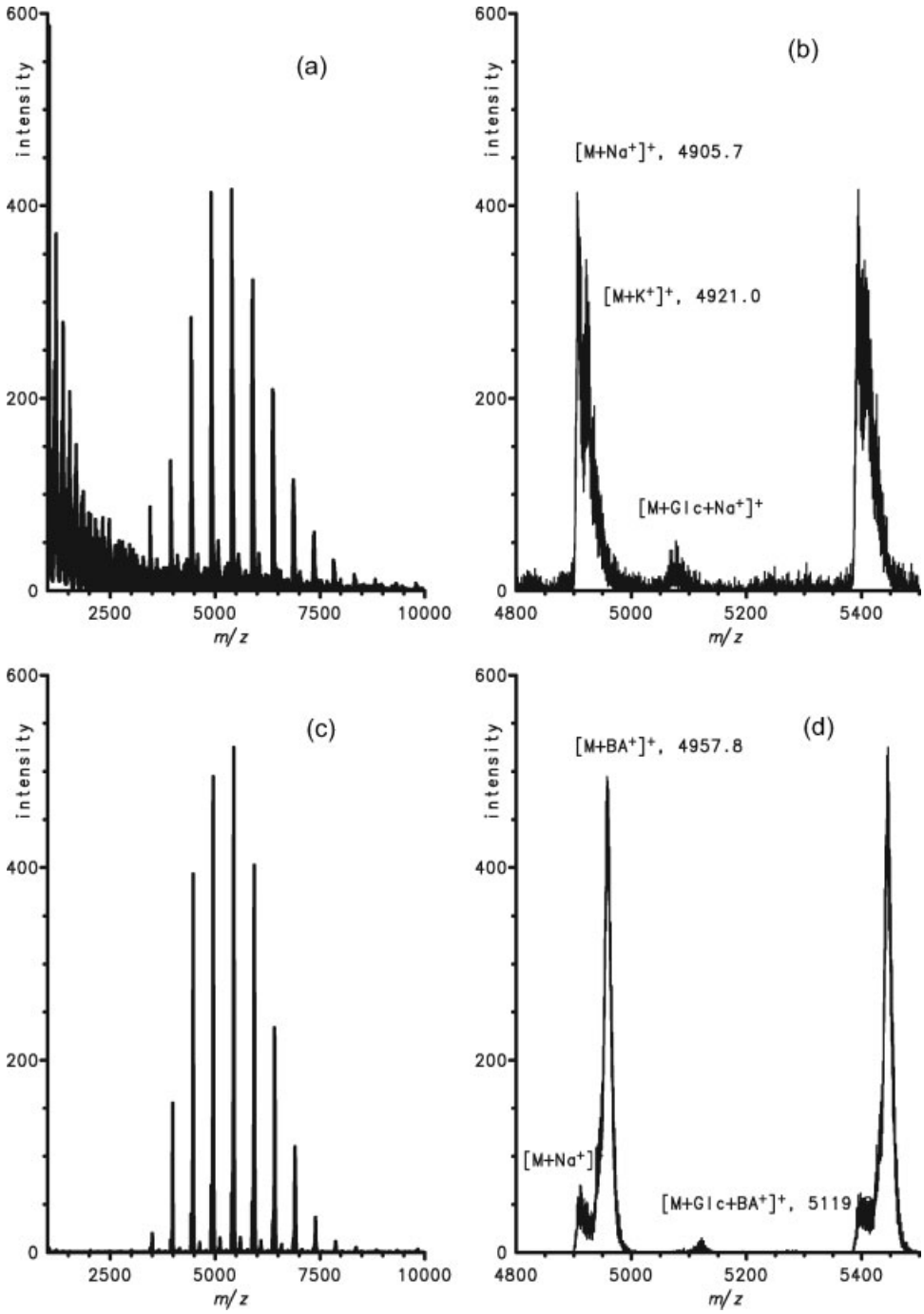

Figure 1. MALDI-TOF spectra of the standard sample Pul-5,900 measured with the matrices DHB (a, b) and DHBB (c, d). The enlarged sections shown in (b) and (d) reveal the adducts and fragments formed. Intensities are given in arbitrary units (a.u.).

Importantly, no ions were found below *m/z* 3000. This observation corroborates the view that the low-mass ions observed with the crystalline DHB matrix in Fig. 1(a) are probably in-source fragmentation products. An alternative explanation is that these fragments stem from hydrolysis of the pullulans upon their co-crystallization in the acidic matrix. Experiments done with acidified and heated samples subsequently mixed with DHBB matrix, however, gave no ions in the lower mass range (data not shown) which seems to exclude the hypothesis of on-target degradation by hydrolysis. It follows that this fragmentation may be associated with the ionization event and that the rigidity of the crystalline structure might contribute to the higher extent of in-source fragmentation of these oligosaccharides.

Very low abundance ions can be seen in Fig. 1 between the major ions, with Δm values of 162 *m/z* units. In the absence of any prominent extent of fragmentation with DHBB matrix, these ions can be ascribed to the natural occurrence of one tetraose unit. Interestingly, ions corresponding to the presence of one pentaose unit are missing.

Copyright © 2008 John Wiley & Sons, Ltd.

DOI: 10.1002/rcm

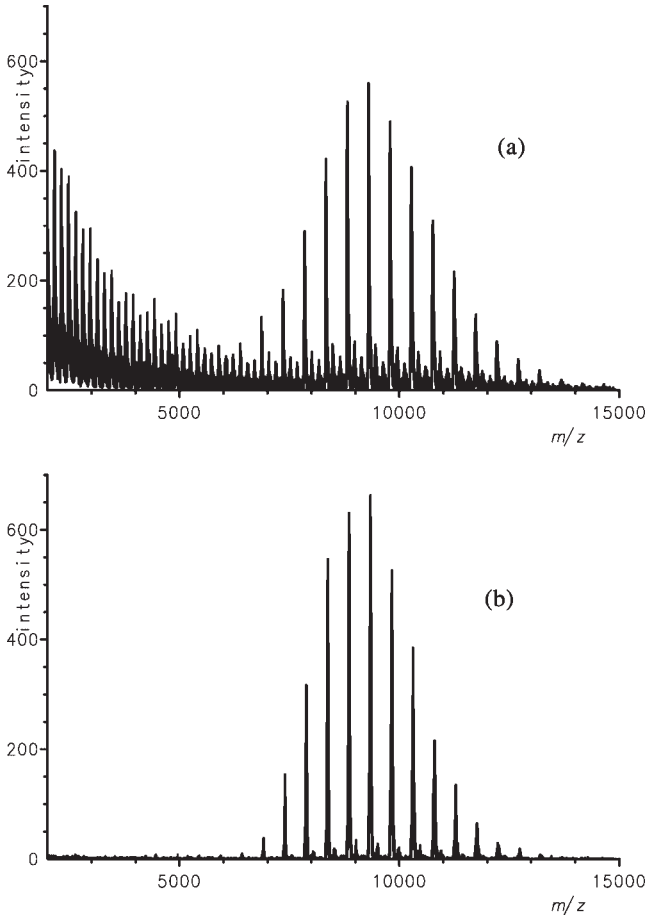

Figure 2. MALDI-TOF spectra of the standard sample Pul-11,800 measured with the matrices (a) DHB and (b) DHBB.

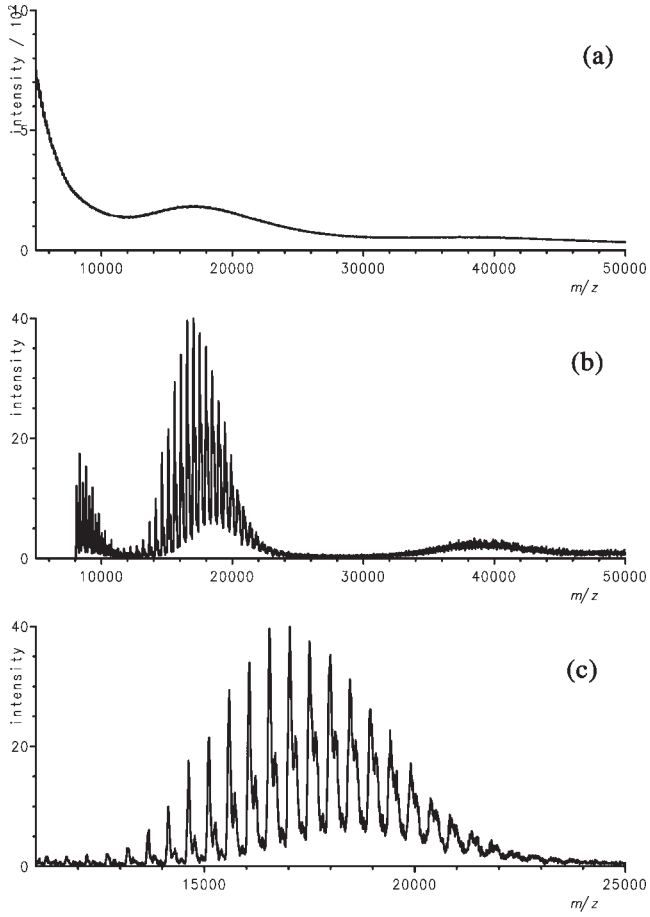

Figure 3. MALDI-TOF spectra of the standard sample Pul-22,800 measured with the matrices DHB (a) and DHBB (b, c). The latter shows an enlarged part of the smoothed distribution given in (b).

Pullulans with intermediate chain length

Pullulan 11,800. The molecular mass distributions for the pullulan standard Pul-11,800 are shown in Fig. 2 as measured with DHB and DHBB matrices. Again, a significant extent of fragmentation becomes obvious in the case of the DHB matrix, whereas fragment ions in the low molecular mass region are nearly absent with DHBB. In agreement with this observation the abundances of the ions between the major ions (corresponding to pullulans containing one tetra- and one pentasaccharide unit) are considerably higher when using DHB. This finding indicates that with pullulans of increased size these measured low abundance distributions might already be affected by the extent of fragmentation with the DHB matrix, but not with the DHBB matrix.

Pullulan 22,800. Mass distributions of pullulans of even higher molecular masses, e.g. Pul-22,800, cannot be successfully determined when using the crystalline DHB matrix. A high extent of fragmentation leads to a noisy spectrum and after application of the standard smoothing algorithm (Savitzky-Golay) a quasi-continuous distribution with high signal intensities at low m/z values is obtained, as shown in Fig. 3(a).

The 'polymer' routine of the instrument software had already failed to calculate the average molar masses M_n and M_w as well as the molar mass of the monomer unit, M_0. Contrary to this situation, when using the ILM DHBB individual ions are still distinguishable (even without any smoothing algorithm). Again, the major ions are separated by the mass of the anhydrotriose unit ((n3)-distribution), but pullulans with one more glucose unit ((n3+1)-distribution, originating, e.g., from the presence of one tetraose unit, can be observed to a considerable extent, and even those containing two more glucose units ((n3+2)-distribution), originating, e.g., from the presence of one pentaose or two tetraose units, were observed. The signal intensities of the (n3+1)-distribution increased relative to the (n3)-distribution, as seen in Fig. 3(c), when compared with lower mass pullulans. Maltotetraose units occur naturally in pullulans (cf. the results shown in Figs. 1(c) and 2 and refs.[32,33]) and one has to assume that the probability of the presence of such units increases with increasing chain length. However, it is likely that the pullulans of the (n3+1) and (n3+2) series originate in addition partially from fragmentation events. In fact, the presence of ions in the m/z range below 10 000 makes it evident that fragmentation already occurs to a significant extent even with the DHBB matrix when dealing with these long-chain pullulans.

Pullulans with molecular masses above 40,000

Even for pullulans of such high molecular masses useful spectra could be obtained when using the ILM DHBB matrix,

Copyright © 2008 John Wiley & Sons, Ltd.

DOI: 10.1002/rcm

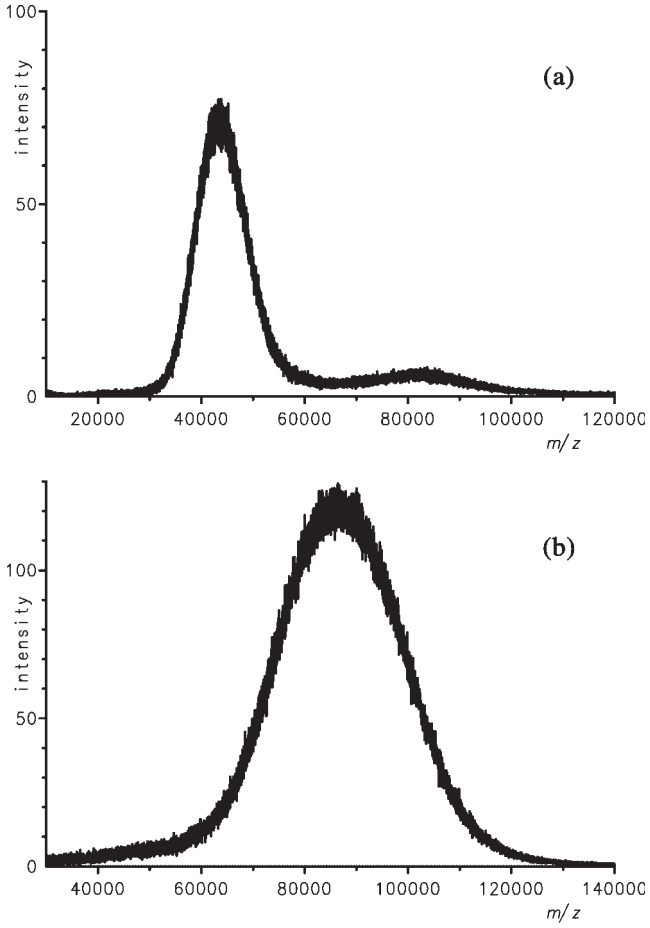

Figure 4. MALDI-TOF spectra of the standard samples Pul-47,300 (a) and Pul-112,000 (b) measured with DHBB matrix; smoothing according to the Savitzky-Golay algorithm, width 30.

as shown in Fig. 4 for pullulans Pul-47,300 and Pul-112,000. The Savitzky-Golay option was used as the smoothing algorithm. A good S/N ratio was obtained in both cases and the extent of the presence of a dimer peak or a doubly charged distribution depended on sample preparation and laser fluence. Considerable fragmentation was manifested by the ions present with pronounced signal intensities in the range below m/z 3800 (region not shown).

Accuracy of measured weight average of molar mass and polydispersity

When discussing the possibility of estimating fairly accurate weight average molar masses, M_w, and polydispersities, D, from the measured distributions, one has to evaluate how far the increasing extent of fragmentation observed for higher pullulans might alter the original distribution. This was done by comparing the determined M_w and D values of the samples measured with the matrices DHB and DHBB which differ in the extent of fragmentation. These data are compiled in Table 1 and compared with the specifications given by the supplier.

The M_w values obtained with the two different matrices were in excellent agreement with each other but considerably lower (by 10–25%) than the supplier's specification data. Similarly, the determined D values deviated only slightly when using the different matrices, but they were between 5 and 10% lower than those specified by the supplier.

The difference between the MALDI-MS data and the specifications might be based on a bias inherent in the specification methods employed by the suppliers. Of the alternative methods SEC is the standard technique, due to its versatility. However, the polymer distribution with D values smaller than 1.2 is always broadened when determined by SEC because of inevitable chromatographic band broadening.[34,35] This means that SEC traces falsely indicate the presence of polymers with higher and lower masses than really present and consequently M_w and D values are overestimated. The calculation of the 'true' distribution from a SEC peak is in principle possible[36,37] but it is a delicate (mathematical inversion) problem in practice, even if the band-broadening parameters are known. Furthermore, continuous signals obtained by SEC provide no information about the smallest repeating units.

With respect to MALDI the accuracy of the measured mass distribution depends first on the extent of discrimination of oligomers and polymers with higher masses during the ionization process and, second, on the extent of in-source fragmentation. The measurement of an equimolar mixture of the pullulan standards Pul-5,900 and Pul-11,800 with DHBB as matrix confirmed the occurrence of a certain extent of discrimination of higher mass oligomers (spectra not shown) even at laser intensities markedly above the threshold value. However, for polymers with narrow distributions (D values less than 1.10) such an effect is usually regarded as less significant.[38] Ionization-associated high-mass discrimination might become important when using laser intensities below the threshold value of the higher mass polymers, conditions which were avoided here. Regarding the extent of fragmentation, no evidence for the presence of fragment ions was found with the samples Pul-5,900 and Pul-11,800 when measured with DHBB matrix. It is thus assumed that the mass distributions seen in these spectra are close to the 'true' ones.

The mass of the repeating unit calculated from the experimental distribution was found to be very near to the theoretical value of 486.43. For the Pul-22,800 standard, a too low value of 478 was obtained, and this is regarded as being due to the limited resolution of the peaks.

It is remarkable that, despite the experimental evidence for significant polymer fragmentation with the DHB matrix, the M_w values obtained with both matrices are in excellent agreement when choosing the given integration limits to be equal for both matrices. A similar low sensitivity of M_w data with respect to improperly chosen baselines[39] or the occurrence of mass discrimination[40] during the ionization process has already been demonstrated in previous studies.

Qualitative model regarding the probability of chain-length dependent fragmentation

A simple qualitative model is presented to explain the increasing extent of fragmentation with higher polymer chain length and higher matrix rigidity. The model is based on the commonly accepted idea that the conformation of a

Copyright © 2008 John Wiley & Sons, Ltd.

DOI: 10.1002/rcm

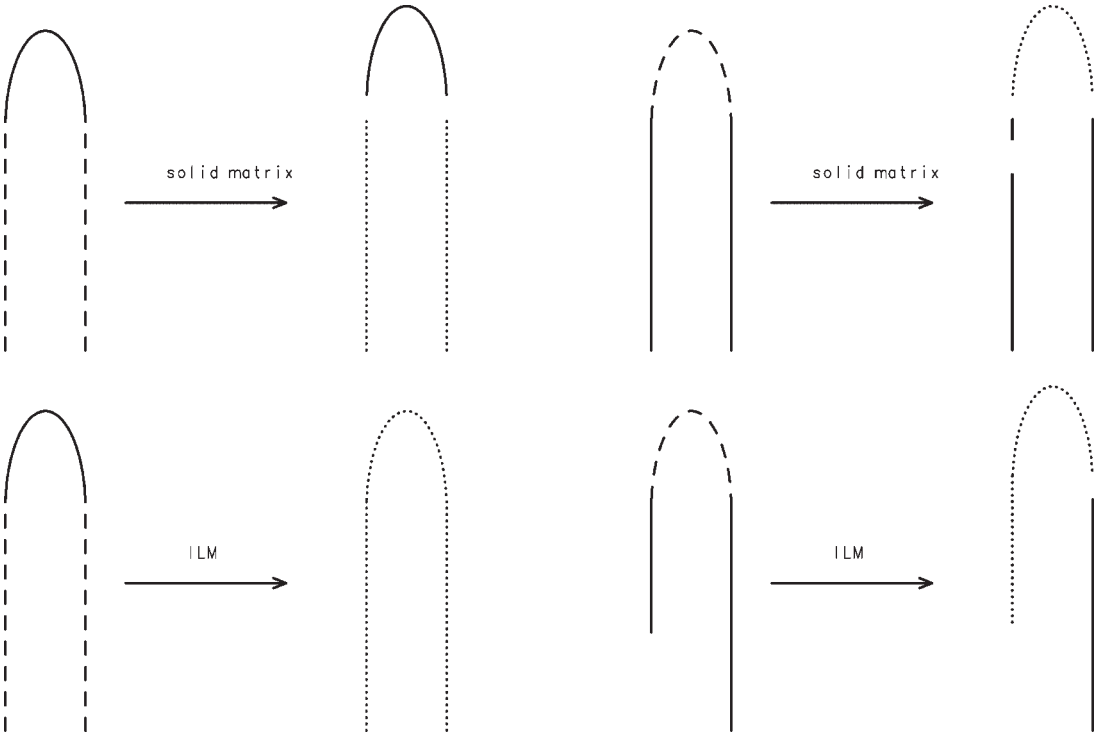

Scheme 1. Model visualizing partially irradiated polymer loops present in a crystalline and a liquid matrix. Upper panel: solid matrix, lower panel: liquid matrix; full lines: polymer in the matrix, dashed lines: irradiated parts of the polymer chain in the matrix, dotted lines: desorbed polymer fragments.

polymer (with flexible links) in solution is not an extended linear chain but can be described by a non-spherical coil[41] characterized by its radius of gyration.[42] This implies that each chain must fold several times, in this way building several loops. The individual polymer segments are surrounded by solvent molecules and, in the case of complete miscibility, also by the matrix molecules. In dilute polymer solutions the coils are separated from each other and can be regarded as isolated. When the polymer concentration is greater than a critical concentration, an entanglement of coils can occur.[41] Due to the spatial extension of the polymer coil it can be envisaged that some polymer molecules lie completely and others only partially in the irradiated volume. Assuming a cylindrical geometry for the illuminated volume and a quite limited penetration depth of the UV laser (usually not more than some tens of molecular layers of the matrix) the fraction of partially irradiated polymers will be quite high. This should be more or less irrespective of the laser beam width.

The logical connection between partial illumination of the polymers and fragmentation is illustrated in Scheme 1. In this presentation the polymer fraction exposed to partial illumination is indicated by the dashed curves. In the irradiated volume the matrix material is desorbed and exerts a drag on the neighbouring polymer segments. In a solid matrix the polymer in the non-irradiated area is retained by the matrix (full curves) and chain rupture at two sites of the loop liberates one or two polymer fragment into the gas phase (dotted curves) depending on which part of the polymer lies within the irradiated volume. As a result the polymer is in many cases fragmented into more than two fragments with a high probability for the formation of smaller fragments. The experimental data reported above indicated that the degree of fragmentation was significantly lower when using liquid matrices. This finding can be explained within the given model by the higher mobility given to the polymer segments when embedded in a liquid matrix. In this instance parts of the pending short polymer chain or even small loops might be pulled away by the volatilized matrix materials without causing chain ruptures (cf. lower part of Scheme 1). This model can also explain the experimental finding that the probability of fragmentation increases with the molecular mass of the pullulans. Of course, assuming such a mechanism does not necessarily exclude that fragmentation events might also result from other causes.

Quantitative mathematical model for simulating polymer distributions after fragmentation events

A quantitative model is introduced that allows one to simulate the effect of fragmentation on the mass distribution curve, particularly its shape and the M_n and M_w values. For this quantitative treatment we start with a simple Gaussian-type number distribution $n(P)$ being a function of the degree of polymerization, P ($P = M/M_0$), and the respective polydispersities, D (as a function of the variance, σ^2), and a function $p(P)$ describing the probability of a fragmentation event. This function is based on the following assumptions: (i) For any value of P above an upper limit, P_u, all polymers are fragmented, i.e., $p(P) = 1$. (ii) Between the upper and a

Copyright © 2008 John Wiley & Sons, Ltd.

DOI: 10.1002/rcm

lower limit $p(P)$ decreases continuously from 1 to zero. From a mathematical point of view any continuous function is a possible candidate for this equation. (iii) Below a certain lower limit of chain length, P_l, no fragmentation occurs; i.e., $p(P) = 0$. By the choice of the limits one can account for different stabilities of linkages. In principle, even polymers with low masses could fragment as is known in practice for some labile acidic oligosaccharides.[27,28] In such a case P_l is simply set equal to 1. On the other hand, if fragmentation seems to be absent this can be taken into account by choosing P_l higher than the mass range of the measurement. If fragmentation is less prominent and almost constant over the mass range a very high value for P_u should be chosen. (iv) The absolute number of molecules fragmented depends on their initial concentration and the fragmentation probability, i.e., $n(P)\cdot p(P)$. (v) Fragmentation occurs in such a way that the fragment distribution does not overlap with that of the intact sample. This last assumption implies that the chosen model is only applicable to samples with narrow distributions.

Based on these assumptions two different functions, p_1 and p_2, were deliberately chosen for $p(P)$:

$$p_1 = 0.5 * \{1 + \tanh(x)\} \quad x = 3.8 \cdot \frac{2 \cdot P - P_u - P_l}{P_u - P_l} \tag{1}$$

$$p_2 = \frac{P - P_l}{P_u - P_l} \quad \text{and} \quad p_2 = 0 \text{ for } P < P_l \text{ and } p_2 = 1 \text{ for } P > P_u \tag{2}$$

and applied to Gaussian functions, $g(P_0, \sigma^2)$, characterized by the mean value P_0 and the variance, σ^2. The concentration of the polymers which are still intact (not fragmented) is then given by:

$$n(P)_u = \frac{1}{\sqrt{2\pi}\sigma} \exp\left\{-\frac{(P - P_0)^2}{2\sigma^2}\right\} \cdot \{1 - p_i\} = g(P_0,\sigma^2)(1-p_i) \quad i = 1,2 \tag{3}$$

The functions, p_1 (dashed curves) and p_2 (dotted lines), are illustrated in Fig. 5(a) with the lower limit $P_l = 25$ and two upper limits $P_u = 250$ and 300 (depicted as grey and black curves), respectively. The limits were deliberately chosen based on the experimental observation of almost no fragmentation for Pul-5,900 and Pul-11,800 and the possibility of even obtaining spectra for the highest molecular masses when working with an ILM. In Fig. 5(b), two original Gaussian distributions (full curves) differing in P_0 and the widths (as indicated) are compared with those calculated for the non-fragmented polymers making use of the p_i functions. From the diagrams in Fig. 5(b) it can be seen that in the case where P_u is far greater than P_0 (left peak group) the modifying influence of fragmentation is almost negligible but increases the closer P_u is to P_0 (right peak group). The absolute intensity is always reduced by the occurrence of fragmentation thus worsening the S/N ratio until in the most unfavourable case the signal is of comparable intensity to the noise.

It is worthwhile mentioning that the proposed approach is by no means limited to simulating the distortion of the measured polymer distribution by fragmentation events, but can be applied equally well to the analogous treatment of changes due to ionization-related mass discrimination.

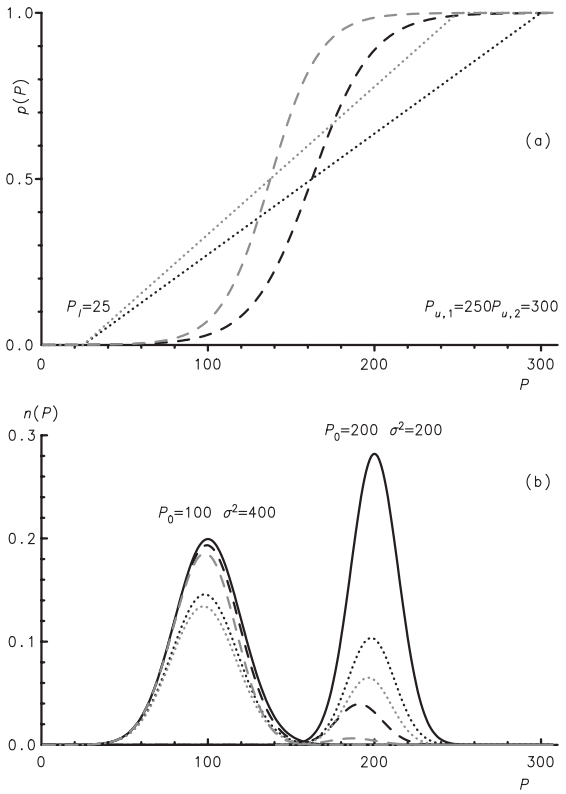

Figure 5. Model calculation describing the impact of the fragmentation probability on the residual non-fragmented polymer distribution. (a) Fragmentation probabilities, p_i, as given by Eqns. 1 (dashed line), and 2 (dotted line) for two different upper limits ($P_u = 250$ and 300, black and grey, respectively); (b) original Gaussian distribution (solid line) and resulting residual non-fragmented polymer distributions as calculated according to Eqn. (3) and applying Eqn. (1) (dashed curve) and Eqn. (2) (dotted curve).

For a quantification of the fragmentation impact the values concerning the weight average degree of polymerization, P_w ($P_w = M_w/486.3$), and the polydispersity, D, were calculated and are listed in Table 2. The width of the distributions was chosen to conform to one or two times the value of the respective Poisson distribution. Those examples where the deviation in P_w is smaller than 5% are regarded as the favourable cases whereas those leading to a reduction in P_w by more than 10% represent worse case scenarios. Given the high signal intensities of intact high-mass pullulans, it is likely that a realistic value of P_u might be even higher than the one assumed for this simulation and that the deviations in P_w might be accordingly smaller.

The following trends can be deduced from the data in Table 2. (i) The agreement between the original and residual non-fragmented polymer distribution becomes better the narrower the original distribution is. (ii) The steeper the slope of the fragmentation function, p_i, the stronger is the distortion of the resulting distribution; in certain cases the symmetry is lost. (iii) Fragmentation leads to a slight reduction of P_w and

Copyright © 2008 John Wiley & Sons, Ltd.

DOI: 10.1002/rcm

Table 2. Calculated values for the weight average degree of polymerization, P_w, and polydispersity, D, of the original Gaussian distributions centred around P_0 (100 and 200, respectively) and the residual non-fragmented polymer distributions simulated by means of Eqn. (3), assuming a fragmentation probability as described by Eqns. (1) and (2), respectively. P_l is chosen in all cases as 25 (calculated P_w values differing from the 'true' ones by more than 10% are indicated in italics)

	p_1		p_2		p_1		p_2	
	P_w	D	P_w	D	P_w	D	P_w	D
P_u	original distribution: $P_0 = 100$, $\sigma^2 = 100$				original distribution: $P_0 = 100$, $\sigma^2 = 400$			
'true'	101	1.010	101	1.010	104	1.040	104	1.040
300	101	1.010	101	1.010	103	1.039	102	1.041
250	100	1.010	100	1.010	101	1.037	101	1.041
200	98.8	1.009	100	1.010	95.5	1.034	100	1.042
150	93.3	1.010	99.0	1.010	*84.0*	1.032	95.7	1.040
130	*89.6*	1.010	97.6	1.010	*77.7*	1.032	*91.0*	1.037
110	*85.0*	1.012	*92.9*	1.007	*68.5*	1.033	*82.8*	1.032
	original distribution: $P_0 = 200$, $\sigma^2 = 200$				original distribution: $P_0 = 200$, $\sigma^2 = 800$			
'true'	201	1.005	201	1.005	204	1.020	204	1.020
300	192	1.005	199	1.005	*176*	1.018	196	1.020
270	190	1.005	198	1.005	*168*	1.020	192	1.019
250	188	1.005	197	1.005	*163*	1.021	188	1.018
230	187	1.006	194	1.004	*157*	1.023	*181*	1.016
210	185	1.006	188	1.003	*150*	1.024	*172*	1.014

the change in D is always very small. Even in the case of a strong impact on P_w the value of D can still be regarded as fairly correct (cf. last line in Table 2).

The comparison of the D values of the pullulans determined by MALDI-MS with those given by the supplier reveals that the discrepancy is higher than the potential error predicted on the basis of the proposed fragmentation model. This corroborates the assumption that the discrepancies in D shown in Table 1 are mainly due to the known overestimation of D by SEC and alternative methods.

CONCLUSIONS

A series of matrices was tested for the MALDI-TOFMS-based characterization of pullulans. The comparison of the spectra obtained either with a solid or with a liquid matrix revealed that for the investigated carbohydrate polymers the ionic liquid matrix (ILM) DHBB was much superior to the crystalline matrices DHB and THAP. This was particularly with respect to the following features. (i) When using the ILM, repetition of measurements led to almost identical results and there was no necessity to find a sweet spot. This result was also obtained by other scientists for other types of analytes[24,26] and is plausible because of the greater homogeneity of the spotted sample. (ii) When using DHBB, fragmentation of the sample is less pronounced and for pullulan samples with molecular masses up to 12 000 Da fragmentation was almost absent. (iii) Very low chemical noise was observed up to a molecular mass of about 12 000 Da. (iv) The ILM enabled the measurement of samples with molecular masses up to 100 kDa, a mass range where DHB had previously failed to give results.

It is very likely that, at least for pullulans up to medium chain lengths, the distribution established by MALDI-TOFMS measurements using the DHBB matrix provides a good approximation for the original, 'true' distribution. For narrow distributions ($D < 1.10$) the ionization-associated effect of high-mass discrimination can be expected to be small when using laser intensities above the threshold of the high-mass polymers. Up to molecular masses of 12 000 Da the fragmentation was found to be negligible when using ILM.

This conclusion is corroborated by our simulation which was based on the assumption of an increasing fragmentation probability with increasing molecular mass that was observed in the experiments. The influence of the degree of fragmentation on the shape of the distribution of the residual non-fragmented polymers, the weight average degree of polymerization, P_w, and the polydispersity was determined assuming an ideal Gaussian distribution as the original one. A slight shift in the P_w values to lower values upon non-negligible fragmentation was predicted. The strongest deviation from the original distribution has to be expected when (i) the mass distribution is broad, (ii) the broad distribution overlaps with the range where fragmentation occurs, and (iii) the fragmentation probability increases steeply.

Assuming reasonable data of fragmentation probabilities from the obtained spectra, a maximum decrease in the M_w values for the samples with molar masses in the 50 and 100 kDa range of less than 1% ($D = 1.01$, $P_0 = 100$) and 14% ($D = 1.02$, $P_0 = 200$), respectively, can be expected based on the presented model calculations. In addition, the simulations revealed that the deviation in D was always less than 1%.

Regarding the important aspect of the accuracy of M_w determinations carried out by different methods, it became evident that in all cases, and even with the short-chain pullulans, the M_w values determined by MALDI-MS and by the use of both types of matrix were always smaller than those given by specifications of the supplier. This was found even for samples under measuring conditions for which a significant extent of fragmentation was unlikely. Our model calculations revealed that the uncertainties in the M_w and D data determined by MALDI-TOF with the DHBB matrix (<14%) were far below the differences found between our MALDI-MS-based data and the supplier's specifications (~25%). This evaluation points to a major bias of the methods employed for these specifications.

The given data provide some confidence that, even for the analysis of carbohydrate polymers, in which the labile glycosidic bond is very susceptible to fragmentation, the molecular mass distribution curves assessed by use of liquid ion-pair matrices is fairly accurate with respect to the distribution itself, but even more with respect to the characteristic numbers, M_w, M_n and polydispersity, D. Such a confidence might also be justified when using ILMs for the investigation of other oligo- and polysaccharides which usually display fragmentation with conventional matrices.

Copyright © 2008 John Wiley & Sons, Ltd.

DOI: 10.1002/rcm

REFERENCES

1. Lin Y, Zhang Z, Thibault J. *Process Biochem.* 2007; **42**: 820.
2. Akiyoshi K, Deguchi S, Moriguchi N, Yamaguchi S, Sunamoto J. *Macromolecules* 1993; **26**: 3062.
3. Forabosco A, Bruno G, Sparavano L, Liut G, Marino D, Delben F. *Carbohydr. Polym.* 2006; **63**: 535.
4. Dubin PL. *Carbohydr. Polym.* 1994; **25**: 295.
5. Kawahara K, Ohta K. *Carbohydr. Polym.* 1984; **4**: 335.
6. Ward RM, Gao Q, de Bruyn H, Gilbert RG, Fitzgerald MA. *Biomacromolecules* 2006; **7**: 866.
7. Roger P, Axelos MAV, Colonna P. *Macromolecules* 2000; **33**: 2446.
8. Yeung B, Marecak D. *J. Chromatogr. A* 1999; **852**: 573.
9. Shingel KI. *Carbohydr. Res.* 2004; **339**: 447.
10. Petrov PT, Shingel KI, Scripko AD, Tsarenkov VM. *Biotechnolgiya* 2002; **1**: 36.
11. Wiley BJ, Ball DH, Arcidiacono SM, Sousa S, Mayer JM, Kaplan DL. *J. Environ. Polym. Degrad.* 1993; **1**: 3.
12. Roukas T, Mantzouridou FJ. *J. Chem. Technol. Biotechnol.* 2001; **76**: 371.
13. Eckelt J, Sugaya R, Wolf BA. *Carbohydr. Polym.* 2006; **63**: 205.
14. Kasaai MR. *J. Appl. Polym. Sci.* 2006; **100**: 4325.
15. Schriemer DC, Li L. *Anal. Chem.* 1996; **68**: 2721.
16. Zhu H, Yalcin T, Li L. *J. Am. Soc. Mass Spectrom.* 1998; **9**: 275.
17. Montaudo G, Samperi F, Montaudo MS. *Progr. Polym. Sci.* 2006; **31**: 277.
18. Stahl B, Steup M, Karas M, Hillenkamp F. *Anal. Chem.* 1991; **63**: 1463.
19. Garozzo D, Spina E, Cozzolino R, Cescutti P, Fett WF. *Carbohydr. Res.* 2000; **323**: 139.
20. Tang K, Allman SL, Chen CH. *Rapid Commun. Mass Spectrom.* 1993; **7**: 943.
21. Hsu NY, Yang WB, Wong CH, Lee YC, Lee RT, Wang YS, Chen CH. *Rapid Commun. Mass Spectrom.* 2007; **21**: 2137.
22. Fukuyama Y, Kolender AA, Nishioka M, Nonami H, Matulewicz MC, Erra-Balsells R, Cerezo AS. *Rapid Commun. Mass Spectrom.* 2005; **19**: 349.
23. Wallace WE, Arnould MA, Knochenmuss R. *Int. J. Mass Spectrom.* 2005; **242**: 13.
24. Armstrong DW, Zhang LK, He L, Gross ML. *Anal. Chem.* 2001; **73**: 3679.
25. Tholey A. *Rapid Commun. Mass Spectrom.* 2006; **20**: 1761.
26. Mank M, Stahl B, Boehm G. *Anal. Chem.* 2004; **76**: 2938.
27. Fukuyma Y, Nakaya S, Yamazaki Y, Tanaka K. *Anal. Chem.* 2008; **80**: 2171.
28. Laremore TN, Murugesan S, Park TJ, Avci FY, Zagorevski DV, Linhardt RJ. *Anal. Chem.* 2006; **78**: 1774.
29. Zifferer G. Institute for Physical Chemistry, University of Vienna, Austria.
30. Yamagaki T, Ishizuka Y, Kawabata SI, Nakanishi H. *Rapid Commun. Mass Spectrom.* 1997; **11**: 527.
31. Beavis RC, Chait BT, Fales HM. *Rapid Commun. Mass Spectrom.* 1989; **3**: 432.
32. Wallenfels W, Kreilich G, Brechtler G, Freudenberger D. *Biochem. Zeitschr.* 1965; **341**: 433.
33. Carolan G, Catley BJ, McDougnal FJ. *Carbohydr. Res.* 1983; **114**: 237.
34. Knox JH, McLennan F. *J. Chromatogr.* 1979; **185**: 289.
35. Schnöll-Bitai I. *J. Chromatogr. A* 2006; **1084**: 160.
36. Baumgarten JL, Busnel JP, Meira GR. *J. Liq. Chromatogr. Relat. Technol.* 2002; **25**: 1967.
37. Meira GR, Vega JR. In *Dekker Encyclopedia of Chromatography*, (2nd edn), Cazes J (ed). Marcel Dekker, CRC Publishers: New York, 2005; 159.
38. Byrd HCM, Mc Ewen CN. *Anal. Chem.* 2000; **72**: 4568.
39. Schnöll-Bitai I, Hrebicek T, Rizzi A. *Macromol. Chem. Phys.* 2007; **208**: 485.
40. Kornherr A, Olaj OF, Schnöll-Bitai I, Zifferer G. *Macromol. Theory Simul.* 2006; **1**: 215.
41. Elias HG. *Makromoleküle, Physikalische Strukturen und Eigenschaften*. Wiley-VCH: Weinheim, 2001; **66**: 292.
42. Viebke C, Williams PA. *Anal. Chem.* 2000; **72**: 3896.

Copyright © 2008 John Wiley & Sons, Ltd.

DOI: 10.1002/rcm

Summary

This thesis deals with the analysis of glycopeptides, glycans and polysaccharides by means of MALDI mass spectrometry (MS). It comprises three original research articles which address the improvement of MS signal intensities of biopolymers containing carbohydrate structures. These molecules show especially in combination with other analytes, *e.g.*, peptides, a reduced ionization yield, the associated signals appear in the mass spectrum with very low intensity or are completely suppressed. There are different approaches to overcome this problem and improve the analysis of carbohydrates. One possibility is the separation of the analytes before the mass spectrometric measurement in order to minimize the suppression of ionization. A second strategy is based on chemical derivatization to achieve better stabilized ions, a third one is the development of alternative MALDI matrices and preparation methods.

The first publication investigates a derivatization procedure aimed to increase the ionization yield of glycosylated peptides. The chosen AQC-derivatization enabled a more comprehensive MALDI-MS analysis of glycopeptides in the presence of non-glycosylated peptides, particularly those containing a small backbone but relatively large carbohydrate moieties.

In the second work a newly developed ionic liquid matrix was investigated which turned out to be especially useful for the analysis of glycopeptides and glycans as significantly higher relative signal intensities could be achieved compared to conventional crystalline matrices. With this matrix it was possible to analyze glycans enzymatically cleaved off from glycopeptides without further treatment or separation, *i.e.*, in the presence of all other peptides of a tryptic digest.

In the third publication an already established ionic liquid matrix was investigated with regard to its suitability to analyze the mass distribution of relatively simple composed polysaccharides, namely pullulans. Although these carbohydrates are prone to easy fragmentation during the MALDI process, accurate mass distribution and polydispersity data could be assessed. The exact knowledge of these data is of importance when using these compounds as calibration standards for aqueous size-exclusion chromatography.

Zusammenfassung

Diese Doktorarbeit beschäftigt sich mit der Analyse von Glykopeptiden, Glykanen und Polysacchariden in der MALDI-Massenspektrometrie (MS). Sie besteht aus drei originalen Forschungsartikeln, die die Verbesserung der Signalintensitäten von aus Kohlenhydraten aufgebauten Biopolymeren zum Ziel haben. Diese Moleküle zeigen vor allem in der Mischung mit anderen Analyten, zum Beispiel Peptiden, eine verminderte Ionenausbeute, die dazugehörigen Signale erscheinen im Massenspektrum entweder mit sehr geringer Intensität oder sind vollständig unterdrückt. Es gibt verschiedene Ansätze um dieses Problem zu umgehen und die Analyse von Kohlenhydraten zu verbessern. Eine Möglichkeit ist die Trennung der Analyte vor der massenspektrometrischen Messung um dadurch die Unterdrückungserscheinungen zu minimieren. Eine zweite Variante ist die chemische Derivatisierung, um eine bessere Stabilisierung der Ionen zu erreichen, eine weitere ist die Entwicklung alternativer MALDI-Matrices oder Präparationsmethoden.

Die erste Publikation beschäftigt sich mit einer Derivatisierungsreaktion, die die Ionenausbeute von glykosylierten Peptiden erhöht. Durch die gewählte AQC-Derivatisierung konnten Glykopeptide, die einen kleinen Peptid- aber einen relativ großen Kohlenhydratanteil besitzen, in der Mischung mit nicht-glykosylierten Peptiden analysiert werden.

In der zweiten Arbeit wird eine neu entwickelte ionisch-flüssige Matrix vorgestellt, die besonders für Glykopeptide und Glykane geeignet ist, da mit deren Hilfe deutlich höhere relative Signalintensitäten erzielt wurden als mit herkömmlichen kristallinen Matrices. Mit dieser Matrix war es möglich, die von Glykopeptiden enzymatisch abgespalteten Glykane ohne weitere Behandlung oder Trennung mittels MALDI-MS zu analysieren, d.h. in Gegenwart aller anderen Peptide eines tryptischen Verdaus.

In der dritten Publikation wurde eine bereits etablierte ionisch-flüssige Matrix in Bezug auf ihre Eignung für die Bestimmung der Massenverteilung von relativ einfach aufgebauten Polysacchariden, nämlich Pullulanen, untersucht. Obwohl diese Kohlenhydrate relativ leicht während des MALDI-Prozesses fragmentieren, konnten präzise Daten für die Massenverteilung und Polydispersität berechnet werden. Die genaue Kenntnis dieser Daten ist von Bedeutung, da diese Verbindungen als Kalibrier-Standards in der wässrigen Size-Exclusion-Chromatographie Verwendung finden.

Lebenslauf

PERSÖNLICHE DATEN

Name	Roman Ullmer
Anschrift	Leystraße 42/33
	1200 Wien, Österreich
Geboren	6. April 1978 in Wien
Staatsbürgerschaft	Österreich
Familienstand	verheiratet

AUSBILDUNG

09/1984 bis 06/1988	Volksschule, 1180 Wien
09/1988 bis 06/1996	Bundesrealgymnasium, 1190 Wien
10/1996 bis 12/2004	Diplomstudium Chemie an der Universität Wien
10/1997 bis 09/1998	Zivildienst bei der Johanniter Unfallhilfe Wien
02/2005	Beginn der Dissertation am Institut für Analytische Chemie und Lebensmittelchemie der Universität Wien, Arbeitsgruppe Prof. Andreas Rizzi

PUBLIKATIONEN

April 2006	R. Ullmer, A. Plematl and A. Rizzi *„Derivatization by 6-aminoquinolyl-N-hydroxy-succinimidyl carbamate for enhancing the ionization yield of small peptides and glycopeptides in matrix-assisted laser desorption/ionization and electrospray ionization mass spectrometry“*, Rapid Commun. Mass Spectrom. 2006; 20: 1469-1479

September 2008	I. Schnöll-Bitai, R. Ullmer, T. Hrebicek, A. Rizzi, I. Lacik *„Characterization of the molecular mass distribution of pullulans by matrix-assisted laser desorption/ionization time-of-flight mass spectrometry using 2,5-dihydroxybenzoic acid butylamine (DHBB) as liquid matrix”*, Rapid Commun. Mass Spectrom. 2008; 22: 2961-2970
Oktober 2008	R. Ullmer, A. Rizzi *„Use of a novel ionic liquid matrix for MALDI-MS analysis of glycopeptides and glycans in total tryptic digests”*, submitted to J. Mass Spectrom.

VORTRÄGE

Februar 2006	*„AQC-Derivatization of peptides and glycopeptides in MALDI- and ESI-MS”* 17. Massenspektrom. Diskussionsveranstaltung Wien
Februar 2008	*„Determination of the Molar Mass Distribution of Oligo- and Poly-Saccharides (Pullulans) by MALDI- and ESI-TOF-MS”* 19th MassSpec Vienna

POSTER

Oktober 2007	*„Analysis of fluorophore-labeled human rhinovirus by capillary electrophoresis coupled to matrix-assisted laser desorption/ionization mass spectrometry”* HUPO 6th Annual World Congress 2007, Seoul, Korea

LEHRTÄTIGKEIT

2004 bis 2008	Tutor und Lektor an der Fakultät für Chemie der Universität Wien